Referee#1 comment RC2

This study investigates the ice nucleation characteristics of two samples of Asian dust collected from the west coast of Japan. Particles with diameters > 1.1 μ m were deposited on a hydrophobic Si waver using an impactor. The ice nucleation ability of the collected particles was investigated in immersion freezing mode in a closed cell mounted onto a cold stage of an optical microscope. The ice nucleating particles (INPs) together with a number of inactive particles were characterized first with AFM and micro-Raman spectroscopy followed by SEM-EDX. For comparison several reference samples were investigated with the same methods. This study presents a new approach to characterize atmospheric INPs on an individual particle basis. It is a welcome complement to other combinations of methods used to characterize atmospheric INPs on a single particle basis. It shows once more how complex the composition of aged aerosol particles in the coarse mode is, rendering a clear classification of particles difficult. Nevertheless, the authors succeeded to identify physical and chemical characteristics that increase or decrease the ice nucleation ability of the particles. I recommend this paper for publication in ACP after revisions. Specifically, the experimental procedure needs to be explained in more detail. For the validation of the method, the reference samples need to be analyzed more quantitatively and compared more thoroughly with available literature. Moreover, more references need to be added to the introduction and the formulation of some sentences needs to be improved (see specific comments below).

The authors would like to thank the reviewer for providing positive comments and constructive suggestions by thoroughly going through the manuscript. As suggested by the reviewer, we added more details on the experimental procedures. We have conducted additional and thorough analysis on the reference samples to validate our method, and quantitatively compared the results with the available literature. Please find our response to each of the comments below (in blue italic).

Page 1, line 19: what is meant by "slower"? At lower temperature?

We changed the corresponding sentence as follows:

'Meanwhile, most of the IN active atmospheric particles formed ice below -28 °C, i.e. at lower temperatures than the standard mineral dust samples of pure components.'

Page 2, line 9: reference to Murray et al. (2012) only is somewhat arbitrary. Add more references or "e.g." in front of the reference to the Murray et al.review..

We added Murray et al., (2010) and Rosenfeld and Woodley, (2000) as the references which also reported that the homogeneous nucleation takes place below -37°C.

Page 2, line 21 – 22: This sentence needs to be reformulated.

We changed the corresponding sentence as follows and added few more references:

'Based on these results, while mineral dust and biological particles are generally regarded as efficient ice nuclei (Morris et al., 2004; Connolly et al., 2009; Niemand et al., 2012), ice nucleation within mixed phase clouds involving soot and organic particles is still not as clearly demonstrated due to the diverse chemical composition and different experimental conditions (DeMott, 1990; Kireeva et al., 2009).'

Page 2, line 23: "sea salt and sulfates are often not considered as efficient ice nuclei.": This is not generally true for sulfates. Ammonium sulfate is found to be ice nucleating at lower temperatures as is also stated later in the manuscript by referring to e.g. Abbatt et al. (2006). The sentence here needs to be corrected, e.g. by adding "under mixed phase conditions".

Indeed, we should state more clearly that we are referring specifically to the mixed phase conditions here. We made the following change as suggested.

'On the other hand, sea salt and sulfates are often not considered as efficient ice nuclei under mixed phase conditions.'

Page 2, lines 30 – 31: This sentence needs to be improved.

We changed the corresponding sentence as:

'This enabled direct and detailed investigation on the particles representative of the actual deposition mode ice nuclei in cirrus clouds.'

Page 3, lines 1 – 3: this statement should be supported by more recent references.

We added Prenni et al., (2012) and Ardon-Dryer and Levin, (2014) as the references.

Page 3, lines 3 – 5: this statement should be supported by a reference.

We added Korolev, (2007) as the reference.

Page 3, line 12: which "above mentioned artifacts" are meant here? Please, be more explicit.

We made the following changes to be more explicit:

'However, they also reported discrepancies between the results obtained from the three different sampling techniques, and attributed them to potential bias arising from the artifacts such as the possible generation of particles within the instruments and the inherently scarce number of ice nuclei in the atmosphere.'

Page 3, line 20: more than just one reference should be given here to support this statement.

We added Zhang et al., (2003), Sullivan et al., (2007), and Iwasaka et al., (2009) as the references.

Page 3, lines 21 - 22: again, more than one reference should be given to support this statement.

We added Maring et al., (2003) as the reference.

Page 4, lines 25 – 28: Was the dew point kept constant at -6 to -3°C during cooling? Also, the degree of dilution of the particle should be estimated based on the size of the developing droplet. This is important to judge whether a freezing point depression as discussed later on in the manuscript is relevant at all.

The air supply to the chamber is cut during the cooling phase, so the dew point of the supplied air is not actively controlled or monitored during this time. Nonetheless, as the course of the cooling down to -30°C, the remaining water vapor in the chamber is expected to be maintained slightly above the saturation. This is consistent with the fact that the growth in particle size due to condensation can be visually observed.

The dry and wet particle diameters before and after the condensational growth are shown in Table S-1. The degree of dilution was estimated based on the growth rate. As a result, the average concentration of the solution droplets of the atmospheric particles were estimated to be approximately 0.074 g/ml.

Table S-1: The diameters and volumes of the particles before (dry) and after (wet) the condensational growth. Corresponding concentrations of the sample and test solute particles in the solution droplets are also shown. Here, D_{dry} and D_{wet} denote the circle equivalent diameters obtained from the 2D silhouette of the particles in the microscopic images taken before and after (at approximately -25 ˚C) the cooling experiment, respectively. The number of the particles observed by the microscope is shown as n. V_{dry} is the sphere equivalent volume calculated from the corresponding D_{dry}. V_{wet} was calculated by assuming droplets having contact angle of 110˚ relative to the substrate. The droplet volumetric growth factor GF was determined by the ratio of V_{wet} relative to V_{dry}. By assuming following densities (sampled particles: 2.00 g/cm^3, NaCl: 2.16 g/cm^3, $Ca(NO_3)_2$: 2.36 g/cm^3), The calculated mass and molar concentrations of the droplet are shown in terms of m and M, respectively. The test solute particles of NaCl and $Ca(NO_3)_2$ were aerosolized by atomizing their solutions (0.005g/ml) and collected on the substrate with an impactor.

	Sampled particles (n = 144)	NaCl (n = 97)	$Ca(NO_3)_2$ (n = 102)
D_{dry} (μm)	3.9 ± 0.8	4.8 ± 1.4	4.0 ± 1.0
D_{wet} (μm)	9.2 ± 1.8	14.7 ± 4.7	12.9 ± 2.5
V_{dry} (μm^3)	4.4 ± 2.2	9.0 ± 7.6	4.9 ± 2.2
V_{wet} (μm^3)	156.9 ± 75.0	750.0 ± 677.0	429.2 ± 191.0
GF	43.9 ± 25.0	94.3 ± 55.7	123.7 ± 101.4
m (g/ml)	0.074 ± 0.112	0.029 ± 0.015	0.024 ± 0.009
M (mol/l)	-	0.49 ± 0.25	0.15 ± 0.05

Page 5, lines 26 – 27: This sentence needs to be improved.

We changed the corresponding sentence as follows:

'Both the IN active and non-active particles collected in the atmosphere were analyzed on an individual particle basis using a series of microscopic techniques. Firstly, an AFM (CombiScope™ 1000, AIST-NT, Inc., USA) was used to characterize the three-dimensional morphology, followed by micro-Raman spectroscopy to detect chemical compounds.'

Page 7, lines 11 – 16: Here, the freezing onset temperatures of the reference samples are compared with literature (Atkinson et al., 2013) and it is concluded that they are consistent. However, this comparison does not take the surface area present in the samples into account. The comparison needs to be based on the surface area present in the investigated reference sample of this study multiplied with published ice nucleating active sites (INAS) surface densities e.g. from Peckhaus et al. (2016) or Harrison et al. (2016) for feldspars. Moreover, It should be specified what frozen fraction was taken as the onset condition.

We have to admit that our technique is not a perfect method that can resolve all technical issues encountered in the ice nucleation experiments. The biggest advantage of course is that we can keep track and be sure which single particle was actually nucleating ice. In return, we have to sacrifice the accuracy and quantitative evaluation of freezing temperatures based on INAS in relation to the evaporation of droplets in the vicinity of the frozen particles (Bergeron-Findeisen effect), as well as due to the limited number and size (d>1.1µm) of the particles that can be analyzed.

The number of ice crystals formed are compromised especially at lower temperatures as the number and size of ice crystals increase and more droplets in the vicinity of the growing ice are subjected to evaporation. When comparing our results with those found in literature, we must also note that strict comparison is difficult because of the uncertainties and differences related to the size distribution and composition of dust particles used in different experiments. Assumptions made to

calculate the surface area can also be a source of bias. The K-feldspar used in this study as a reference mineral dust was purchased from the same supplier, but the lot number is different (i.e. different source rock) from the K-feldspar used in Atkinson et al (2013). Therefore, composition of K-feldspar used in the current study and that used in Atkinson et al. (2013) are not exactly the same. Nevertheless, we added the ice nucleation active sites (INAS) of the 4 standard mineral particles measured by the current IDFM (Fig. S-2).

The ice nucleation active sites (INAS) obtained in this study agreed within an order of magnitude difference compared to those found in the literature (despite many different experimental conditions). Further, we would like to emphasize that the relative order of the onset temperatures found for different particles is always consistent (i.e. K-feldspar > Na-feldspar > quartz > kaolinite >> pure water) and even the range of the freezing temperatures are not far off from the reported values.

It was probably not clearly stated in the manuscript, so the following change was made with regard to the onset temperatures:

'Heterogeneous ice nucleation observed in all standard mineral samples tested in this study (K-feldspar, Na-feldspar, quartz, kaolinite) consistently occurred at higher temperatures than the homogeneous freezing temperature. The reference mineral samples were milled to fine grains before being collected on Si wafer substrate by an impactor. Three set of samples were made for each reference mineral to ensure large enough observation area for the IDFM. The total number of the particles monitored during the ice nucleation experiment by IDFM was 4,509, 2,271, 4,759, and 1,435 particles, respectively. In this study, the freezing onset temperature of the sample was defined as the temperature at which the IN active fraction of the total observed particles reached 0.01. As a result, the freezing onset temperatures for K-feldspar, Na-feldspar, quartz, and kaolinite ranged between -22.2 to -24.2 ˚C, -24.7 to -25.7˚C, -24.8 to -26.8 ˚C and -27.2 to -29.2 ˚C, respectively (Fig. S-1). Therefore, the ice nucleation activity of K-feldspar was the highest and that of kaolinite was the lowest. The order and the range of observed onset temperatures for these minerals were consistent with the results found in the literature (Atkinson et al., 2013; Murray et al., 2011).'

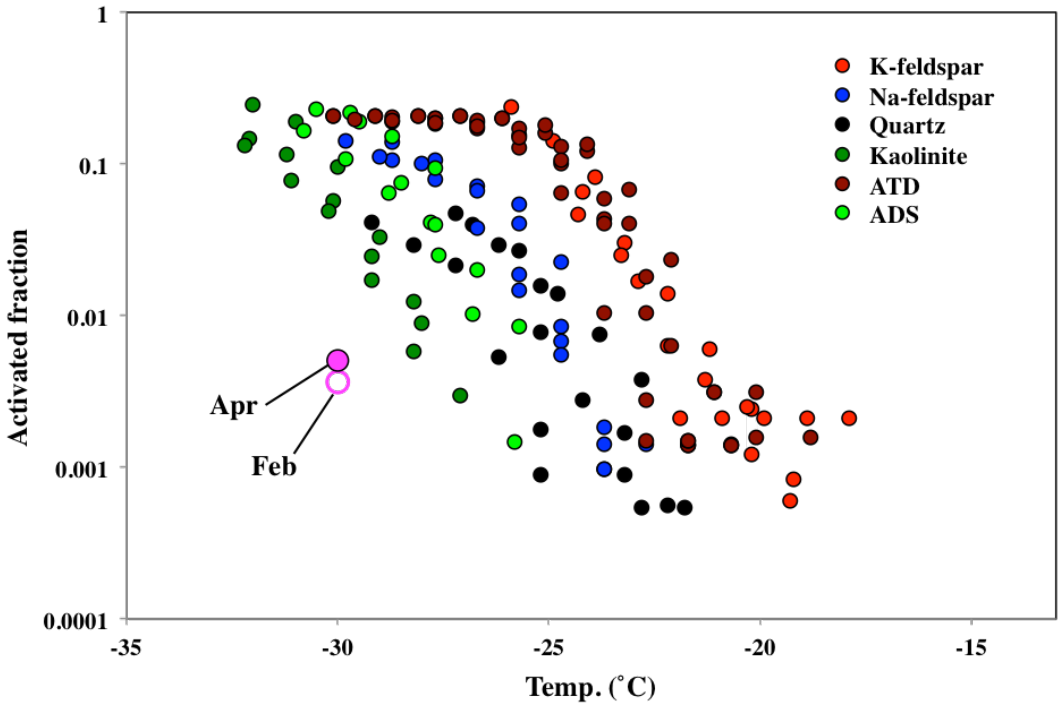

Figure S-1: Activated fractions of the reference mineral dust particles. Results of the atmospheric samples collected in February and April are also shown for comparison.

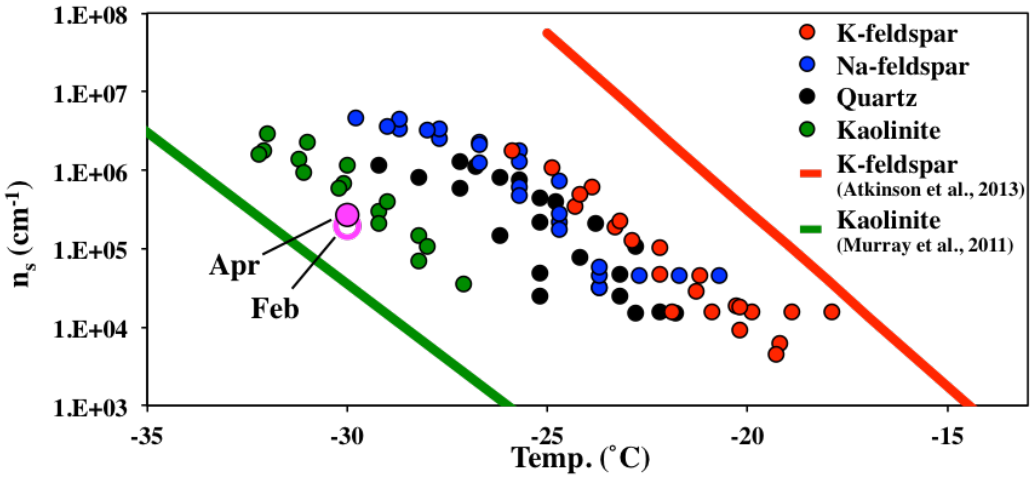

5

Figure S-2: the ice nucleation active site (INAS) densities for the reference single component mineral dust samples. These INAS densities were calculated from the activated fractions (Fig. S-1) and the averaged sphere equivalent surface areas obtained from the 2D silhouette of individual particles in the microscopic image.

Page 7, line 18: The ATD and ADS samples should be discussed in more detail. How many particles were analyzed? Comparison of freezing temperatures with relevant literature is needed.

In response to the above comment, we added the ice nucleation active sites measured for ATD and ADS, and compared with the natural dust sample found in literature (Niemand et al., 2012)

We also made the following change in the manuscript:

'For comparison, the freezing onset temperatures of the ATD and ADS were -22.1 to -23.7 °C and -25.2 to -27.2 °C, for 2,019 and 1,354 monitored particles, respectively.'

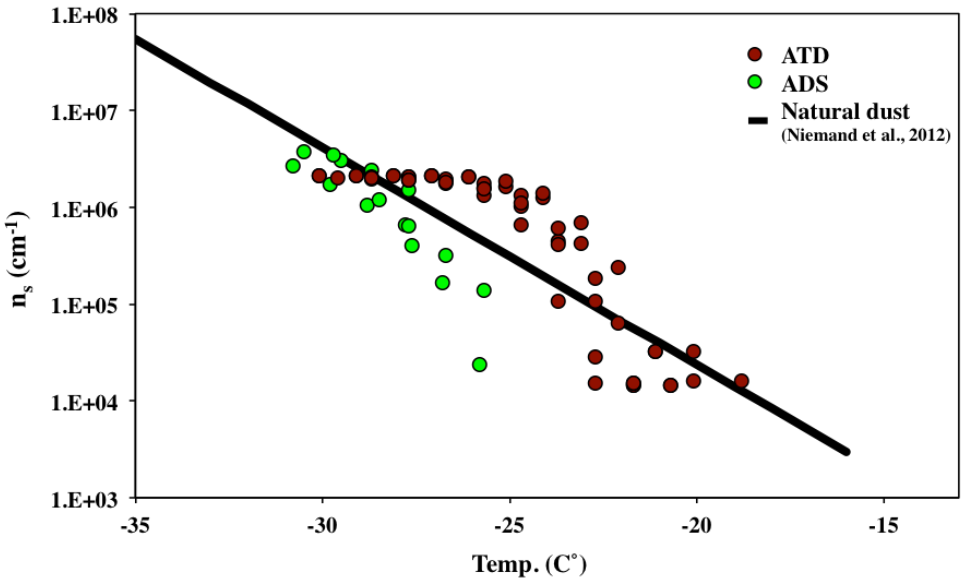

Figure S-3: the ice nucleation active site densities for ATD and ADS.

Page 7, line 19 – 21: the measurement procedure needs to be explained better. Was the same sample cooled repeatedly to investigate the ice nucleation activity of the 10,188 and 24,145 particles? If yes, what were the heating/drying conditions between the cooling cycles to remove the ice crystals?

No we did not repeat the freezing and heating/drying cycles though it would be an interesting experiment to show the robustness and reproducibility of the results. To minimize the impact of repeated activation on the particle properties, we limited it to be just one freezing and heating cycle. Besides, it is very labor intensive to go through that many particles for a repeated number of cycles.

The heating/drying condition is described in section 2.1 in the manuscript. We added following explanation in the manuscript:

'For ambient samples, we first determined the total number of target particles by analyzing the optical images recorded with x50 magnification. As a result, ice nucleation activity of 10,188 and 24,145 particles were monitored by the IDFM for the February and April samples, respectively. To avoid too many particles in contact or in proximity to each other in the same field of view, multiple samples were collected during the sampling period on separate silicon wafer substrates to gain a good total number of particles. '

Page 7, lines 22 – 23: Ice nucleation active fractions should also be given for the reference samples.

We added those results in Fig. S-1.

Page 7, line 24: specify "onset temperature" in terms of a frozen fraction.

We added the following description in section 3.1 as the definition of the onset temperature.

'In this study, the freezing onset temperature of the sample was defined as the temperature at which the ice nucleation active fraction of the total observed particles reached 0.01.'

Pages 9 – 10, Section 3.4: The elements C, N, O and Si could not be identified by SEM-EDX. The influence of this restriction should be discussed more explicitly. It should be analyzed whether based on the Raman spectra, some particles might be dominated by organics. In general, it might be helpful to combine the results of the Raman spectra and the SEM-EDX analysis already in the results section and not only in the discussion section. Also, do the compositions derived from the two techniques support each other or are they in some cases contradictory? At the end of this section, it is stated that the Raman peaks are "not necessarily representative of a major component of the particle". This is certainly true for large samples. However, in case of particles with diameters < 5 μ m, the laser spot penetrates the whole sample. This is supported by the presence of Raman peaks from the substrate present in the spectra. Moreover, in the method section, it is stated that Raman spectra were taken "each 750 nm step". This should lead to a full coverage of the particles in the x- and y-directions.

The restriction of not being able to take into account C, N, O and Si peaks are that we cannot detect organic containing particles by SEM-EDX analysis alone. As a result, if an organic dominant particle is present, it should be identified by the presence of organic related peaks in Raman and absence of other particular elements in the EDX spectra. This restriction however, does not lead to miscounting of mineral dust particles since even a quartz enriched particle can be detected with inclusions of small amount of Al. We added the following description in section 3.4.

'Note however, that elements C, N, O, and Si were not taken into account in the EDX semi-quantitative analysis. Therefore, we cannot rule out the possibility that organic dominant particles may be overlooked by EDX analysis alone.'

In relation to the results obtained by Raman spectra and EDX analysis, we found that the compositions derived from the two techniques are generally complementary to each other rather than being contradictory. But it is difficult to obtain a 100% match because the Raman peaks depend on the amount, Raman active cross section and peak overlaps of the compounds. And we also cannot determine if the organic matter is the dominant component in a particle or not solely from the obtained Raman peaks.

As pointed out, the following statement "not necessarily representative of a major component of the particle" and the related paragraph (Page 10, 1-9) is omitted from the text since it is true that we cannot prove it. We made following change in the manuscript:

'Particle classification with SEM-EDX relies on characteristic X-ray signals, which are used to estimate the major elemental composition of a particle. This information can be considered to reflect the bulk elemental distribution within a particle and has been commonly used for particle classification in many previous studies. In contrast, micro-Raman spectroscopy detects slight shifts of wavelength in the scattered light that reflect the vibrations of molecular bonds specific to the compounds contained in a sample. Therefore the Raman spectrum was used rather to complement the bulk particle type classification by the EDX analysis, and to detect the internally mixed compounds.'

Page 10 – 12, Section 4.1: This section needs to be improved. The assignment of clay minerals is solely based on a fluorescence signal in the Raman spectra. However, fluorescence is also often taken as an indication for the presence of biological aerosol particles (e.g. Twohy et al., 2016). How can a biological origin of the fluorescence signal be excluded?

Actually, the assignment of clay minerals is not solely based on a fluorescence signal but also taking into account the subsequent SEM-EDX analysis on the same particles. Our conclusion is based on the fact that 87% of the fluorescent particles contained dust related elements such as Mg, Al, Fe.

Indeed, we are aware of the biological fluorescence and it is also stated in Page 8, 29-31 'Fluorescence from a particle is typically attributed to a certain group of organics of biological origin, or the intercalated impurities of humic or humic-like substances in clay minerals and amorphous alumino-silicates (Sobanska et al., 2012; Jung et al., 2014).'

Possibility remains that part of the fluorescence results from internal mixing of biological matter attached to the mineral dust. To make it more clear, the following explanation is now added in the manuscript:

*'Subsequent SEM-EDX analysis showed that most of the fluorescent particles (87 %) contained elements that indicate a mineral composition. The fluorescence is also often taken as an indication for the presence of biological aerosols (Twohy et al., 2016), but considering the fact that all the ADS also showed similar fluorescence, and the relatively small abundance of biological particles as compared to mineral dust in general (*Huffman et al., 2012*), these fluorescence signals are mostly associated with mineral dust (especially those enriched in clay minerals) rather than pure biological particles. Possibility remains however, that a fraction of the fluorescence signal results from biological matters attached to the clay minerals. In any case, both the SEM-EDX and micro-Raman analyses indicated that mineral dust particles act as efficient ice nuclei under conditions relevant for mixed phase cloud formation.'*

Page 11. lines 5 – 6: An Al-K-(Ca+Na) ternary plot is not a typical way to discriminate K-feldspars from Na/Ca-feldspars. For this purpose a K-Na-Ca plot is usually used.

The ternary plot in Figure 7 is replaced with the K-Na-Ca plot. In any case, atmospheric particles are not gathering at a certain corner but they are rather scattered and show quite mixed characteristics.

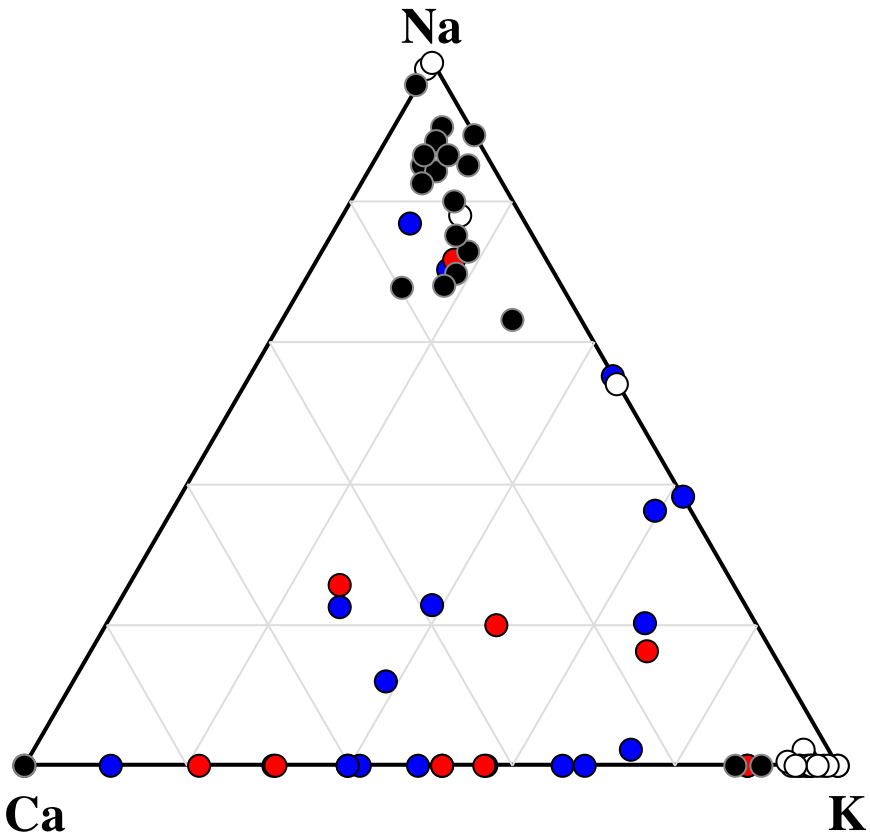

Page 11, lines 6 – 7: Why should clay minerals and mica appear in the middle of an Al-K-(Ca+Na) ternary plot? The clay mineral kaolinite contains only Al but no K nor Ca/Na. It should appear therefore at the Al corner. The clay mineral illite contains Al and K but no Ca/Na. It should therefore appear on the Al-K line. The same with the common mica muscovite: it contains Al and K but no Ca/Na.

From our years of experience of SEM-EDX analysis on natural Asian dust aerosols, it is very rare to see a single component dust particle. It is commonly the case that several mineral components are internally mixed within a particle so that plots do not usually stick to Al corner or Al-K line.

Page 11, line 8: How was the presence of mica inferred?

According to Yabuki et al., (2003), mica appears in the center rather than along the Al-(Ca+Na+K) line of the ternary Al-(Ca+Na+K)-(Fe+Mg) plot. Most of our dust particles (both IN and non-IN active) also fall in the area where plots of mica, feldspars, clay minerals appear. Most particles do not show characteristic elemental composition of specific mineral types, which is another indication that particles are forming complex mineral mixtures.

Page 11, lines 17 – 19: Only one study is cited although the sentence starts with "Previous studies". Either give reference to at least one more study or change to "A previous study".

We changed to "A previous study".

Page 11, line 23: improve formulation, e.g. reformulate: “most IN particles active above -30°C.”

Reformulated accordingly to the suggestion as follows.

‘most IN particles active above -30°C.’

Page 11, lines 23 – 26: The discussion of the origin of the fluorescence signal needs to be improved.

The fluorescence signal may come naturally from the crystal structural defect and/or the organic materials contained in the clay mineral particles. As discussed in section 4.4.(page 16, lines 12-16 in the original manuscript), we even found that all the fresh ADS (Asian dust particles believed to be dominated largely by clay minerals) were fluorescent and contained organic matter to some extent. Therefore the fluorescent particles associated with elements of crustal origin (by EDX analysis) were suggested as clay minerals. We made the following changes to be more explicit:

‘Furthermore, we even found that all the fresh ADS particles (believed to be dominated largely by clay minerals) showed the fluorescence. This fluorescence is likely derived from the defects and/or impurities (e.g. humic organics) in their crystal structure (Gaft et al., 2005; Jung et al., 2014; Sovanska et al., 2014). Therefore, the fluorescent particles associated with elements of crustal origin (by EDX analysis) were regarded as clay minerals. It was also demonstrated that the most IN particles active above -30 °C were dominated by such fluorescence mineral dust particles.'

Page 12, lines 7 – 8: It should be stated here, that this number has a low bias because contributions from organics are missed in SEM-EDX. An estimate of the contributions of organics based on the Raman spectra might be added.

Following sentence is added to the corresponding section:

‘Note however, that this elemental fraction of sea salt components is based on SEM-EDX and does not reflect potential contribution from organics and therefore must be regarded as the upper limit.’

Page 12,. line 23: “at any event” seems a too strong conclusion considering that aged sea salt particles + inclusions were also found as a small fraction in the IN active particle fraction.

We changed the corresponding part as follows:

'Based on the results of this study, we suggest that large and aged sea salt particles internally mixed with sulfates, nitrates, or organics are less likely to nucleate ice, although the possibility remains for ice nucleation by sea spray organic particles in the atmosphere.'

Page 13, line 30 – 31: "Therefore, the liquefied Ca(NO3)2 coating is expected to show strong molar depression of freezing point, which could explain their weak IN ability". This argumentation is only valid in the case of concentrated solutions. Its validity in the present case depends on the degree of dilution of the soluble material in the droplet. The dilution should be estimated to test the validity of this argumentation.

As shown in Table S-1, the average mass concentration of the suspension droplets formed by the atmospheric particles was estimated to be 0.074 g / ml. Similarly, the mass concentrations of droplets formed by pure NaCl and $Ca(NO_3)_2$ measured for comparison were 0.029 g / ml and 0.024 g/ ml, respectively. These concentrations are equivalent to 0.49 mol / l and 0.15 mol / l.

We conducted additional experiments to compare the freezing temperatures of pure water and NaCl solution and found that the droplets formed by NaCl particles froze consistently at lower temperatures than the pure water droplets by the current method (Fig. S-4). this result suggests that the molar depression of freezing point by NaCl or Ca $(NO_3)_2$ may occur within the range of concentrations expected in the current ice crystal formation experiment, unless there is an inclusion of extremely active ice nuclei. Furthermore, Pruppacher and Neiburger (1963) suggested that the freezing point depression by inorganic salt may be significant with concentrations down to 10^{-3} mol / l. Therefore, with the degree of dilution involved in the current experiment, freezing point depression may be effective and act to hinder freezing of droplets activated from NaCl or Ca $(NO_3)_2$ enriched particles.

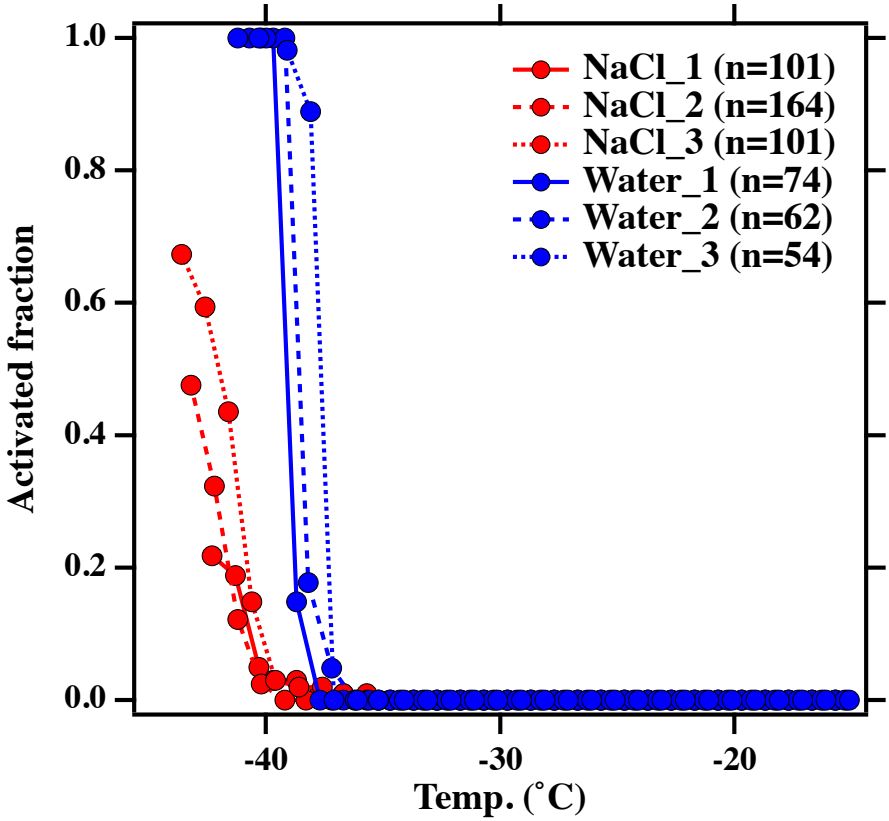

Figure S-4: Activated fractions of NaCl and pure water droplets. Three set of samples were tested for both NaCl and water. The number of particles and droplets observed under the microscope is shown as n.

The test NaCl particles were aerosolized by atomizing their solutions (0.005g/ml) and collected on the substrate with an impactor. The pure water droplets were also collected by spraying directly onto the substrate.

Page 14. Line 31: Can the OH peaks be associated with either alcohol or carboxy functionalities?

Detections of both the OH peak (3200 – 3650 cm^{-1}) and the organic peak (2,800 – 3,100 cm^{-1}) in this study suggest that the detected particles are highly oxidized organic matter containing hydroxyl group (Laskina et al., 2013). Although it is difficult to draw any conclusions, these Raman spectral features are also similar to OH bands observed for glassy oxygenated organic material (Tong et al., 2011; Baustian et al., 2012).

Page 15, lines 25 – 26: improve this sentence. You might split it: "…mainland Japan. Further upstream…"

The sentence was now split accordingly to the suggestion as the follows:

'The study area, Kanazawa City, is located along the west coast of mainland Japan. Further upstream of the westerly continental outflow are the vast arid regions of inland China and Mongolia. Every spring, frequent dust outbreaks are

observed, transporting a massive amount of mineral dust aerosols (Asian dust) across the region and beyond (Iwasaka et al., 2009).'

Page 16, line 2: why exactly 3.27±1.80 particles/cm3? Please explain.

This value is basically what we observed as an average concentration during Asian dust events in February 2016 at our monitoring station. This is explained in the manuscript for better clarity as follows:

'The average concentration observed during Asian dust events in February 2016 was 3.27 ± 1.80 particles/cm^3, so the concentrations observed during February sampling period were not as high as that expected during major Asian dust events.'

Page 16, line 8: how far away is NOTOGRO from the sampling location?

We added the following information in the manuscript:

'(NOTOGRO; 37.45°N, 137.36°E; 116km north east of the sampling location)'

Page 16, lines 20 – 27: this paragraph reads like a conclusion and might be deleted here and merged with the conclusion section.

The corresponding paragraph is now merged with the conclusion.

Page 17, line 5: the text in the bracket needs to be formulated better. Is it meant that mineral components such as clay minerals have defects in their crystal structure and contain impurities?

Yes, the corresponding part is now changed accordingly to the suggestion:

These mineral dust particles were suggested to be mixtures of several clay mineral components rather than single mineral species, having defects in their crystal structure and contain impurities.

Page 28, Fig. 3 and page, 35, Fig. 10: the line along which the transect of the particle was scanned should be indicated. The length bar of 0.5 µm given on top of the AFM images does not seem to correspond with the length axis given at the bottom in some images. Please check.

We checked and changed Fig.3 and Fig. 10 as follows:

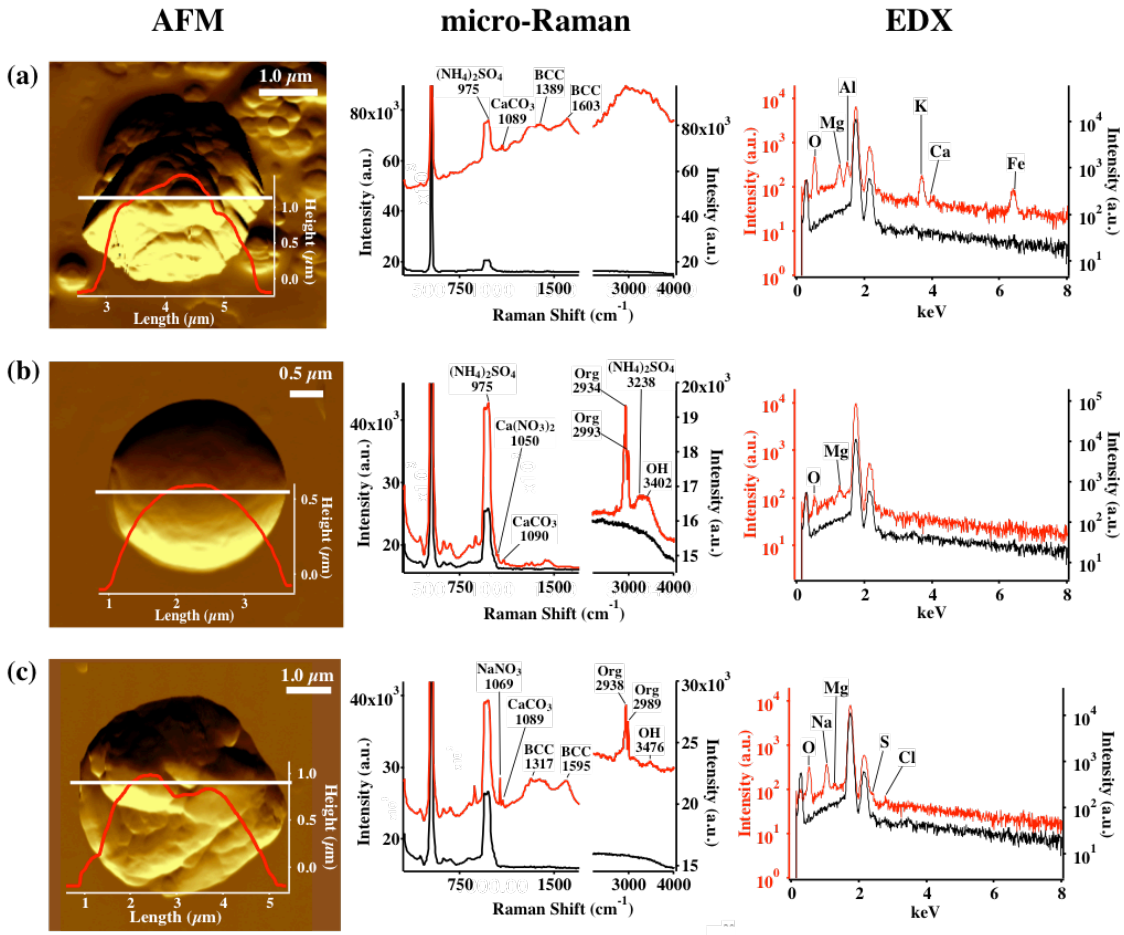

Figure 3: AFM topographic images of representative IN active particle (a) and non-active particle (b, c) groups, and their corresponding Raman and EDX spectra. The AFM images were obtained in probe amplitude mode. The inset in the AFM image shows the scanned height along the white transect of each particle. The red and black curves indicate the spectra of the particles and the substrate background, respectively.

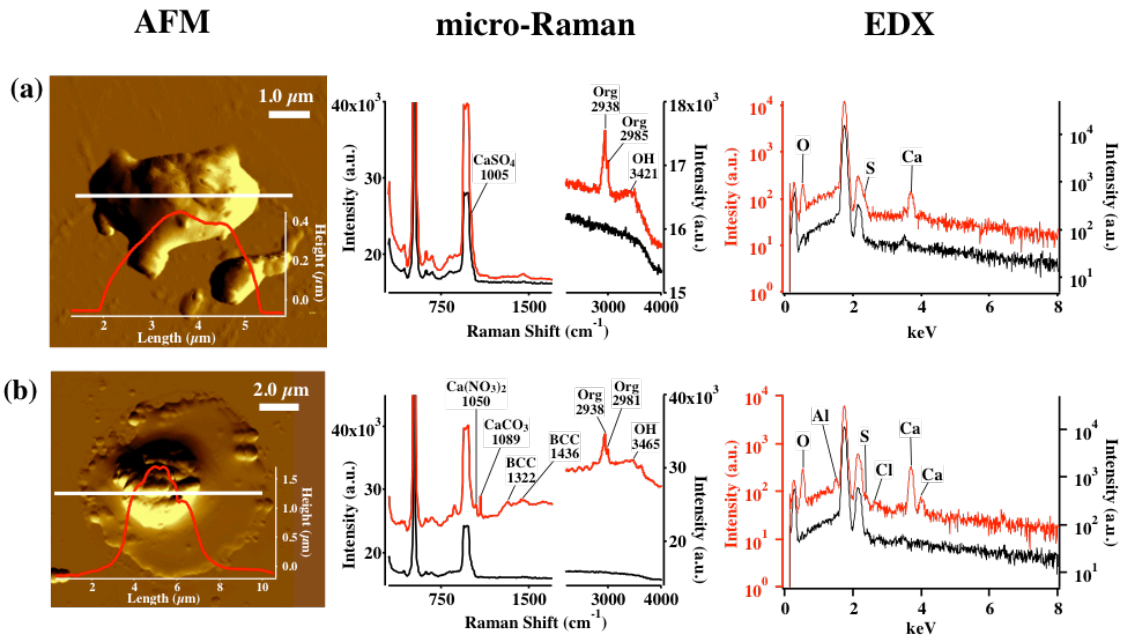

Figure 10: AFM topographic images of representative Ca-rich particles in IN active (a) and non-active (b) groups, and their corresponding Raman and EDX spectra. The AFM images were obtained in probe amplitude mode. The inset in the AFM image shows the scanned height along the white transect of each particle. The red and black curves indicate the spectra of the particle and the substrate background, respectively

Page 30, Fig. 5: what sulfates are meant here if not ammonium sulfate or calcium sulfate?

This sulfates in Fig. 5 means the detection frequency of either ammonium sulfate or calcium sulfate. We also changed Fig. 5 to for better clarity as the follows:

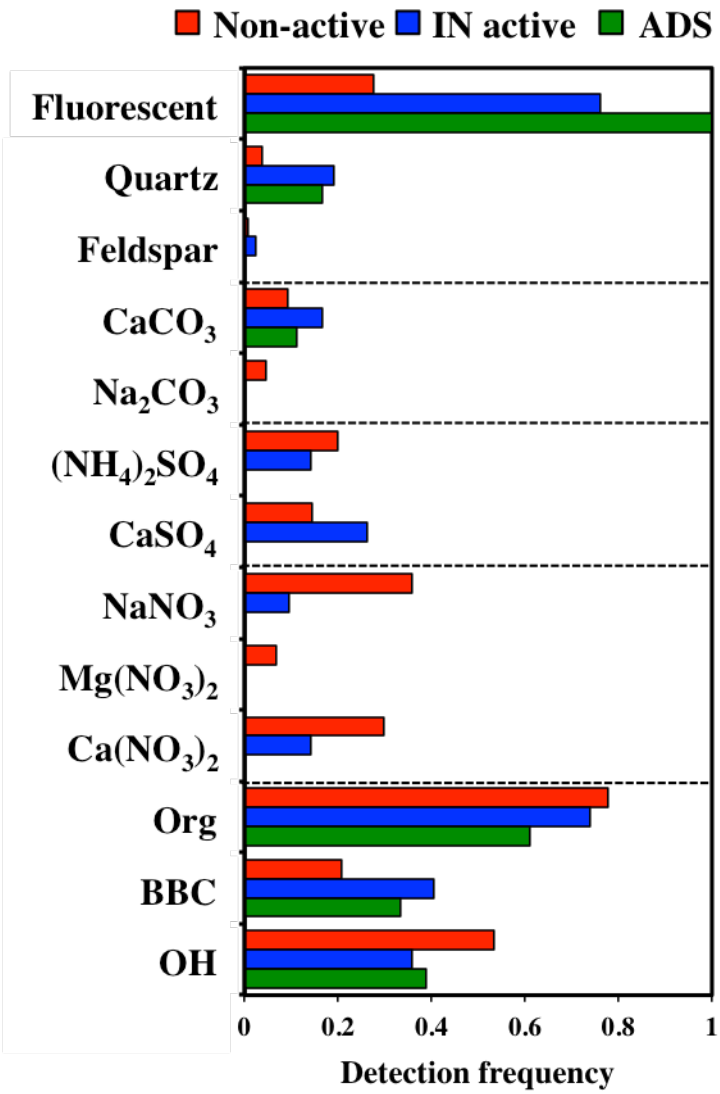

Figure 5: Summary of the detection frequencies of the assigned components in non-active and IN active particles by micro-Raman analysis. Data from Asian dust source (ADS) particles are shown for comparison.

Page 3, line 9: "residues" instead of "residue".

Corrected accordingly.

Page 8, line 31: Sobanska et al. (2012) is missing from the reference list.

Corrected accordingly.

Page 14, line 4: “nucleus” instead of “nuclei”

Corrected accordingly.

Page 26: figure caption: “supersaturation” instead of “super saturation”.

Corrected accordingly.

Page 27, Figure 2: the axis numbers are too small to be readable.

Corrected accordingly as follow.

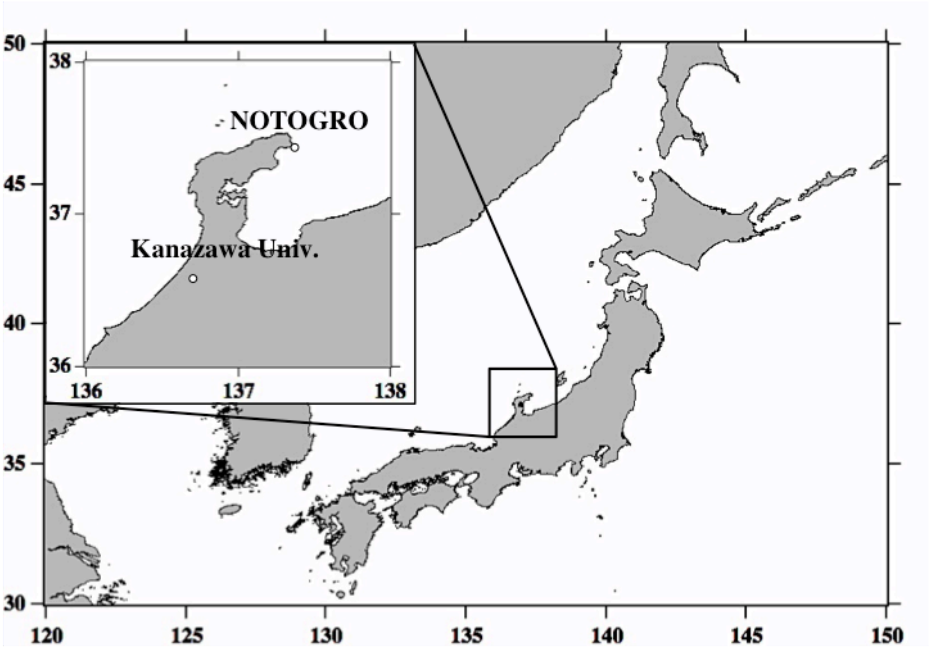

Page 28, Fig. 3 and page, 35, Fig. 10: The label “BCC” in the Raman spectra should read “BBC”.

Corrected accordingly.

References:

Ardon-Dryer, K., and Levin, Z.: Ground-based measurements of immersion freezing in the eastern Mediterranean, Atmos. Chem. Phys., 14, 5217–5231, doi:10.5194/acp-14-5217-2014, 2014.

Atkinson, J.D., Murray, B.J., Woodhouse, M.T., Whale, T.F., Baustian, K.J., Carslaw, K.S., Dobbie, S., O’Sullivan, D., and Malkin, T.L.: The importance of feldspar for ice nucleation by mineral dust in mixed-phase clouds, Nature, 498, 355-358, doi: 10.1038/nature12278, 2013.

Baustian, K.J., Cziczo, D.J., Wise, M.E., Pratt, K.A., Kulkarni, C., Hallar, A.G., and Tolbert, M.A.: Importance of aerosol composition, mixing state, and morphology for heterogeneous ice nucleation: A combined field and laboratory approach, J. Geophys. Res., 117, D06217, doi: 10.1029/2011JD016784, 2012.

Connolly, P.J., Möhler, O., Field, P.R., Saathoff, H., Burgess, R., Choularton, T., and Gallagher, M.: Studies of heterogeneous freezing by three different desert dust samples, Atmos. Chem. Phys., 9, 2805–2824, doi:10.5194/acp-9-2805-2009, 2009.

DeMott, P.J.: An exploratory study of ice nucleation by soot aerosols, J. Appl. Meteorol., 29, 1072–1079, doi: 10.1175/1520-0450(1990)029<1072:AESOIN>2.0.CO;2, 1990.

Gaft, M., Reisfeld, R., and Panczer, G.: Modern Luminescence Spectroscopy of Minerals and Materials; Springer-Verlag: Berlin, Heidelberg, doi: 10.1007/b137490, 2005.

Huffman, J. A., Sinha, B., Garland, R. M., Snee-Pollmann, A., Gunthe, S. S., Artaxo, P., Martin, S. T., Andreae, M. O., and Pöschl, U.: Size distributions and temporal variations of biological aerosol particles in the Amazon rainforest characterized by microscopy and real-time UV-APS fluorescence techniques during AMAZE-08, Atmos. Chem. Phys., 12, 11997–12019, doi:10.5194/acp-12-11997-2012, 2012.

Iwasaka, Y., Shi, G. Y., Yamada, M., Kobayashi, F., Kakikawa, M., Maki, T., Chen, B., Tobo, Y., and Hong, C.: Mixture of Kosa (Asian dust) and bioaerosols detected in the atmosphere over the Kosa particles source regions with balloon-borne measurements: possibility of long-range transport, Air. Qual. Atmos. Health., 2, 29–38, 2009.

Jung, H.J., Eom, H.J., Kang, H.W., Moreau, M., Sobanska, S., and Ro, C.U.: Combined use of quantitative ED-EPMA, Raman microspecrometry, and ATR-FTIR imaging techniques for the analysis of individual particles, Analyst, 139, 3949–3960, doi: 10.1039/c4an00380b, 2014.

Kireeva, E.D., Popovicheva, O.B., Persiantseva, N.M., Khokhlova, T.D., and Shonija, N.K.: Effect of black carbon particles on the efficiency of water droplet freezing, Colloid J., 71, 353–359, doi: 10.1134/S1061933X09030090, 2009.

Korolev, A.: Limitations of the Wegener-Bergeron-Findeisen Mechanism in the Evolution of Mixed-Phase Clouds, J. Atmos. Sci., 64, 3372–3375, doi:10.1175/JAS4035.1, 2007.

Laskina, O., Young, M.A., Kleiber, P.D., and Grassian, V.H.: Infrared extinction spectroscopy and micro-Raman spectroscopy of select components of mineral dust mixed with organic compounds, J. Geophys. Res. Atmos, 118, 6593–6606, doi:10.1002/jgrd.50494, 2013.

Maring, H., Savoie, D. L., Izaguirre, M. A., Custals, L., and Reid, J. S.: Mineral dust aerosol size distribution change during atmospheric transport, J. Geophys. Res., 108(D19), 8592, doi:10.1029/2002JD002536, 2003.

Morris, C.E., Georgakopoulos, D.G., Sands, D.C.: Ice nucleation active bacteria and their potential role in precipitation. J. Phys. IV. Fr., 121, 87-103, doi: 10.1051/jp4:2004121004, 2004.

Murray, B. J., Broadley, S. L., Wilson, T. W., Atkinson, J. D., and Wills, R. H.: Heterogeneous freezing of water droplets containing kaolinite particles, Atmos. Chem. Phys., 11, 4191–4207, doi:10.5194/acp-11-4191-2011, 2011.

Murray, B.J., Broadley, S.L., Wilson, T.W., Bull, S.J., Wills, R.H., Christenson, H.K., and Murrary, E.J.: Kinetics of the homogeneous freezing of water, Phys. Chem. Chem. Phys., 12, 10380–10387, doi: 10.1039/C003297B, 2010.

Niemand, M., Möhler, O., Vogel, B., Vogel, H., Hoose, C., Connolly, P., Klein, H., Bingemer, H., DeMott, P., Skrotzki, J., and Leisner, T.: A particle-surface-area-based parameterization of immersion freezing on desert dust particles, J. Atmos. Sci., 69, 3077–3092, doi:10.1175/Jas-D-11-0249.1, 2012.

Prenni, A. J., DeMott, P. J., Sullivan, A. P., Sullivan, R. C., Kreidenweis, S. M., and Rogers, D. C.: Biomass burning as a potential source for atmospheric ice nuclei: Western wildfires and prescribed burns, Geophys. Res. Lett., 39, L11805, doi:10.1029/2012GL051915, 2012.

Rosenfeld, D., and Woodley, W.L.: Deep convective clouds with sustained supercooled liquid water down to -37.5 ˚C, Nature, 405, 440–442, doi: 10.1038/35013030, 2000.

Sobanska, S., Falgayrac, G., Rimetz-Planchon, J., Perdrix, E., Brémard, C., and Barbillat, J.: Resolving the internal structure of individual atmospheric aerosol particle by the combination of Atomic Force Microscopy, ESEM–EDX, Raman and ToF–SIMS imaging, Microchem. J., 114: 89–98, doi: 10.1016/j.microc.2013.12.007, 2014.

Sullivan, R. C., Guazzotti, S. A., Sodeman, D. A., and Prather, K. A.: Direct observations of the atmospheric processing of Asian mineral dust, Atmos. Chem. Phys., 7, 1213–1236, 10 doi:10.5194/acp-7-1213-2007, 2007.

Tong, H.-J., Reid, J. P., Bones, D. L., Luo, B. P., and Krieger, U. K.: Measurements of the timescales for the mass transfer of water in glassy aerosol at low relative humidity and ambient temperature, Atmos. Chem. Phys., 11, 4739–4754, doi:10.5194/acp-11-4739- 2011, 2011.

Twohy, C. H., McMeeking, G. R., DeMott, P. J., McCluskey, C. S., Hill, T. C. J., Burrows, S. M., Kulkarni, G. R., Tanarhte, M., Kafle, D. N., and Toohey, D. W.: Abundance of fluorescent biological aerosol particles at temperatures conducive to the formation of mixed-phase and cirrus clouds, Atmos. Chem. Phys., 16, 8205–8225, https://doi.org/10.5194/acp-16-8205-2016, 2016.

Zhang, D., Iwasaka, Y., Shi, G., Zang, J., Matsuki, A., and Trochkine, D.: Mixture state and size of Asian dust particles collected at southwestern Japan in spring 2000. J. Geophys. Res., 108, 4760, doi: 10.1029/2003JD003869, 2003.

Anonymous Referee #2 RC3

The manuscript "Characterization of individual ice nuclei by the single droplet freezing method: a case study in the Asian dust outflow region" by Ayumi Iwata and Atsushi Matsuki describes an application of a droplet freezing apparatus to the characterization of the ice nucleating (IN) particles sampled during two Asian dust events. The authors report on the application of several microanalysis techniques (AFM, Micro-Raman, SEM, EDX) to reveal the chemical composition and morphology of the most IN active particle in a subset of a sample, identified by the droplet freezing technique. A combination of the single-particle microanalysis techniques with droplet freezing assay methods is a very promising development in the field of the ice nucleating particle research. An important advantage of the method described in the manuscript is the realization of a "single IN particle per water droplet" approach, which greatly reduces uncertainty associated with preparation of suspensions, characterization of particle size and surface distribution, and variability of particle properties across the droplet population, which are the common issues in a conventional cold stage experiment. However, before starting characterizing the most active ice nucleating particles with all the modern and expensive single particle techniques, one has to be completely sure that the particles identified as the most IN active are really such particles. To be honest, I am not convinced that this is the case. I would nevertheless support the publication of the manuscript provided that authors carefully address the multiple critical issues listed below. This might require a tedious re-evaluation of the results or even new experiments because some issues cannot be resolved without repeating the experiments.

We appreciate all the positive comments and valuable feedbacks the reviewer provided us. We carefully examined and addressed the issues raised by the reviewer, which also involved thorough re-evaluation of the results and new experiments to validate our experimental method. We believe that the additional information will help improve the technical soundness of our paper. Please find our response to each of the comments below (in blue italic).

1. I would like to draw the author's attention to the both papers of Schrod at al., AMT 2016, and ACP 2017, who essentially describes a similar but much better characterized setup (FRIDGE) to study the deposition freezing of ice on the atmospheric IN particles collected with an unmanned aircraft over eastern Mediterranean. This group has gone a long way improving their instrument and achieving reliable results, you can learn a lot from them. These papers have to be mentioned and discussed.

Thank you for reminding us of the works using FRIDGE. We have certainly learned a lot form FRIDGE. We added Ardon-Dryer and Levin, (2014), Schrod at al., (2016) and Schrod at al., (2017) as the references which also reported the measurements of the atmospheric ice nuclei using cold stage. Now they are discussed in the context of the limitations and the merits of IDFM, and cited in the result section as follows:

'The advantage of IDFM is that we can keep track and be sure which of the collected single particle was actually nucleating ice. Thus the IN active particles identified by IDFM can be studied in detail by various particle analysis techniques. Comparing IDFM with the other methods such as FRIDGE used primarily to measure ice nuclei concentration (Ardon-Dryer and Levin, 2014; Schrod at al., 2016; Schrod at al., 2017), we have to compromise the accuracy and quantitative

evaluation of IN activity since the evaporation of droplets around frozen particles by the Bergeron-Findeisen effect can affect the activated fraction. Therefore, by selecting the higher cooling rate and -30 °C as the end cooling temperature, we minimized the evaporation and the scavenging of the droplets around the rapidly growing ice crystals in the experiments of atmospheric particles. By this way, most of the atmospheric particle (excluding those very close to the ice crystals) were not dried and remained as droplets until temperature reached -30 °C. Note however, that the selected cooling rate is considerably faster when compared with the typical cooling rate found in the convective cloud updraft. Also, we cannot fully rule out the possibility that droplets very close to an ice crystal may had been fully evaporated.'

2. The method description is incomplete. Many important details are missing, preventing the objective evaluation of method applicability. The only reference supposedly describing the setup (Akizawa et al., 2016), refers to an application of a Linkam stage for mineralogical samples. I wonder how is that related to the IN study discussed in the manuscript. Peckhaus et al., ACP 2016, also used a Linkam stage for a cold stage experiments.

We added and changed the introduction and the method section as follows:

'Several laboratory studies used similar cold stage to test the ice nucleation activities of various atmospherically relevant standard particles (Fornea et al., 2009; Baustian et al., 2010; Mason et al., 2015; Whale et al., 2015; Knopf et al., 2014), but not enough studies have been made so far to investigate on the immersion-mode ice nucleation (mixed phase cloud) by the individual particles in the actual atmosphere.'

'The sample particles were deposited onto a Si wafer substrate with a hydrophobic coating (Glaco, Soft99 Corporation, Japan). Particles were observed for their position, size, and shape under an optical microscope with x50 magnification (Olympus, Japan) as shown in Fig. 1a. Subsequently, the substrate was transferred onto a cold stage in a closed cell (THMSG600, Linkam Scientific Instruments, UK). Since the cold stage used in this study is cooled by liquid nitrogen, the exposed tube through which the liquid nitrogen passes in the cold cell becomes a cold trap which can act as an additional sink for the water vapor. Therefore, in this study, all cooling parts except the cold stage surface were covered by insulating material. The temperature measured at the cold stage was calibrated by the substances of known melting points (Akizawa et al., 2016). Furthermore, we confirmed that the temperature gap between the substrate and the cold stage was consistently smaller than 0.3 °C by observing the melting of water. During the ice nucleation experiment by atmospheric particles, the stage temperature and the dew point were recorded every 1 seconds. The temperature measurement and the images were synchronized with the PC internal clock.'

3. The method described in the manuscript allows identifying the first particle within the field of view that initiated the freezing. This particle is then labeled the "ice nucleating" particle, and the others as "non-nucleating" particles. I wonder what happens with all other particles on the substrate? Do they initiate freezing too? Please explain this clearly in the manuscript.

It is a very important point. We do not have uniform distribution of particles on the substrate, because impinging jet of the impactor concentrates particles closer to the nozzle center, and there is a hotspot where we see too many particles that are close to each other. We discard these areas with too many (right in the center) or too sparse particles (far from center), so we do not keep track on what happened to all other particles on the substrate outside the field of view. We do see cases with multiple particles freezing in the same field of view by monitoring the collected particles in a relatively wide area (Fig.1) and it is not necessarily only one particle that we are labeling as "ice nucleating". We added this in the method section as follows:

'By comparing the optical images before and after the ice nucleation experiments, the individual particles that formed ice crystals (excluding those coalescing with adjacent droplets or crystals) were identified and regarded as IN active particles. Most of the particles collected on the substrates were monitored under an optical microscope with x5 magnification (Fig. 1a). We did see multiple particles freezing in the same field of view. However, we did not cover all of the collected particles. Therefore we must note that the Non-active particles or IN active particles outside of our field of view are not included in our counts.'

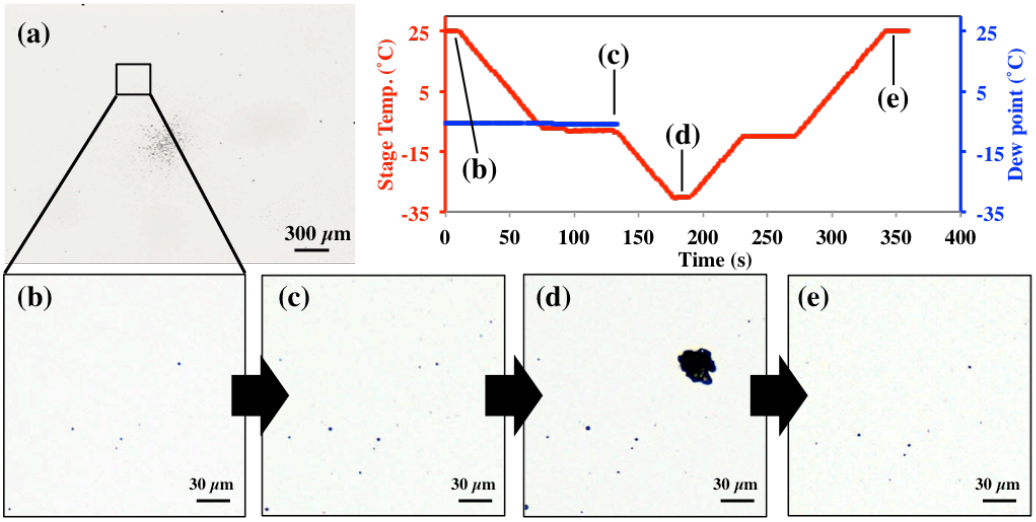

Figure 1: Optical images of sample particles deposited on Si wafer substrate before the freezing experiment (a, b), after exposure to water super saturation conditions at -9 ˚C (c), after cooling to -30 ˚C (d), and after sublimation and evaporation by dry air (e). The inset graph shows the stage temperature and the dew point of the wet air introduced into the cell before exposing the stage to water super saturation.

4. The setup description in the manuscript doesn't have it very clear, but if I understand correctly, the method has a very important limitation. In a closed cell with the humidified gas disconnected from the cell, the droplets are in equilibrium with the water vapor. The moment the first crystal appears, it grows very fast because the vapor is supersaturated with respect to the ice surface. Now that the system contains all three phases of water, droplets start evaporating and some of them would

evaporate completely without having a chance to freeze. To prevent complete evaporation, you use the very fast cooling rate (30 K/min), but this reduces the time remaining for the other droplets to freeze to less than 20 s (if the first droplet freeze at -30_C and the homogeneous freezing is over at -40 °C). Ice nucleation is a stochastic process described by a rate equation, so that the probability of freezing at given temperature is a function of time spent at this temperature. At such cooling rate, the freezing of "second-best" IN particles can be inhibited by this time-dependent issue and all the droplets will freeze homogeneously concealing the potential freezing activity of the IN particles. A chance of freezing is further reduced by droplets evaporation.

It is a very important point. It is true that part of the reason we selected the higher cooling rate is to prevent the evaporation of the droplets. Another reason is to restrict the final size of the growing ice crystals so that they do not coagulate with, or dry many of the surrounding droplets. By selecting the higher cooling rate and -30 °C as the end cooling temperature, we minimized the evaporation and the scavenging of the droplets around the rapidly growing ice crystals in the experiments of atmospheric particles. By this way, most of the atmospheric particle (excluding those very close to the ice crystals) were not dried and remained as droplets until temperature reached -30 °C. However, as the reviewer points out, we cannot fully rule out the possibility that droplets very close to an ice crystal may be fully evaporated. Therefore, it is possible that a moderately IN active particle may be miss-interpreted as non-active particles. We admit that the current method still has limitations and space for future improvements with respect to the quantification and accuracy of the IN counting. The fast cooling rate may also cause "second-best" IN to be overlooked in the current method. These limitations are now clearly explained in the section 3.1 (also as a response to the first comment). However, our primary objective here is to identify the properties of the individual ice nucleating particle in the actual atmosphere, by realizing a clear-cut identification of IN active particles. Therefore, we believe being able to identify even the most active fraction (with potential miss counting of the "second best" IN) from the actual atmosphere is still an important step forward towards our understanding of the IN behaviors of atmospheric aerosols, which are often found in complex mixtures (both internally and externally).

5. In this way, only one ice nucleating particle can be identified per sample. The other, just very slightly less active ice nucleating particles would have no chance to initiate freezing and would be labeled as non-nucleating. This would result in a wrong statistics of the IN vs the non-IN particles, and as a consequence in a biased composition of non- IN active particles. If I am wrong, please show your results in form of "the number of frozen droplets as a function of the substrate temperature". Such curves can be used to retrieve the so-called ice nucleating active site (INAS) densities, that can be better compared with the measurements of other groups.

We have to admit that our technique is not a perfect method that can resolve all technical issues encountered in the ice nucleation experiments. The biggest advantage of course is that we can keep track and be sure which single particle was actually nucleating ice. In return, we cannot fully rule out the possibility that the "second-best" IN particles may had been overlooked due to the evaporation of droplets in the vicinity of the frozen particles. Therefore, accuracy and the quantitative evaluation of freezing temperatures based on the activated fraction and the INAS could be biased to some extent. The

number of ice crystals formed are compromised especially at lower temperatures as the number and size of ice crystals increase and more droplets in the vicinity of the growing ice are subjected to evaporation.

In this study, only a small number of particles collected in the atmosphere formed ice crystals in a limited temperature range between -26 ℃ and - 30 ℃. so it is difficult to present the "the number of frozen droplets as a function of the substrate temperature". Instead, we show INAS and activated fraction of standard samples, and the validity of this experimental method is discussed by comparing these result with previous studies.

When comparing our results with those found in literature, we must also note that strict comparison is difficult because of the uncertainties and differences related to the size distribution and composition of dust particles used in different experiments. Assumptions made to calculate the surface area can also be a source of bias. The K-feldspar used in this study as a reference mineral dust was purchased from the same supplier, but the lot number is different (from different source rock) from the K-feldspar used in Atkinson et al (2013). Therefore, composition of K-feldspar used in the current study and that used in Atkinson et al. (2013) are not exactly the same. Nevertheless, we added the ice nucleation active sites (INAS) of the 4 standard mineral particles measured by the current IDFM (Fig. S-2).

The ice nucleation active sites (INAS) obtained in this study agreed within an order of magnitude difference compared to those found in the literature(despite many different experimental conditions). Further, we would like to emphasize that the relative order of the onset temperatures found for different particles is always consistent (i.e. K-feldspar > Na-feldspar > quartz > kaolinite >> pure water) and even the range of the freezing temperatures are not far off from the reported values.

It was probably not clearly stated in the manuscript, so the following change was made with regard to the onset temperatures:

'Heterogeneous ice nucleation observed in all standard mineral samples tested in this study (K-feldspar, Na-feldspar, quartz, kaolinite) consistently occurred at higher temperatures than the homogeneous freezing temperature. The reference mineral samples were milled to fine grains before being collected on Si wafer substrate by an impactor. Three set of samples were made for each reference mineral to ensure large enough observation area for the IDFM. *The total number of the particles monitored during the ice nucleation experiment by IDFM was 4,509, 2,271, 4,759, and 1,435 particles, respectively. In this study, the freezing onset temperature of the sample was defined as the temperature at which the IN active fraction of the total observed particles reached 0.01. As a result, the freezing onset temperatures for K-feldspar, Na-feldspar, quartz, and kaolinite ranged between -22.2 to -24.2 °C, -24.7 to -25.7°C, -24.8 to -26.8 °C and -27.2 to -29.2 °C, respectively (Fig. S-1). Therefore, the ice nucleation activity of K-feldspar was the highest and that of kaolinite was the lowest. The order and the range of observed onset temperatures for these minerals were consistent with the results found in the literature (Atkinson et al., 2013; Murray et al., 2011).'*

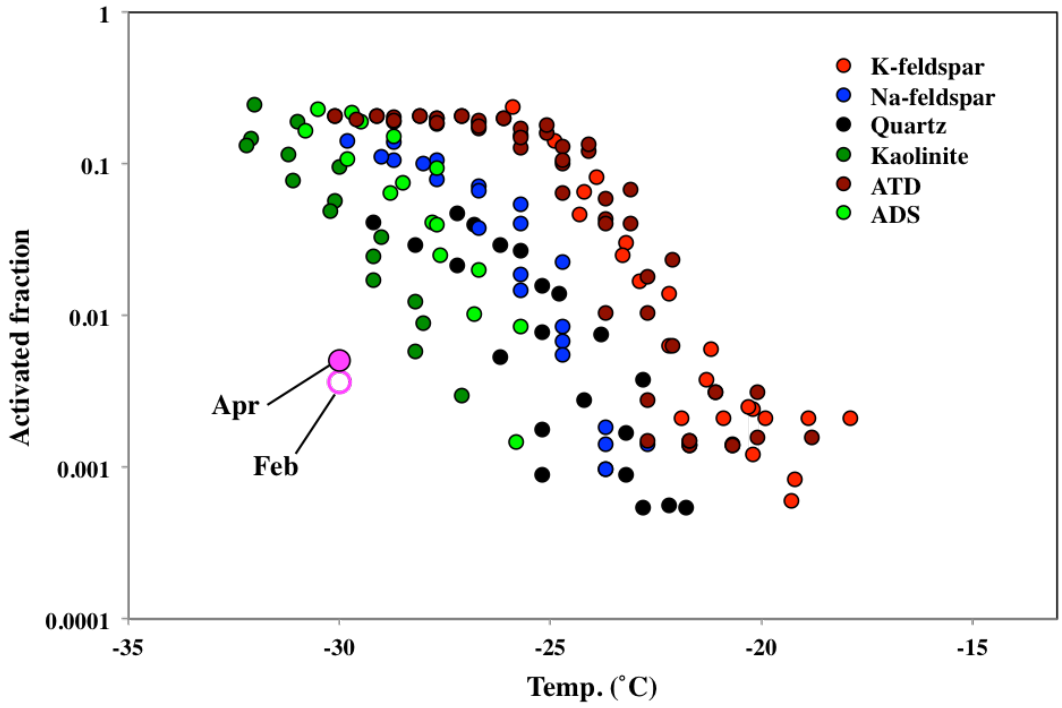

Figure S-1: Activated fractions of the reference mineral dust particles. Results of the atmospheric samples collected in February and April are also shown for comparison.

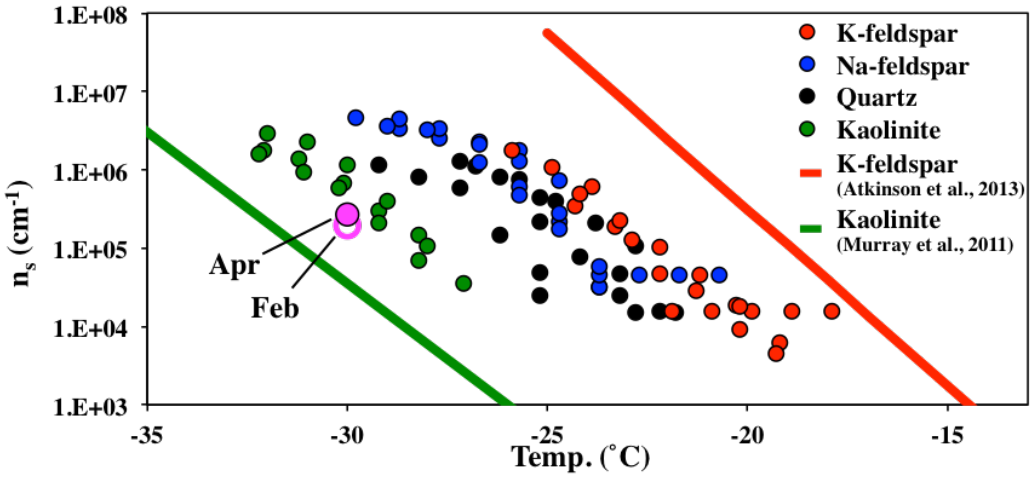

5

Figure S-2: the ice nucleation active site (INAS) densities for the reference single component mineral dust samples. These INAS densities were calculated from the activated fractions (Fig. S-1) and the averaged sphere equivalent surface areas obtained from the 2D silhouette of each particles in the microscopic image.

6. The critical issue discussed in the above comments can be also a consequence of the Linkam stage design. The standard cell of a Linkam stage has the metal coolant tubing exposed to the environment, making this tubing the coldest spot inside the cell. Water condensed on the tubing during the condensation step must freeze first during the cooling. As explained above, such ice surface would immediately become a strong sink for the water vapor. If the cooling rate is too slow, the liquid droplets condensed on the residual particles would evaporate before having a chance to freeze. I suspect that this is the reason for using a cooling rate of 30 K/min. If this is the case, it is a serious drawback of the system and has to be clearly stated in the manuscript. For the future work, I would recommend enclosing the substrate with the collected particles into a separate cell, so that just this area of the substrate is exposed to the supersaturated vapor.

We are aware of this issue of the Linkam stage design. Before the experiment, we made a slight modification in the Linkam stage such that the metal coolant tube is covered by the insulating material and made sure that the condensation on this tube does not act as a strong sink for the water vapor. This is better explained in the revised manuscript as follows:

'Since the cold stage used in this study is cooled by liquid nitrogen, the tube through which the liquid nitrogen passes in the cold cell becomes a cold trap which can act as an additional sink for the water vapor. Therefore, in this study, all cooling parts except the cold stage surface were covered by insulating material.'

7. At the cooling rate this high, a strong temperature gradient across the substrate can arise. The freezing temperature can be biased towards low values. Was temperature measured on the surface of a substrate or taken from the Linkam stage internal measurement? How was the temperature of the freezing onset determined? Have you been recording the microscope images? If yes, what was the image acquisition rate? Was it synchronized with temperature measurements? Since this is the first time you report the measurements with the new setup, you should convince the reader that the setup is well characterized.

The temperature measured on the surface of a substrate and the Linkam stage internal measurement is calibrated based on the melting experiment of some materials as described in Akizawa et al., 2016. The temperature difference between the substrate surface and the stage, as well as the temperature gradient was determined to be less than 0.3 °C based on the observation of melting of pure ice.

The microscopic images were recorded with the maximum rate of (5 fps). During the ice nucleation experiment by atmospheric particles, the stage temperature and the dew point were recorded every 1 seconds. The temperature measurement and the images were synchronized with the PC internal clock. This is better explained in the revised manuscript as follows

'The sample particles were deposited onto a Si wafer substrate with a hydrophobic coating (Glaco, Soft99 Corporation, Japan). Particles were observed for their position, size, and shape under an optical microscope with x50 magnification

(Olympus, Japan) as shown in Fig. 1a. Subsequently, the substrate was transferred onto a cold stage in a closed cell (THMSG600, Linkam Scientific Instruments, UK). Since the cold stage used in this study is cooled by liquid nitrogen, the exposed tube through which the liquid nitrogen passes in the cold cell becomes a cold trap which can act as an additional sink for the water vapor. Therefore, in this study, all cooling parts except the cold stage surface were covered by insulating material. The temperature measured at the cold stage was calibrated by the substances of known melting points (Akizawa et al., 2016). Furthermore, we confirmed that the temperature gap between the substrate and the cold stage was consistently smaller than 0.3 °C by observing the melting of pure ice. During the ice nucleation experiment by atmospheric particles, the stage temperature and the dew point were recorded every 1 seconds. The temperature measurement and the images were synchronized with the PC internal clock.'

8. What is the relationship between the field of view of the microscope and the sampling area containing droplets condensed on the aerosol particles? What if the first ice crystals are located outside of the view area? In this case, the initial ice crystals would not be detected but the local vapor pressure would be reduced due to the vapor deposition on the growing crystals, leading to evaporation of droplets and inhibition of freezing. Please give a detailed assessment of this effect. Given the uncertainty of the method of identifying the most active IN particles, I don't see the point of discussing the single particle microanalysis. If possible, give the maximum detail of the cold stage operation and detection techniques. If the measurements data permit, present your data not just in form of on-set freezing temperature, but in form of temperature dependent freezing curves. Otherwise, the measurements have to be repeated with a lower or variable cooling rate, and the results analyzed as discussed above.

Monitoring of ice crystal formation by the optical microscope covers most of the sampled atmospheric particles (please refer to our response corresponding to the 3rd comment) By selecting the higher cooling rate, we minimized the evaporation and the scavenging of the droplets around the rapidly growing ice crystals. Then, most of atmospheric particle (excluding the very close droplets of ice crystals) were not completely dried the formed droplets until temperature reached -30 °C in this study. Therefore we believe that suppression of ice crystal formation by local vapor pressure reduction has been minimized at least down to -30 °C. However, as shown in temperature dependent freezing curve for the standard dust samples in Fig. S-1, the quantification of the activated fraction especially at lower temperatures is compromised as a result of the drying of droplets by growing crystals. In return, this method enables direct identification of individual particles with high IN activity within the ambient samples.

We also added the following explanations of the both limitation for detection of particle and quantitative for ice nucleation in IDFM in the section 3.1 as follows:

'The advantage of IDFM is that we can keep track and be sure which of the collected single particle was actually nucleating ice. Thus the IN active particles identified by IDFM can be studied in detail by various particle analysis techniques. Comparing IDFM with the other methods such as FRIDGE used primarily to measure ice nuclei concentration (Ardon-Dryer and Levin, 2014; Schrod at al., 2016; Schrod at al., 2017), we have to compromise the accuracy and quantitative

evaluation of IN activity since the evaporation of droplets around frozen particles by the Bergeron-Findeisen effect can affect the activated fraction. Therefore, by selecting the higher cooling rate and -30 °C as the end cooling temperature, we minimized the evaporation and the scavenging of the droplets around the rapidly growing ice crystals in the experiments of atmospheric particles. By this way, most of the atmospheric particle (excluding those very close to the ice crystals) were not dried and remained as droplets until temperature reached -30 °C. Note however, that the selected cooling rate is considerably faster when compared with the typical cooling rate found in the convective cloud updraft. Also, we cannot fully rule out the possibility that droplets very close to an ice crystal may had been fully evaporated.'

With respect to the particle size detection/limit, the impactor already size segregates particles and limit the test particles in the super-micron range. The diameter of the collected atmospheric particles whose ice crystal formation could be monitored ranged between 1.16 and 5.47 µm through the identification by the optical microscope. Meanwhile, the laser spot size (i.e. spatial resolution) of micro Raman spectroscopy approaches the diffraction limit of approximately 1 µm in diameter. All in all, the size of IN active particles that can be analyzed by this method is limited to super micron particles.'

References

Akizawa, N., Tamaru, A., Fukushi, K., Yamamoto, J., Mizukami, T., Python, M., and Arai, S.: High-temperature hydrothermal activities around suboceanic Moho: An example from diopsidite and anorthosite in Wadi Fizh, Oman ophiolite, Lithos, 263, 66-87, 2016.

Ardon-Dryer, K., and Levin, Z.: Ground-based measurements of immersion freezing in the eastern Mediterranean, Atmos. Chem. Phys., 14, 5217–5231, doi:10.5194/acp-14-5217-2014, 2014.

Atkinson, J.D., Murray, B.J., Woodhouse, M.T., Whale, T.F., Baustian, K.J., Carslaw, K.S., Dobbie, S., O'Sullivan, D., and Malkin, T.L.: The importance of feldspar for ice nucleation by mineral dust in mixed-phase clouds, Nature, 498, 355-358, doi: 10.1038/nature12278, 2013.

Baustian, K.J., Wise, M.E., and Tolbert, M.A.: Depositional ice nucleation on solid ammonium sulfate and glutaric acid particles, Atmos. Chem. Phys., 10, 2307–2317, 2010.

Fornea, A.P., Brooks, S.D., Dooley, J.B., and Saha, A.: Heterogeneous freezing of ice on atmospheric aerosols containing ash, soot, and soil, J. Geophys. Res., 114, D13201, doi:10.1029/2009JD011958, 2009.

Knopf, D. A., Alpert, P. A., Wang, B., O'Brien, R. E., Kelly, S. T., Laskin, A., Gilles, M. K., and Moffet, R. C.: Microspectroscopic imaging and characterization of individually identified ice nucleating particles from a case field study, J. Geophys. Res. Atmos., 119, JD021866, doi:10.1002/2014JD021866 , 2014.

Mason, R.H., Chou, C., McCluskey, C.S., Levin, E.J.T., Schiller, C.L., Hill, T.C.J., Huffman, J.A., DeMott, P.J., and Bertram, A.K.: The micro-orifice uniform deposit impactor–droplet freezing technique (MOUDI-DFT) for measuring concentrations of ice nucleating particles as a function of size: improvements and initial validation, Atmos. Meas. Tech., 8, 2449–2462, doi: 10.5194/amt-8-2449-2015, 2015.

Murray, B. J., Broadley, S. L., Wilson, T. W., Atkinson, J. D., and Wills, R. H.: Heterogeneous freezing of water droplets containing kaolinite particles, Atmos. Chem. Phys., 11, 4191–4207, doi:10.5194/acp-11-4191-2011, 2011.

Schrod, J., Danielczok, A., Weber, D., Ebert, M., Thomson, E. S., and Bingemer, H. G.: Re-evaluating the Frankfurt isothermal static diffusion chamber for ice nucleation, Atmos. Meas. Tech., 9, 1313–1324, doi:10.5194/amt-9-1313-2016, 2016.

Schrod, J., Weber, D., Drücke, J., Keleshis, C., Pikridas, M., Ebert, M., Cvetkovic, B., Nickovic, S., Marinou, E., Baars, H., Ansmann, A., Vrekoussis, M., Mihalopoulos, N., Sciare, J., Curtius, J., and Bingemer, H. G.: Ice nucleating particles over the Eastern Mediterranean measured by unmanned aircraft systems, Atmos. Chem. Phys., 17, 4817–4835, https://doi.org/10.5194/acp- 17-4817-2017, 2017.

Whale, T.F., Murray, B.J., O'Sullivan, D., Wilson, T.W., Umo, N.S., Baustian, K.J., Atkinson, J.D., Workneh, D.A., and Morris, G.J.: A technique for quantifying heterogeneous ice nucleation in microlitre supercooled water droplets, Atmos. Meas. Tech., 8, 2437–2447, doi: 10.5194/amt-8-2437-2015, 2015.

Anonymous Referee #3 RC1

The authors attempted to characterize the physico-chemical properties of atmospherically relevant ice-nucleating particles with the new off-line approach (i.e., a combination of several off-the-shelf techniques), which could potentially complement the in situ approach of ice residual studies. The topic itself is an important addition to ACP and the atmospheric science community. However, the experimental and analytical methods are unfortunately poorly explained and partly erroneous. Further, the manuscript contains a number of ambiguous statements and over-interpreted results without proper quantitative analyses as well as conclusive performance verifications. I have numerous suggestions for critical revisions. Additional tests of IDFM are necessary, and I do believe that the revision of the manuscript could be time consuming and result in a significantly different paper.

First of all, we would like to express our gratitude to the reviewer for carefully going through our manuscript and providing highly relevant remarks and suggestions for improvements. We took the comments very seriously, and hence made substantial efforts to conduct additional tests on our method (IDFM). We believe that the major concerns raised in the comments are now addressed. Please find our response to each of the comments below (in blue italic).

The title is misleading. "Characterization of individual ice nuclei: : :" should read ": : :ice residual: : :" unless the authors could provide the evidence of particular individual particles repeatedly form ice over several cooling-thawing cycles. The properties of the particle may alter during/after ice activation, and the particle should be considered as a residual after thawing.

In a strict sense it is true that it is an ice residual particle that we characterized. We changed the title as suggested and now we use the term "ice residual particle". Now the title appears as:

'Characterization of individual ice residual particles by the single droplet freezing method: a case study in the Asian dust outflow region'

In the introduction section, the authors need to logically address why it is particularly important to study the aerosol mixing state to improve our understanding of atmospheric ice nucleation in mixed-phase clouds. What is special about the mixing state on ice nucleation as compared to other general properties, such as size and bulk composition?

The authors may want to do a careful and rigorous literature review, digest the contents in a diplomatic manner and describe your thoughts to the reader along with your own story line.

The extremely small fraction of IN particles in the total atmospheric particles precludes us from using bulk aerosol sample for characterizing the IN property. In addition to the various external mixing states expected in the ambient aerosols, we believe that the internal mixing commonly found in the atmosphere is equally important. Therefore, the detailed information on the individual particles is indispensable for better understanding the ice crystals formation in the real atmosphere. This is now explained more clearly in the introduction (Page 3,Lline 20) of the manuscript.

'Internal mixing of aerosols commonly takes place during long-range transport in the atmosphere (e. g. Zhang et al., 2003, Sullivan et al., 2007, and Iwasaka et al., 2009). The surface properties of the internally mixed particles following atmospheric processing (reaction, coagulation and aging) can dramatically change from their original properties (Maring et al., 2003; Trochkine et al., 2003). The internal mixing of particles is an important factor that contributes to the complexity of atmospheric aerosol particles. Although efforts have been made to address the effects of internal mixing on the IN activity of aerosols under conditions relevant for the mixed phase cloud formation (Sullivan et al., 2010; Kulkarni et al., 2014; Augustin-Bauditz et al., 2016), the complexity of the ambient aerosol has not yet been fully represented by the laboratory generated aerosols. Therefore, detailed investigation based on the individual particle analysis is necessary to relate the internal mixing state of aerosols in the actual atmosphere and their IN activity.'

Why did the authors arbitrarily pick -30 dC as the end cooling T (no explanation given)?

Why didn't the authors carry out the T-binned analyses (e.g., up to -20 dC cooling vs. up to -30 dC cooling)? Such capability (seemingly feasible) and approach can resolve the issue, which the authors point out in the manuscript (e.g., P15L15-23).

We observed that the atmospheric particles started to form ice crystals only below -25 °C. The reason why we did not go below -30 °C is that it was difficult to keep track on the Non-IN and IN particles due primarily to the fact that initially formed ice crystals were growing too big and the impact on the surrounding particles became too obvious (scavenging and evaporation of droplets around the rapidly growing ice crystals). Also, if we start dividing the already few number of total IN particles into different temperature bins, it further degrades the counting statistics and makes the comparison of particle types more difficult. Therefore, we had to give up discussing on the problems that require the statistical comparisons by the T - bin analysis in the narrow temperature range (e.g. "P15L15-23" which need to clarify the detailed freezing temperature difference among various organics in atmospheric particles).

Because differences in particle composition may be correlated with particle size, it is difficult to determine which characteristic fundamentally drives cloud-nucleating ability. Why didn't the authors conduct the size dependent analysis (i.e., coarse vs. fine) to examine if the size can be a nucleation-triggering factor? It is not appropriate to generalize the results based on all-size population.

We agree on the importance of size dependent analysis. However, the number of IN in the atmosphere is generally extremely small, and as a result the total number of particles we could identify as ice residues became rather limited. If we further group and divide the already few ice residues into different size groups, it becomes even more difficult to compare the ice-nucleating ability among the particles with diverse mixing states and chemical compositions. All of the particles analyzed in this study are already larger than 1.1µm due to technical limitations, and the largest size was 5.47 µm, thus our result is representative only for this rather narrow range of the coarse particles, and it is now explained more clearly in section 3.1 as follows:

'With respect to the particle size detection/limit, the impactor already size segregates particles and limit the test particles in

the super-micron range. The diameter of the collected atmospheric particles whose ice crystal formation could be monitored ranged between 1.16 and 5.47 µm through the identification by the optical microscope. Meanwhile, the laser spot size (i.e. spatial resolution) of micro Raman spectroscopy approaches the diffraction limit of approximately 1 µm in diameter. All in all, the size of IN active particles that can be analyzed by this method is limited to super micron particles.'

The cooling rate of 0.5 K/s seems aggressive and not atmospherically relevant (i.e., 1 K/m may simulate a typical convective cloud updraft). Why not 1 K/min just like other numerous cold stage techniques do?

It is a very important point. We admit that our cooling rate is considerably faster when compared with the typical cooling rate in the convective cloud updraft. Part of the reason we selected the higher cooling rate is to minimize the chance of scavenging and drying nearby droplets because if we select a slower cooling rate, the resulting ice crystal size became too large. To avoid this from happening and facilitate precise isolation of the ice-nucleating particles, we had to choose the faster rate. However, we did confirm that pure water droplets do not freeze until the stage reaches down to -36.5 degrees even at this cooling rate, which coincides rather well with the results by several previous laboratory experiments (Pruppacher and Klett, 1997;Koop et al., 2000; Murray et al., 2010; Murray et al., 2012) and the observations of deep convective clouds (Rosenfeld and Woodley, 2000). The reason for selecting this cooling rate is now explained in section 3.1 as follows:

'The advantage of IDFM is that we can keep track and be sure which of the collected single particle was actually nucleating ice. Thus the IN active particles identified by IDFM can be studied in detail by various particle analysis techniques. Comparing IDFM with the other methods such as FRIDGE used primarily to measure ice nuclei concentration (Ardon-Dryer and Levin, 2014; Schrod at al., 2016; Schrod at al., 2017), we have to compromise the accuracy and quantitative evaluation of IN activity since the evaporation of droplets around frozen particles by the Bergeron-Findeisen effect can affect the activated fraction. Therefore, by selecting the higher cooling rate and -30 °C as the end cooling temperature, we minimized the evaporation and the scavenging of the droplets around the rapidly growing ice crystals in the experiments of atmospheric particles. By this way, most of the atmospheric particle (excluding those very close to the ice crystals) were not dried and remained as droplets until temperature reached -30 °C. Note however, that the selected cooling rate is considerably faster when compared with the typical cooling rate found in the convective cloud updraft. Also, we cannot fully rule out the possibility that droplets very close to an ice crystal may had been fully evaporated.'

Show the profiles of dew point and T throughout the experiment rather than show snapshot pictures (i.e., Fig. 1).

We added the corresponding temperature profile and the time when the images were taken as follows. As described in the manuscript, moist air supply is stopped and the cooling stage is isolated during the cooling process, so the dew point is expected to vary and closely follow the stage temperature while the saturated vapor continued to condense onto the activated droplets.

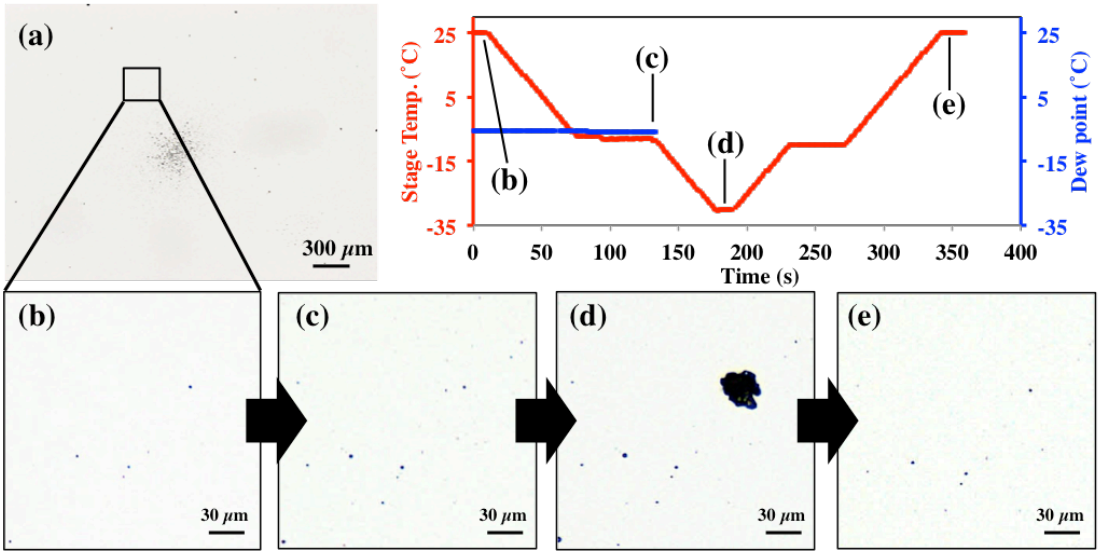

Figure 1: Optical images of sample particles deposited on Si wafer substrate before the freezing experiment (a, b), after exposure to water super saturation conditions at -9 °C (c), after cooling to -30 °C (d), and after sublimation and evaporation by dry air (e). The inset graph shows the stage temperature and the dew point of the wet air introduced into the cell before exposing the stage to water super saturation.

Quantitatively evaluate the capability of immersion/condensation freezing method relative to other cold stages using the ice nucleation parameters, such as frozen fraction or ice nucleation active surface site density. The onset discussion (P711-18) seems qualitative, speculative and over-simplified.

We have to admit that our technique is not a perfect method that can resolve all technical issues encountered in the ice nucleation experiments. The biggest advantage of course is that we can keep track and be sure which single particle was actually nucleating ice. In return, we have to sacrifice the accuracy and quantitative evaluation of freezing temperatures based on INAS in relation to the evaporation of droplets in the vicinity of the frozen particles (Bergeron-Findeisen effect), as well as due to the limited number and size (d>1.1μm) of the particles that can be analyzed.

The number of ice crystals formed are compromised especially at lower temperatures as the number and size of ice crystals increase and more droplets in the vicinity of the growing ice are subjected to evaporation. When comparing our results with those found in literature, we must also note that strict comparison is difficult because of the uncertainties and differences related to the size distribution and composition of dust particles used in different experiments. Assumptions made to calculate the surface area can also be a source of bias. The K-feldspar used in this study as a reference mineral dust was purchased from the same supplier, but the lot number is different (from different source rock) from the K-feldspar used in Atkinson et al (2013). Therefore, composition of K-feldspar used in the current study and that used in Atkinson et al. (2013)

are not exactly the same. Nevertheless, we added the ice nucleation active sites (INAS) of the 4 standard mineral particles measured by the current IDFM (Fig. S-2).

The ice nucleation active sites (INAS) obtained in this study agreed within an order of magnitude difference compared to those found in the literature (despite many different experimental conditions). Further, we would like to emphasize that the relative order of the onset temperatures found for different particles is always consistent (i.e. K-feldspar > Na-feldspar > quartz > kaolinite >> pure water) and even the range of the freezing temperatures are not far off from the reported values. It was probably not clearly stated in the manuscript, so the following change was made with regard to the onset temperatures:

'Heterogeneous ice nucleation observed in all standard mineral samples tested in this study (K-feldspar, Na-feldspar, quartz, kaolinite) consistently occurred at higher temperatures than the homogeneous freezing temperature. The reference mineral samples were milled to fine grains before being collected on Si wafer substrate by an impactor. Three set of samples were made for each reference mineral to ensure large enough observation area for the IDFM. *The total number of the particles monitored during the ice nucleation experiment by IDFM was 4,509, 2,271, 4,759, and 1,435 particles, respectively. In this study, the freezing onset temperature of the sample was defined as the temperature at which the IN active fraction of the total observed particles reached 0.01. As a result, the freezing onset temperatures for K-feldspar, Na-feldspar, quartz, and kaolinite ranged between -22.2 to -24.2 ˚C, -24.7 to -25.7˚C, -24.8 to -26.8 ˚C and -27.2 to -29.2 ˚C, respectively (Fig. S-1). Therefore, the ice nucleation activity of K-feldspar was the highest and that of kaolinite was the lowest. The order and the range of observed onset temperatures for these minerals were consistent with the results found in the literature (Atkinson et al., 2013; Murray et al., 2011).'*

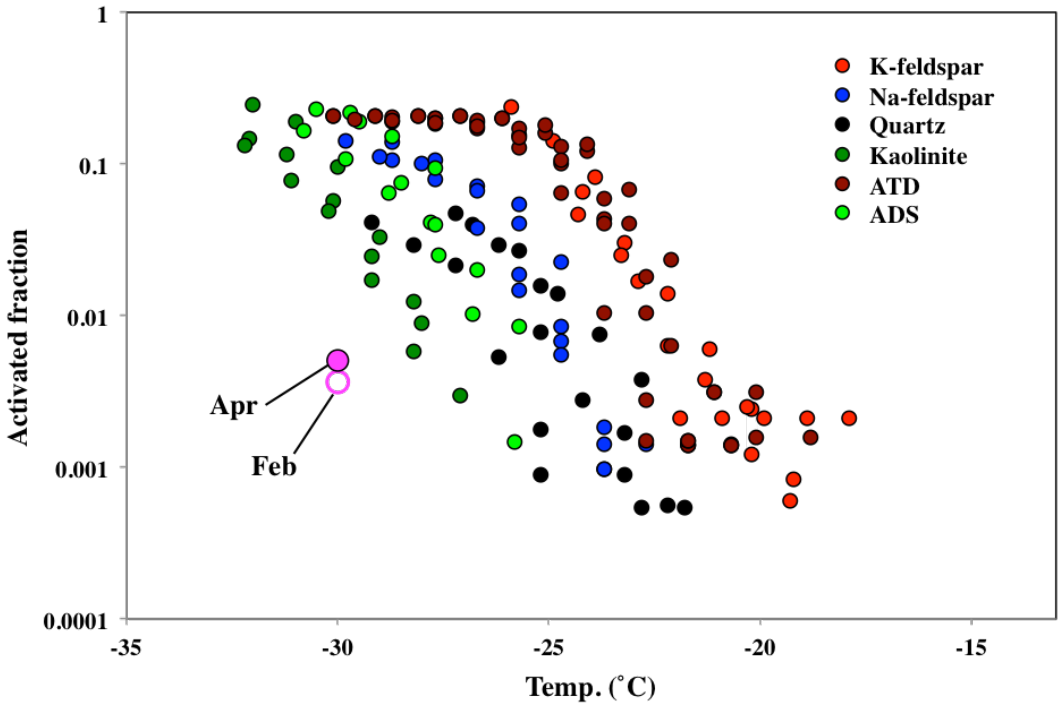

Figure S-1: Activated fractions of the reference mineral dust particles. Results of the atmospheric samples collected in February and April are also shown for comparison.

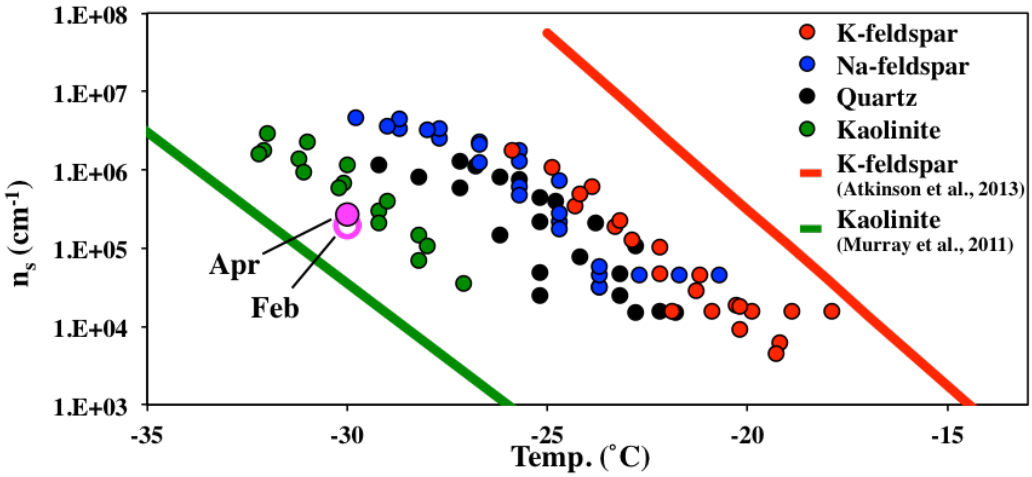

5

Figure S-2: the ice nucleation active site (INAS) densities for the reference single component mineral dust samples. These INAS densities were calculated from the activated fractions (Fig. S-1) and the averaged sphere equivalent surface areas obtained from the 2D silhouette of each particles in the microscopic image.

Description of the background contribution (contamination/impurity) should be included. The authors can assess it by putting soluble salts (e.g., NaCl) on the silicon wafer and cooling the cold stage down to the homogeneous freezing T.

We are aware of the importance of the background contribution (contamination/impurity). As suggested, we conducted additional measurements on the atomized NaCl particles and the activated fractions as a function of temperature are shown in Fig. S-4. At least, the ice nucleation was not observed above -34 °C for both NaCl particles and pure water. Therefore, we believe that there is no significant impact from contamination/impurity both during the water vapor condensation and the cooling processes affecting the ice nucleation down to -30 °C.

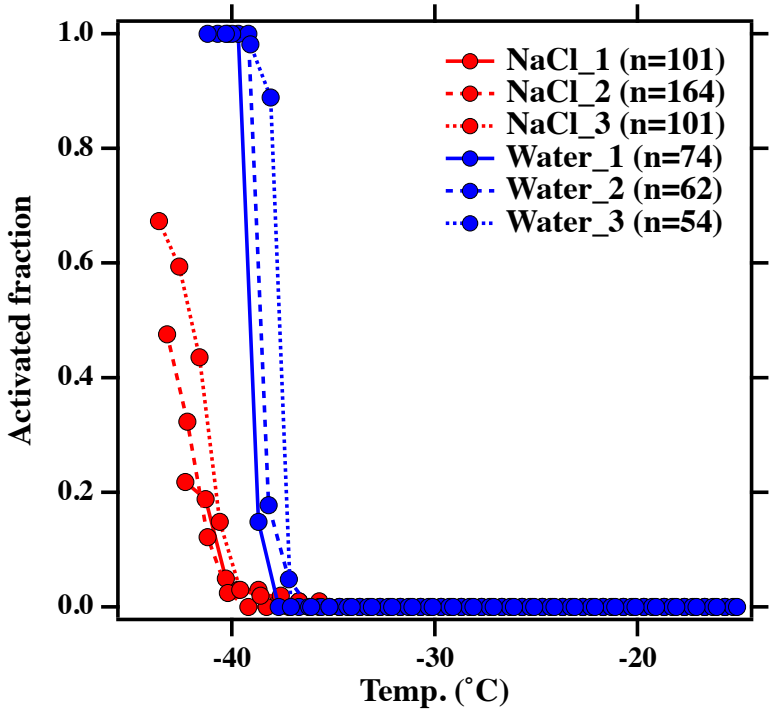

Figure S-4: Activated fractions of NaCl and pure water droplets. Three set of samples were tested for both NaCl and water. The number of particles and droplets observed under the microscope is shown as n.

The test NaCl particles were aerosolized by atomizing their solutions (0.005g/ml) and collected on the substrate with an impactor. the pure water droplets were also collected by spraying directly onto the substrate..

Why the homogeneous freezing occurs over 3.5 K (P7L6-8)? It should be abruptly spontaneous in a narrow range of T, if the water saturation condition is well-controlled.

The size of droplets might not be a substantial factor for the observed deviation. Technical validations seem necessary.

We believe there was an obvious lack of explanation. In the same freezing run, all droplets freeze in a much narrower range and almost spontaneously at the same temperature, like the reviewer points out (Fig.S-4). -36.5 degrees is the highest $T_{0.5}$ (temperature when freezing fraction is 0.5) that was recorded among the multiple freezing experiments, and all the droplets were frozen before the temperature reached -40 degrees. This explanation is added in the manuscript (Page 7, line 6-8) as follows:

'Before evaluating the ice nucleation activity of the standard samples by IDFM, we measured the freezing temperature of pure water droplets using the same method, which can be regarded as the onset temperature of homogeneous freezing. As a result, homogeneous ice nucleation was initiated at approximately -36.5 °C or below, and all droplets spontaneously froze in a narrow temperature range within the same experimental run. All droplets froze before the temperature reached down to -40 °C in all experimental runs. This homogeneous freezing temperature coincides with those reported by several previous laboratory experiments (Pruppacher and Klett, 1997; Murray et al., 2010; Murray et al., 2012) and from observations of deep convective clouds (Rosenfeld and Woodley, 2000).'

Fig 1: What particles are they? Regardless, the immersion freezing active fraction at -30 dC is 1/16. Is it comparable to other cold stage techniques?

The particles shown in Fig 1 are atmospheric particles collected in April, 2016. The original image shown in Fig. 1 was for a small area on the substrate which was enlarged for better visibility. Now Fig. 1 is modified (as shown above in response to earlier 9 comment) and the entire observation area is also shown. The actual activated fractions was 5.6E -03 as stated in the manuscript, which was significantly smaller than 1/16.

The authors may want to test reference samples (K-feldspar, quartz etc.) and estimate their n_s for to quantitatively compare to Atkinson et al. (2013, Nature).

As shown in response to earlier comments, the INAS obtained in this study agreed within an order of magnitude difference compared to those found in the literature (Fig. S-2).

Fig. 6: Two more pie charts should be added. Show the composition of total aerosols measured before cooling as well as that of after thawing to eliminate the artifact of cooling-thawing.

It would be better if we can show the additional two pie charts, however, conducting analysis before the cooling-thawing experiment will be an additional source of artifacts, for example, SEM analysis involves electron irradiation under high vacuum and can potentially damage the sample and evaporate semi-volatile materials. In addition, it is already quite labor intensive and very difficult to repeat three multiple individual particle analyses on the same particles. The idea was to preserve the original particle properties as much as possible until the cooling experiment. We cannot fully rule out the

possibility of the impact of cooling-thawing on the particle properties, but it is beyond the scope of our current study, and must be incorporated in the future course of the study.

Sea salts are not ice nucleation inhibitors (P1L23), it is just not as active as other known INPs (e.g., aluminosilicate).

We believe there is also a lack of explanation and overstatement here. The results showed that the particles grouped as mineral dust were the most abundant ice residues in our study, with no obvious dependence on the elemental composition (EDX). On the other hand, most of the particles internally mixed with sea salt were not found as ice residues. This internal mixing counterpart included mineral dust. Therefore, (instead of clearly placing them as an inhibitor) we suggest the internal mixing of mineral dust with sea salt may reduce the chance of the mineral dust to act as ice nuclei.

P2L9: Koop, 2000 (Nature) missing

Thank you for pointing out the error. We added it in the reference.

How were reference sample powders dispersed/aerosolized onto silicon wafers?

We added the following line to be more explicit on the preparation of the standard mineral samples:

'The reference mineral samples were milled to fine grains before being collected on Si wafer substrate by an impactor. Three set of samples were made for each reference mineral to ensure large enough observation area for the IDFM.'

Some details of single particle techniques (laser intensity of Raman, and its influence on composition detection) are also missing.

We added following information in the method section:

'The Raman spectra of individual particles were obtained using a 532 nm excitation laser with the intensity fixed at 4.906 mW. This laser wavelength was used to detect C-H vibrational mode that appears as peaks or a broad peak in the range 2,800 cm^{-1} and 3,100 cm^{-1}, and the laser intensity was chosen to minimize damage to the sample.'

Describing the experimental uncertainties in temperature measurement, particle size detection/limit etc. would be beneficial to the reader.

The temperature measured on the surface of a substrate and the Linkam stage internal measurement is calibrated based on the melting point of materials with known properties as described in Akizawa et al., 2016. The temperature difference between the substrate surface and the stage, as well as the temperature gradient is less than 0.3 ˚C based on the observation of melting pure ice. This explanation is added in the section 2.1 as follows:

'The sample particles were deposited onto a Si wafer substrate with hydrophobic coating (Glaco, Soft99 Corporation, Japan). Particles were observed for their position, size, and shape under an optical microscope with x50 magnification (Olympus, Japan) as shown in Fig. 1a. Subsequently, the substrate was transferred onto a cold stage in a closed cell

(THMSG600, Linkam Scientific Instruments, UK). Since the cold stage used in this study is cooled by liquid nitrogen, the exposed tube through which the liquid nitrogen passes in the cold cell becomes a cold trap which can act as an additional sink for the water vapor. Therefore, in this study, all cooling parts except the cold stage surface were covered by insulating material. The temperature measured at the cold stage was calibrated by the substances of known melting points (Akizawa et al., 2016). Furthermore, we confirmed that the temperature gap between the substrate and the cold stage was consistently smaller than 0.3 ˚C by observing the melting of pure ice. During the ice nucleation experiment by atmospheric particles, the stage temperature and the dew point were recorded every 1 seconds. The temperature measurement and the images were synchronized with the PC internal clock.'

Experimental limitations related to the particle size is discussed earlier in response to the comment made in relation to the size dependent analysis.

References:

Akizawa, N., Tamaru, A., Fukushi, K., Yamamoto, J., Mizukami, T., Python, M., and Arai, S.: High-temperature hydrothermal activities around suboceanic Moho: An example from diopsidite and anorthosite in Wadi Fizh, Oman ophiolite, Lithos, 263, 66-87, 2016.

Ardon-Dryer, K., and Levin, Z.: Ground-based measurements of immersion freezing in the eastern Mediterranean, Atmos. Chem. Phys., 14, 5217–5231, doi:10.5194/acp-14-5217-2014, 2014.

Atkinson, J.D., Murray, B.J., Woodhouse, M.T., Whale, T.F., Baustian, K.J., Carslaw, K.S., Dobbie, S., O'Sullivan, D., and Malkin, T.L.: The importance of feldspar for ice nucleation by mineral dust in mixed-phase clouds, Nature, 498, 355-358, doi: 10.1038/nature12278, 2013.

Augustin-Bauditz, S., Wex, H., Denjean, C., Hartmann, S., Schneider, J., Schmidt, S., Ebert, M., and Stratmann, F.: Laboratory generated mixtures of mineral dust particles with biological substances: characterization of the particle mixing state and immersion freezing behavior, Atmos. Chem. Phys., 16, 5531–5543, doi:10.5194/acp-16-5531-2016, 2016.

Iwasaka, Y., Shi, G. Y., Yamada, M., Kobayashi, F., Kakikawa, M., Maki, T., Chen, B., Tobo, Y., and Hong, C.: Mixture of Kosa (Asian dust) and bioaerosols detected in the atmosphere over the Kosa particles source regions with balloon-borne measurements: possibility of long-range transport, Air. Qual. Atmos. Health., 2, 29–38, 2009.

Koop, T., Luo, B. P., Tsias, A., and Peter, T.: Water activity as the determinant for homogeneous ice nucleation in aqueous solutions, Nature, 406, 611–614, 2000.

Kulkarni, G., Sanders, C., Zhang, K., Liu, X., and Zhao, C.: Ice nucleation of bare and sulfuric acid-coated mineral dust particles and implication for cloud properties, J. Geophys. Res. Atmos., 119, 9993–10011, doi:10.1002/2014JD021567, 2014.

Maring, H., Savoie, D. L., Izaguirre, M. A., Custals, L., and Reid, J. S.: Mineral dust aerosol size distribution change during atmospheric transport, J. Geophys. Res., 108(D19), 8592, doi:10.1029/2002JD002536, 2003.

Murray, B.J., Broadley, S.L., Wilson, T.W., Bull, S.J., Wills, R.H., Christenson, H.K., and Murrary, E.J.: Kinetics of the homogeneous freezing of water, Phys. Chem. Chem. Phys., 12, 10380–10387, doi: 10.1039/C003297B, 2010.

Murray, B. J., Broadley, S. L., Wilson, T. W., Atkinson, J. D., and Wills, R. H.: Heterogeneous freezing of water droplets containing kaolinite particles, Atmos. Chem. Phys., 11, 4191–4207, doi:10.5194/acp-11-4191-2011, 2011.

Murray, B.J., O'Sullivan, D., Atkinson, J.D., and Webb, M.E.: Ice nucleation by particles immersed in supercooled cloud droplets, Chem. Soc. Rev., 41, 6519–6554, doi: 10.1039/C2CS35200A, 2012.

Pruppacher, H.R., and Klett, J.D.: Microphysics of Clouds and Precipitation, Kluwer Academic Publishers, Dordrecht, The Netherlands,1997.

Rosenfeld, D., and Woodley, W.L.: Deep convective clouds with sustained supercooled liquid water down to -37.5 ˚C, Nature, 405, 440–442, doi: 10.1038/35013030, 2000.

Schrod, J., Danielczok, A., Weber, D., Ebert, M., Thomson, E. S., and Bingemer, H. G.: Re-evaluating the Frankfurt isothermal static diffusion chamber for ice nucleation, Atmos. Meas. Tech., 9, 1313–1324, doi:10.5194/amt-9-1313-2016, 2016.

Schrod, J., Weber, D., Drücke, J., Keleshis, C., Pikridas, M., Ebert, M., Cvetkovic, B., Nickovic, S., Marinou, E., Baars, H., Ansmann, A., Vrekoussis, M., Mihalopoulos, N., Sciare, J., Curtius, J., and Bingemer, H. G.: Ice nucleating particles over the Eastern Mediterranean measured by unmanned aircraft systems, Atmos. Chem. Phys., 17, 4817–4835, https://doi.org/10.5194/acp- 17-4817-2017, 2017.

Sullivan, R. C., Guazzotti, S. A., Sodeman, D. A., and Prather, K. A.: Direct observations of the atmospheric processing of Asian mineral dust, Atmos. Chem. Phys., 7, 1213–1236, 10 doi:10.5194/acp-7-1213-2007, 2007.

Sullivan, R.C., Petters, M.D., DeMott, P.J., Kreidenweis, S.M., Wex, H., Niedermeier, D., Hartmann, S., Clauss, T., Stratmann, F., Reitz, P., Schneider, J., and Sierau, B.: Irreversible loss of ice nucleation active sites in mineral dust particles caused by sulphuric acid condensation, Atmos. Chem. Phys., 10, 11471–11487, doi:10.5194/acp-10-11471-2010, 2010.

Trochkine, D., Iwasaka, Y., Matsuki, A., Yamada, M., Kim, Y.-S., Nagatani, T., Zhang, D., Shi, G.-Y., and Shen Z.: Mineral aerosol particles collected in Dunhuang, China, and their comparison with chemically modified particles collected over Japan, J. Geophys. Res., 108, 8642, doi:10.1029/2002JD003268, 2003.

Zhang, D., Iwasaka, Y., Shi, G., Zang, J., Matsuki, A., and Trochkine, D.: Mixture state and size of Asian dust particles collected at southwestern Japan in spring 2000. J. Geophys. Res., 108, 4760, doi: 10.1029/2003JD003869, 2003.

~~Characterization of individual ice nuclei by the single droplet freezing method: a case study in the Asian dust outflow region~~ *Characterization of individual ice residual particles by the single droplet freezing method: a case study in the Asian dust outflow region*

Ayumi Iwata[1] and Atsushi Matsuki[2]

[1]Graduate School of Natural Science and Technology, Kanazawa University, Kakuma, Kanazawa, Ishikawa, 920-1192, Japan
[2]Institute of Nature and Environmental Technology, Kanazawa University, Kakuma, Kanazawa, Ishikawa, 920-1192, Japan.

Correspondence to: Ayumi Iwata (iayumi@stu.kanazawa-u.ac.jp) and Atsushi Matsuki (matsuki@staff.kanazawa-u.ac.jp)

Abstract. In order to better characterize ice-nucleating (IN) aerosol particles in the atmosphere, we investigated the chemical composition, mixing state, and morphology of atmospheric aerosols that nucleate ice under conditions relevant for mixed phase clouds. Five standard mineral dust samples (quartz, K-feldspar, Na-feldspar, Arizona test dust, and Asian dust source particles) were compared with actual aerosol particles collected from the west coast of Japan (Kanazawa City) during Asian dust events in February and April 2016. Following droplet activation by particles deposited on a hydrophobic Si wafer substrate under supersaturated air, individual IN particles were located using an optical microscope by gradually cooling the temperature to -30 ˚C. For the aerosol samples, both the IN active particles and non-active particles were analyzed individually by Atomic Force Microscopy (AFM), micro-Raman spectroscopy, and Scanning Electron Microscopy (SEM) coupled with Energy Dispersive X-ray spectroscopy (EDX). Heterogeneous ice nucleation in all standard mineral dust samples tested in this study was observed at consistently higher temperatures (-25.7 ˚C) than the homogeneous freezing temperature (-36.5 ˚C). ~~Meanwhile, most of the IN active atmospheric particles formed ice below -28 ˚C and were found to be IN active, but slower than the standard mineral dust samples of pure components~~. *Meanwhile, most of the IN active atmospheric particles formed ice below -28 °C, i.e. at lower temperatures than the standard mineral dust samples of pure components*. The most abundant IN active particles above -30 ˚C were predominantly irregular solid particles that showed clay mineral characteristics (or mixtures of several mineral components). Other than clay, Ca-rich particles internally mixed with other components, such as sulfate, were also regarded as IN active particle types. Moreover, sea salt particles were predominantly found in the non-active fraction, and internal mixing with sea salt clearly acted as a significant inhibiting agent for the ice nucleation activity of mineral dust particles. Also, relatively pure or fresh calcite, $Ca(NO_3)_2$, and $(NH_4)_2SO_4$ particles were more often found in the non-active fraction. In this study, we demonstrated the capability of the combined single droplet freezing method and thorough individual particle analysis to characterize the ice nucleation activity of atmospheric aerosols. We also found that dramatic changes in the particle mixing states during long-range transport had a

complex effect on the ice nucleation activity of the host aerosol particles. A case study in the Asian dust outflow region highlighted the need to consider particle mixing states, which can dramatically influence ice nucleation activity.

1 Introduction

Ice nucleation in clouds substantially affects the climate by significantly impacting the radiation balance and precipitation processes in the Earth's atmosphere (Lohmann and Feichter, 2005; Rosenfeld et al., 2008; Flato et al., 2013). Most of the initial precipitation process in mid-latitude regions involves ice nucleation in mixed phase clouds, where supercooled water droplets and ice crystals co-exist (Pruppacher and Klett, 1997; Murray et al., 2012). Therefore, an understanding of ice nucleation is crucial to predicting precipitation and cloud radiative properties.

Pure water droplets generally maintain their liquid state, even in temperatures below 0 ˚C, and remain as supercooled water droplets. These pure water droplets spontaneously freeze by cooling to approximately -37 ˚C and below (homogeneous nucleation) (*e.g. Koop, 2000; Rosenfeld and Woodley, 2000; Murray et al., 2010;* Murray et al., 2012). However, supercooled water droplets in the atmosphere generally form ice crystals at higher temperatures due to the presence of aerosol particles that can nucleate ice (heterogeneous nucleation). Traditionally, heterogeneous nucleation pathways are categorized into four freezing modes: deposition, condensation, immersion, and contact freezing modes (Pruppacher and Klett, 1997; Cantrell and Heymsfield, 2005). The physical and chemical properties of aerosols, which act as ice nuclei, play an essential role in the formation of ice crystals. However, the response of ice nucleation processes to changes in host aerosol properties is still poorly understood due to a lack of understanding of the basic aerosol particle interactions leading to ice crystal formation. Therefore, considerable uncertainty still exists regarding the prediction of ice nucleation that would lead to climate changes in the atmosphere.

Many previous ice nucleation experiments have been performed under laboratory conditions, providing valuable information on the ice nucleation properties of pure component particles and artificially generated aerosol mixtures (Pruppacher and Klett, 1997; Hoose and Möhler, 2012; Murray et al., 2012). ~~Based on these results, mineral dust and biological particles are generally regarded as efficient ice nuclei (Morris et al., 2004; Connolly et al., 2009; Niemand et al., 2012), while ice nucleation involving soot and organic particles as part of mixed cloud formation is still not clearly indicate because of depending on their composition of particles and experimental conditions (DeMott, 1990; Kireeva et al., 2009). On the other hand, sea salt and sulfates are often not considered as efficient ice nuclei.~~ *Based on these results, while mineral dust and biological particles are generally regarded as efficient ice nuclei (Morris et al., 2004; Connolly et al., 2009; Niemand et al., 2012), ice nucleation within mixed phase clouds involving soot and organic particles is still not as clearly demonstrated due to the diverse chemical composition and different experimental conditions (DeMott, 1990; Kireeva et al., 2009). On the other hand, sea salt and sulfates are often not considered as efficient ice nuclei under mixed phase conditions*. However, the situation is even more complex in the ambient atmosphere, where particles are often present as complex mixtures of different compounds and minerals. Although recent laboratory experiments have considered the influence of aerosol mixing states

(Sullivan et al., 2010; Kulkarni et al., 2014; Augustin-Bauditz et al., 2016), the complexity of the atmosphere has not yet been fully represented.

Over the last decade, several techniques have emerged, such as the counter vertical impactor (CVI), which is capable of distinguishing ice residue particles from background atmospheric particles (non-active particles) (Klein et al., 2010, Cziczo et al., 2013). Using these techniques, several field studies have been conducted to directly extract ice crystal residues from cirrus clouds (i.e. pure ice phase). ~~This has enabled the detailed investigation of particles representing the actual deposition mode of ice nuclei in cirrus clouds.~~ *This enabled direct and detailed investigation on the particles representative of the actual deposition mode ice nuclei in cirrus clouds*.

The investigation of ice nuclei in mixed phase clouds (i.e. dominated by immersion and condensation freezing modes), however, requires a different and much more demanding approach to ensure the complete isolation of ice crystals from numerous supercooled droplets and other interstitial aerosol particles. The accuracy required to ensure complete separation of ice nuclei is very challenging because the number of ice nuclei is believed to be on the order of only 1 out of 10^5 - 10^6 ambient particles and supercooled droplets in the free troposphere (*e. g.* Rogers et al., 1998*; Prenni et al., 2012; Ardon-Dryer and Levin, 2014*). It is also generally accepted that one single ice crystal grows at the expense of 10^5 - 10^6 evaporating droplets inside mixed phase clouds (the Bergeron-Findeisen or so-called "cold rain" process) *(Korolev, 2007)*.

In order to overcome the issue of ice nuclei extraction from mixed phase clouds, several techniques such as the Ice-CVI or the Ice Selective Inlet have been proposed (Mertes et al., 2007; Kupizewski et al., 2014), and efforts have been made to characterize ice nuclei using these instruments (Kamphus et al., 2010; Ebert et al., 2011). Worringen et al. (2015) reported the size distribution and chemical components of ice ~~residue~~ *residues* from mixed phase clouds collected by three different techniques (Ice-CVI, ISI, and ice nuclei counter combined with CVI), and found that silicates, Ca-rich, carbonaceous, and metal oxide particles constitute the major groups of ice nuclei. ~~However, they also reported discrepancies between the results obtained from the three different sampling techniques, and attributed them to potential bias due to the above mentioned artifacts and the scarcity of ice nuclei.~~ *However, they also reported discrepancies between the results obtained from the three different sampling techniques, and attributed them to potential bias arising from the artifacts such as the possible generation of particles within the instruments and the inherently scarce number of ice nuclei in the atmosphere*. Further, it is unknowable whether the ice residues were the actual ice nuclei, because, for example, the riming process can potentially mix cloud condensation nuclei, ice nuclei, and/or interstitial aerosols in the same ice residue.

In addition to these technical difficulties, the number of field studies that have characterized ice residues in mixed phase cloud remains sparse owing to the limited access to research locations where such clouds are directly and frequently accessible. Therefore, there is a further need to conduct field measurements in many different locations in order to reflect the regional variations in IN particles.

~~Internal mixing of aerosols commonly takes place during long-range transport in the atmosphere (Zhang et al., 2003). Through internal mixing, the reaction processes, coatings, and aging states at the surface of the particles can dramatically change from their original properties (Trochkine et al., 2003). It is often the case that internal mixing states can vary from~~

~~particle to particle; therefore, individual particle analysis is necessary for establishing a complete understanding of ice nucleation by ambient aerosol particles.~~ *Internal mixing of aerosols commonly takes place during long-range transport in the atmosphere (e. g. Zhang et al., 2003, Sullivan et al., 2007; Iwasaka et al., 2009b). The surface properties of the internally mixed particles following atmospheric processing (reaction, coagulation and aging) can dramatically change from their original properties (Maring et al., 2003; Trochkine et al., 2003). The internal mixing of particles is an important factor that contributes to the complexity of atmospheric aerosol particles. Although efforts have been made to address the effects of internal mixing on the IN activity of aerosols under conditions relevant for the mixed phase cloud formation (Sullivan et al., 2010; Kulkarni et al., 2014; Augustin-Bauditz et al., 2016), the complexity of the ambient aerosol has not yet been fully represented by the laboratory generated aerosols. Therefore, detailed investigation based on the individual particle analysis is necessary to relate the internal mixing state of aerosols in the actual atmosphere and their IN activity.*

This study is designed to investigate how the morphology, chemical composition, and mixing state of ambient aerosol particles influence their ice nucleation activities under conditions relevant to mixed phase clouds. Following the ice nucleation experiments, comprehensive analysis of the chemical, physical, and mixing properties of individual aerosol particles collected from the atmosphere was conducted. We further demonstrate the ability to monitor individual IN particles by continuously controlling the ambient conditions during the ice nucleation experiments.

The individual droplet freezing method (IDFM) is the experimental method used in this study, with which ice crystal formation on each particle could be monitored under controlled conditions while keeping individual particles distinct. By drying and evaporating the particles that formed ice crystals and/or droplets, their exact location as ice and/or droplet residues can be observed. Instead of deploying state-of-the-art, in-situ ice nuclei samplers into extreme field locations (e.g. low temperature, high altitude, and airborne), this method enables detailed post sampling analysis on both IN active and non-active particles on an individual particle basis using a fairly simple, conventional sampling method.

~~Similar methods have been employed in some laboratory studies to test the ice nucleation activities of various atmospherically relevant standard particles, but for different freezing modes (Fornea et al., 2009; Baustian et al., 2010; Mason et al., 2015; Whale et al., 2015). In particular, Baustian et al. (2012) investigated individual particles that nucleated ice crystals in the deposition freezing mode by locating the samples in saturated conditions with respect to ice at temperatures between −43 ˚C and −63 ˚C.~~ *Several laboratory studies used similar cold stage to test the ice nucleation activities of various atmospherically relevant standard particles (Fornea et al., 2009; Baustian et al., 2010; Mason et al., 2015; Whale et al., 2015; Knopf et al., 2014), but not enough studies have been made so far to investigate on the immersion-mode ice nucleation (mixed phase cloud) by the individual particles in the actual atmosphere.* ~~By employing similar methods, w~~ We exposed sample particles to the conditions relevant for mixed phase cloud formation (i.e. immersion and condensation freezing modes), while monitoring the states of individual particles. The sample particles were collected from the west coast of mainland Japan in spring, which is frequently subjected to the influence of continental outflow; often associated with plumes of Asian dust mixed with bioaerosols and other anthropogenic pollutants (Matsuki et al., 2005; Maki et al., 2010; Tobo et al., 2010).

2 Method

2.1 Individual droplet freezing method (IDFM)

~~The sample particles were deposited onto a Si wafer substrate with a hydrophobic coating (Glaco, Soft99 Corporation, Japan). Particles were observed for their position, size, and shape under an optical microscope with x50 magnification (Olympus, Japan) as shown in Fig. 1a. Subsequently, the substrate was transferred onto a cold stage in a closed cell (Akizawa et al., 2016; THMSG600, Linkam Scientific Instruments, UK).~~ *The sample particles were deposited onto a Si wafer substrate with a hydrophobic coating (Glaco, Soft99 Corporation, Japan). Particles were observed for their position, size, and shape under an optical microscope with x50 magnification (Olympus, Japan) as shown in Fig. 1b. Subsequently, the substrate was transferred onto a cold stage in a closed cell (THMSG600, Linkam Scientific Instruments, UK). Since the cold stage used in this study is cooled by liquid nitrogen, the tube through which the liquid nitrogen passes in the cold cell becomes a cold trap which can act as an additional sink for the water vapor. Therefore, in this study, all cooling parts except the cold stage surface were covered by insulating material. The temperature measured at the cold stage was calibrated by the substances of known melting points (Akizawa et al., 2016). Furthermore, we confirmed that the temperature gap between the substrate and the cold stage was consistently smaller than 0.3 ˚C by observing the melting of pure ice. During the ice nucleation experiment by atmospheric particles, the stage temperature and the dew point were recorded every 1 seconds. The temperature measurement and the images were synchronized with the PC internal clock.*

The dew point of the air introduced into the cell was controlled by mixing dry air (QD10-50, IAC, Japan) and wet air from a water filled gas scrubbing bottle. Both air flows were kept particle free and their mixing ratio was controlled by a pair of mass flow controllers (MQV9005, Azbil Corporation, Japan). The resulting dew point was also monitored by a chilled mirror type hygrometer (OptiSonde^{TM}, General Electric Company, Japan). By adjusting both the dew point of the introduced air flow (0.5 l/min) in the range -6 ˚C to -3 ˚C and the sample temperature on the cold stage in the range -9 ˚C to -7 ˚C, the particles on the substrate were exposed to water super saturation conditions that initiate droplet formation. Thus, increases in particle sizes could be observed ~~(Fig. 1b)~~ *(Fig. 1c)*.

After the air supply was stopped, the temperature of the stage was reduced to -30 ˚C at a rate of -0.5 ˚C/s. As the temperature of the stage decreased, the saturated water vapor was expected to keep condensing onto the droplets. Thus, the degree of water super saturation was assumed to be limited to slightly higher than 100 % in terms of relative humidity. The formation of ice crystals on individual droplets can be visually identified by their rapidly growing size with irregular shapes ~~(Fig. 1c)~~ *(Fig. 1d)*.

After relaxing for 10 seconds once the substrate reached -30 ˚C, the temperature of the stage was increased up to -10 ˚C at 0.5 ˚C/s. After reaching this temperature, dry air flow (0.5 l/min) was introduced into the cell to expose the formed ice crystals and droplets to the sub-saturation conditions for ice. As a result of evaporation and/or sublimation of water, the nuclei particles were exposed and left visible on the substrate. Finally, the positions of the dried particles were again located under the optical microscope ~~(Fig. 1d)~~ *(Fig. 1e)*. ~~By comparing the optical images before and after the ice nucleation~~

~~experiments, the individual particles that formed ice crystals (excluding those coalescing with adjacent droplets or crystals) were identified and regarded as IN active particles.~~ *By comparing the optical images before and after the ice nucleation experiments, the individual particles that formed ice crystals (excluding those coalescing with adjacent droplets or crystals) were identified and regarded as IN active particles. Most of the particles collected on the substrates were monitored under an optical microscope with x5 magnification (Fig. 1a). We did see multiple particles freezing in the same field of view. However, we did not cover all of the collected particles. Therefore we must note that the Non-active particles or IN active particles outside of our field of view are not included in our counts.*

2.2 Preparation of atmospheric aerosol and standard particles

Using the IDFM, we identified IN particles from the ambient aerosol particles and five types of standard samples. We sampled actual aerosol particles at Kanazawa University campus (36.54 ˚N, 136.70 ˚E, 149 m. ASL), Japan (Fig. 2) on 28 February 2016 and 10 April 2016. The particles were collected on the substrate (described above) using an impactor with a 50 % cutoff diameter of 1.1 μm at a flow rate of 1.0 L/min. The sampling period was set to 60 seconds for each substrate. The ambient temperature, pressure, relative humidity, and particle number concentrations were recorded using a mobile meteorological sensor (TR-72Ui, T&D Corporation, Japan) and an optical particle sizer (OPS 3330, TSI, USA) during the sampling periods.

The ambient atmospheric conditions during the ambient aerosol sampling were 16.7 ˚C, 22.7 % RH, and 1004.25 hPa for the February sample, and 11.7 ˚C, 84.0 %, and 994.47 hPa for the April sample. The average concentrations of coarse particles during the two sampling periods (Dp > 1.117 μm) were approximately 1.4E + 02 particles cm^{-3} for February and 4.1E + 02 particles cm^{-3} for April, indicating that the concentration for April was three times higher than for the February sampling period. No significant difference was observed for the fine particles (Dp < 1.117 μm) between the two periods.

The five standard samples include three types of single mineral component samples (quartz, K-feldspar, Na-feldspar) and two types of soil dust samples (Arizona test dust: ATD, and Asian dust source particles: ADS) that consist of multiple mineral components. The ADS were sampled from the surface soil of an arid region near Dunhung, China (40.21 ˚N, 94.68 ˚E). K-feldspar and Na-feldspar were purchased from the Bureau of Analyzed Samples Ltd. K-feldspar has been reported by several studies to show higher ice nucleation activity in mineral dust (Atkinson et al., 2013; Harrison et al., 2016). The quartz sample was purchased from Wako Pure Chemical Industries, Ltd., and it was further crushed with a mortar to decrease the grain size. Both of the soil dust samples (ATD and ADS) were size selected by the impactor and only particles coarser than 1.1 μm were used in the ice nucleation experiments.

2.3 Individual particle analyses

~~Both the atmospheric particles that IN active and non active particles were analyzed on an individual particle basis using an AFM (CombiScope™ 1000, AIST-NT, Inc., USA) and by micro-Raman spectroscopy (Nanofinder® HE, Tokyo Instruments, Inc., Japan) to characterize the three-dimensional morphology and detect surface chemical compounds, respectively.~~ *Both*

the IN active and non-active particles collected in the atmosphere were analyzed on an individual particle basis using a series of microscopic techniques. Firstly, an AFM (CombiScopeTM 1000, AIST-NT, Inc., USA) was used to characterize the three-dimensional morphology, followed by micro-Raman spectroscopy to detect chemical compounds. Furthermore, the exact same particles were analyzed by a SEM (S-3000N, HITACHI, Japan), coupled with EDX (EMAX-500, HORIBA, Japan), in order to obtain their elemental compositions. The reason for conducting AFM observations and micro-Raman analysis prior to SEM-EDX analysis is because the former two methods can be applied under ambient conditions, while the latter requires a high vacuum. The sequence of the multiple analyses was determined by taking into account the potential loss of volatile components within individual particles, especially under conditions of high vacuum and electron beam bombardment. Further, the advantages of AFM over conventional imaging techniques are that it is non-destructive (ambient conditions, no electron beam bombardment, and minimum physical contact), and directly provides the three-dimensional structure of individual particles. The technique does not involve any pre-treatment (e.g. shadowing particles by spattering a Pt/Pd alloy from a certain angle inside the vacuum) or tilting of samples as is conventionally required, especially when obtaining particle height from the inherently two-dimensional electron micrographs (Adachi et al., 2007; Ueda et al., 2011).

In this study, AFM images were obtained in dynamic mode using a silicon tip (ATEC-NC, NANOSENSORS^{TM}, Switzerland) with a spring constant of 45 N/m. The resolution of the measurement was set to 20 nm for each particle. The tip was resonated at approximately 335 kHz. In order to avoid sweeping of the particles by physical contact with the tip, the amplitude of the tip was set to 200 nm, and the rate of scanning speed was set to 0.1 lines per second.

~~The Raman spectra of individual particles were obtained using a 532 nm excitation laser with the intensity fixed at 4.906 mW.~~ *The Raman spectra of individual particles were obtained using a 532 nm excitation laser with the intensity fixed at 4.906 mW. This laser wavelength was used to detect C-H vibrational mode that appears as peaks or a broad peak in the range 2,800 cm^{-1} and 3,100 cm^{-1}, and the laser intensity was chosen to minimize damage to the sample*. With the use of a 100x objective lens, the laser spot size (i.e. spatial resolution) approaches the diffraction limit of approximately 1 μm in diameter. The laser was scanned over the Si wafer substrate containing the particle deposits with an automatically controlled X, Y piezo scanner stage. For each 750 nm step, a Raman spectrum was acquired with an exposure time of 10 s and 5 accumulations.

The compounds and minerals contained in the particles were identified by the main Raman-shift peaks in the spectral range -100 cm^{-1} to 4,000 cm^{-1}. The peaks were assigned to specific compounds and minerals by comparing with reported values from the literature (Tang and Fung, 1989; Ivleva et al., 2007; Freeman et al., 2008; Baustian et al., 2012; Laskina et al., 2013) and Raman databases. The peak positions were also verified by measuring standard pure chemical compounds using the current Raman system. The Raman-shift peak positions used for the identification of compounds and minerals are summarized in Table 1. The identification of organic components was defined by detection of the C-H vibrational mode that appears as peaks or a broad peak in the range 2,800 cm^{-1} and 3,100 cm^{-1} (Baustian et al., 2012; Ault et al., 2013; Laskina et al., 2013). The strong broad peak obtained from atmospheric particles in the range 1,200 cm^{-1} and 1,700 cm^{-1}, such as that shown in Fig. 3a and c, is typically due to the presence of complex organic matter with conjugate double bounds, biological

material, diesel soot, black and brown carbon, or humic-like substances (Escribano et al., 2001; Sadezky et al., 2005; Ivleva et al., 2007). Therefore, we refer to this broad peak as black or brown carbon (BBC) (Hiranuma et al., 2011). Other than peaks assigned to the specific components mentioned here, spectra showing strong fluorescence in the measured range, as shown in Fig. 3a, were further classified as "fluorescent particles".

Following the measurements under atmospheric pressure by AFM and micro-Raman, the particles on the Si wafer substrate were coated by Au approximately 30 nm thick. The coated particles were located under SEM-EDX. The X-ray spectra were collected at 20 kV acceleration voltage and 15 mm working distance. The relative atomic fractions (%) of the detected elements were determined by the ratios of the characteristic X-ray peak areas. Due to the limitations of the method, related to the quantification of lighter elements and elements contained in the coating and substrate, C, N, O, Au, and Si were excluded from the semi-quantitative analysis.

3 Results

3.1 Observation of ice nucleation by IDFM

~~Before evaluating the ice nucleation activity of the standard samples by IDFM, we measured the freezing temperature of pure water droplets using the same method, which can be regarded as the onset temperature of homogeneous freezing. As a result, homogeneous ice nucleation was initiated at approximately -36.5 °C, and all the pure water droplets were frozen by -40 °C. This homogeneous freezing temperature coincides with those reported by several previous laboratory experiments (Pruppacher and Klett, 1997; Murray et al., 2010; Murray et al., 2012) and from observations of deep convective clouds (Rosenfeld and Woodley, 2000).~~

~~Heterogeneous ice nucleation observed in all standard samples tested in this study consistently occurred at higher temperatures than the homogeneous freezing temperature. The standard samples of single mineral components included K-feldspar, Na-feldspar, and quartz, and their freezing onset temperatures were -20.3 °C, -20.7 °C, and -25.7 °C, respectively. Therefore, the ice nucleation activity of K-feldspar was the highest and that of quartz was the lowest. The order and the range of observed onset temperatures for these minerals were consistent with the freezing temperatures based on micro-liter suspension droplets by Atkinson et al. (2013).~~

Before evaluating the ice nucleation activity of the standard samples by IDFM, we measured the freezing temperature of pure water droplets using the same method, which can be regarded as the onset temperature of homogeneous freezing. As a result, homogeneous ice nucleation was initiated at approximately -36.5 °C or below, and all droplets spontaneously froze in a narrow temperature range within the same experimental run. All droplets froze before the temperature reached down to -40 °C in all experimental runs (Fig.S-1). This homogeneous freezing temperature coincides with those reported by several previous laboratory experiments (Pruppacher and Klett, 1997; Murray et al., 2010; Murray et al., 2012) and from observations of deep convective clouds (Rosenfeld and Woodley, 2000).

Heterogeneous ice nucleation observed in all standard mineral samples tested in this study (K-feldspar, Na-feldspar, quartz, kaolinite) consistently occurred at higher temperatures than the homogeneous freezing temperature. The reference mineral samples were milled to fine grains before being collected on Si wafer substrate by an impactor. Three set of samples were made for each reference mineral to ensure large enough observation area for the IDFM. The total number of the particles monitored during the ice nucleation experiment by IDFM was 4,509, 2,271, 4,759, and 1,435 particles, respectively. In this study, the freezing onset temperature of the sample was defined as the temperature at which the IN active fraction of the total observed particles reached 0.01. As a result, the freezing onset temperatures for K-feldspar, Na-feldspar, quartz, and kaolinite ranged between -22.2 to -24.2 ˚C, -24.7 to -25.7˚C, -24.8 to -26.8 ˚C and -27.2 to -29.2 ˚C, respectively (Fig. S-2). Therefore, the ice nucleation activity of K-feldspar was the highest and that of kaolinite was the lowest. The order and the range of observed onset temperatures for these minerals were consistent with the results found in the literature (Atkinson et al., 2013; Murray et al., 2011). For comparison, we also showed the IN activities of the reference samples in terms of ice nucleating active site (INAS) densities (Fig. S-3, S-4), calculated based on the IN active fraction curve shown in Fig. S-2, and the averaged sphere equivalent surface areas obtained from the 2D silhouette of individual particles in the microscopic image.

The fact that the observed freezing temperatures were similar to those reported in previous studies clearly demonstrates the validity of the IDFM for representing immersion and condensation mode ice nucleation. ~~For comparison, the freezing temperatures of ATD and ADS were -22.5 ˚C and -26.6 ˚C, respectively.~~ *For comparison, the freezing onset temperatures of the ATD and ADS were -22.1 to -23.7 ˚C and -25.2 to -27.2 ˚C, for 2,019 and 1,354 monitored particles, respectively (Fig. S-2, corresponding INAS densities estimated for ATD and ADS are shown in Fig. S-4)*

~~For ambient samples, we first determined the total number of target particles by analyzing the recorded optical images. As a result, ice nucleation activity of 10,188 and 24,145 particles were monitored by the IDFM for the February and April samples, respectively.~~ *For ambient samples, we first determined the total number of target particles by analyzing the optical images recorded with x50 magnification. As a result, ice nucleation activity of 10,188 and 24,145 particles were monitored by the IDFM for the February and April samples, respectively. To avoid too many particles in contact or in proximity to each other in the same field of view, multiple samples were collected during the sampling period on separate silicon wafer substrates to gain a good total number of particles.* Among those, the number of IN active particles was 37 for the February samples and 122 for the April samples. Therefore, the ice nucleation active fraction for D_p > 1.1 µm particles was 5.6E -03 for the April samples. This value is 1.5 times higher than that for the February samples (3.6E -03). While most of the IN active particles formed ice below -28 ˚C, the highest onset temperature recorded for these ambient particles was -25 ˚C. Particles with such a relatively high onset temperature tended to grow faster and larger, therefore coalescing with adjacent particles, complicating identification of individual particles following the ice nucleation experiment. As a result, individual analysis of such rapidly growing particles was not performed.

The advantage of IDFM is that we can keep track and be sure which of the collected single particle was actually nucleating ice. Thus the IN active particles identified by IDFM can be studied in detail by various particle analysis techniques.

Comparing IDFM with the other methods such as FRIDGE used primarily to measure ice nuclei concentration (Ardon-Dryer and Levin, 2014; Schrod at al., 2016; Schrod at al., 2017), we have to compromise the accuracy and quantitative evaluation of IN activity since the evaporation of droplets around frozen particles by the Bergeron-Findeisen effect can affect the activated fraction. Therefore, by selecting the higher cooling rate and -30 °C as the end cooling temperature, we minimized the evaporation and the scavenging of the droplets around the rapidly growing ice crystals in the experiments of atmospheric particles. By this way, most of the atmospheric particle (excluding those very close to the ice crystals) were not dried and remained as droplets until temperature reached -30 °C. Note however, that the selected cooling rate is considerably faster when compared with the typical cooling rate found in the convective cloud updraft. Also, we cannot fully rule out the possibility that droplets very close to an ice crystal may had been fully evaporated.

With respect to the particle size detection/limit, the impactor already size segregates particles and limit the test particles in the super-micron range. The diameter of the collected atmospheric particles whose ice crystal formation could be monitored ranged between 1.16 and 5.47 µm through the identification by the optical microscope. Meanwhile, the laser spot size (i.e. spatial resolution) of micro Raman spectroscopy approaches the diffraction limit of approximately 1 µm in diameter. All in all, the size of IN active particles that can be analyzed by this method is limited to super micron particles.

3.2 Observation of individual IN active particles by AFM

Owing to the inherently small number of IN particles in the atmosphere, three different analytical methods were employed to gather as many physical and chemical characteristics as possible from individual IN active particles.

Firstly, the 3D morphological images and the maximum height (h) based on the cross-sectional shape of 22 IN active particles and 67 non-active particles were obtained by AFM (note that the counts are shown as the sum of February and April samples due to the small number of IN active particles). We further determined the surface equivalent diameter (D_S), which is defined as the arithmetic average of the longest axis and its orthogonal axis in the 2D particle silhouette. As a result, the IN active particles were found to fall within the 1.12 - 14.60 µm range for D_S and in the 0.32 - 3.28 µm range for h, while the non-active particles had D_S values of 0.60 - 12.04 µm and h values of 0.07 - 1.98 µm.

In terms of particle shape, we determined the D_S/h ratio, which can be closely linked to the physical state, whereby semi-ellipsoidal particles with high D_S/h ratios tend to be in a liquid or semi-liquid state, while irregular shaped particles with low ratios are most likely in a dry solid phase (Sobanska et al., 2014). As shown in Fig. 4a, while the IN active particles tended to concentrate in low D_S/h ratios, the non-active particles showed a wider range, including relatively high D_S/h ratios. This suggests that the IN active particles were predominantly irregular solid particles.

Aspect ratio was also determined for each particle using the ratio between the major and minor axis of the best fit ellipse of the 2D particle silhouette. Although the number of measured particles was small, the aspect ratio of the IN active particles was not close to 1 (Fig. 4b). In other words, the IN active particles were predominantly irregularly shaped particles (as shown in Fig. 3a), consistent with the results of D_S/h ratio distribution (Fig. 4a). Conversely, the particles shown in Fig. 3b

and c were more representative of non-active particles. It is noteworthy, however, that the analyzed morphology of particles may not necessarily correspond to that in the actual atmosphere, since particles can be flattened upon impaction and particle shape can also be altered following ice nucleation experiments involving ice and/or droplet activation.

3.3 Analysis of individual IN active particles by micro-Raman spectroscopy

Chemical species contained in the 42 IN active particles and 131 non-active particles were identified by Raman spectra mapping (counts include the February and April samples combined). The detection frequencies of the Raman-active molecular compounds among individual particles are summarized in Fig. 5.

It was found that more than 70 % of both IN active particles and non-active particles contained organic matter. Additionally, nitrate and/or sulfate peaks were detected in 50 % and 99 % of the IN active and non-active particles, respectively. These results show that most of the ambient aerosol particles (D_P > 1.1 μm) collected in this study were internally mixed with organic and/or inorganic (sulfates and nitrates) materials.

The fraction of particles containing sulfates, such as $(NH_4)_2SO_4$ and/or $CaSO_4$, was 40 % and 34 % for IN active and non-active particles, respectively. Moreover, a significantly larger fraction (76 %) of the IN active particles showed fluorescence in the Raman spectra. Fluorescence from a particle is typically attributed to a certain group of organics of biological origin, or the intercalated impurities of humic or humic-like substances in clay minerals and amorphous alumino-silicates (Sobanska et al., 2012; Jung et al., 2014). In addition to the fraction of fluorescent particles, BBC, $CaSO_4$, and quartz were detected in the IN active particles with significantly higher frequencies than in non-active particles. In contrast, the particles indicating broad OH peaks and nitrate peaks were more abundant in non-active particles. In terms of the detection frequency of organic matter and $(NH_4)_2SO_4$, we did not find any clear differences between IN active and non-active particles.

We also performed micro-Raman analysis on ADS for comparison. As shown in Fig. 5, all ADS showed fluorescence in the Raman spectra. Organic matter and quartz components were identified in 61 % and 16 % of individual ADS, respectively. Meanwhile, peaks indicating sulfates or nitrates were not detected in any ADS particles. This is consistent with the findings that Asian dust aerosols near the source region are fresher and hence contain less sulfur than in the downwind regions (Trochkine et al., 2003). This result clearly indicates that many mineral dust particles are originally internally mixed with organic matter to some extent, but that the Asian dust source does not contain sulfates or nitrates (Kawamura et al., 2004).

Additionally, the presence of feldspar in the individual particles was tested by comparing spectra with that of the standard mineral samples. However, there were almost no particles showing typical spectra indicating the presence of feldspar in the ambient samples. The possibility remains that the feldspar content was so small that it was below detection limits, or that the feldspar contained impurities or had defects in the crystal structures that may have caused interference in the form of strong fluorescence in the Raman spectrum. Nonetheless, we did not observe any particles predominantly composed of pure feldspar, such as the standard feldspar sample, that indicated characteristic peaks in the Raman spectra.

3.4 Analysis of individual IN active particles by SEM-EDX

Elemental compositions of 37 IN active and 114 non-active particles were analyzed using SEM-EDX (counts include the February and April samples combined). The presence of mineral dust particles can be identified by the dominant X-ray peaks corresponding to Al, Mg, and Fe. Due to interference by the Si wafer substrate, Si was not determined in this study. The particles predominantly composed of Na and Cl were classified as fresh sea salt with a Cl/Na ratio in the 0.8 - 1.2 range. Due to the Cl liberation reaction during transport (Zhang et al., 2003), those particles with lower Cl/Na ratio can be considered as aged sea salt particles. Particles enriched in Ca or S were classified as Ca-rich particles or sulfate particles, respectively. When a particle contained more than 35 % of elements other than the predominant components, we defined it as an internal mixture, which is designated by (+ inclusion) in Fig. 6.

As shown in Fig. 6, the relative abundance of particle groups clearly differed between IN active and non-active particles. The mineral dust particle groups (mineral dust and mineral dust + inclusions) accounted for 55 % of IN active particles and were the most dominant type, while sea salt particles were rarely found (3 %). Conversely, the majority (62 %) of non-active particles was dominated by fresh and aged sea salt particles, suggesting it was internally mixed with other components, such as S. The mineral dust particle group, in turn, comprised a relatively minor fraction (12 %). *Note however, that elements C, N, O, and Si were not taken into account in the EDX semi-quantitative analysis. Therefore, we cannot rule out the possibility that organic dominant particles may be overlooked by EDX analysis alone.*

The Ca-rich and sulfate groups were found in both IN active and non-active particles. However, the pure Ca-rich and sulfate component groups were relatively minor compared to internal mixtures, which contain the latter components plus other matter (+ inclusion), for IN active particles. They were found in similar fractions for non-active particles.

Particles enriched in Pb were reported to be involved in the formation of ice crystals at Jungfraujoch (Cziczo et al., 2009). However, such particles enriched in Pb were neither found in IN active particles nor in non-active particles.

The semi-quantitative comparison of particle composition obtained by micro-Raman spectroscopy and SEM-EDX analyses is hampered by the different principles employed in the two techniques. ~~Particle classification with SEM-EDX relies on characteristic X-ray signals, which are used to estimate the elemental composition of a particle. This information can be considered to reflect the bulk elemental distribution within a particle and has been commonly used for particle classification in many previous studies. In contrast, micro-Raman spectroscopy detects slight shifts of wavelength that reflect the vibrations of molecular bonds contained in a sample. While the laser transmission depth depends on the particle material, and it is not necessarily representative of a major component of the particle. In the following discussion, we considered that micro-Raman spectra are typically representative of a coating and/or components concentrated on the particle surface, i.e. the analytical volume is more surficial than for EDX.~~ *Particle classification with SEM-EDX relies on characteristic X-ray signals, which are used to estimate the major elemental composition of a particle. This information can be considered to reflect the bulk elemental distribution within a particle and has been commonly used for particle classification in many previous studies. In contrast, micro-Raman spectroscopy detects slight shifts of wavelength in the scattered light that reflect*

the vibrations of molecular bonds specific to the compounds contained in a sample. Therefore the Raman spectrum was used rather to complement the bulk particle type classification by the EDX analysis, and to detect the internally mixed compounds.

4 Discussion

4.1 Mineral dust particles

The SEM-EDX analysis indicated that mineral dust particles accounted for 55 % of the IN active particles (Fig. 6). Fluorescent particles identified by micro-Raman spectroscopy were also common (76 %) in IN active particles (Fig. 5). ~~Subsequent SEM-EDX analysis showed that most of the fluorescent particles (87 %) contained elements that indicate a mineral composition. Considering the fact that all the ADS also showed similar fluorescence, these fluorescent particles could be associated with mineral dust (especially those enriched in clay minerals). Both the SEM-EDX and micro-Raman analyses indicated that mineral dust particles act as efficient ice nuclei under conditions relevant for mixed phase cloud formation.~~ *Subsequent SEM-EDX analysis showed that most of the fluorescent particles (87 %) contained elements that indicate a mineral composition. The fluorescence is also often taken as an indication for the presence of biological aerosols (Twohy et al., 2016), but considering the fact that all the ADS also showed similar fluorescence, and the relatively small abundance of biological particles as compared to mineral dust in general (Huffman et al., 2012), these fluorescence signals are mostly associated with mineral dust (especially those enriched in clay minerals) rather than pure biological particles. Possibility remains however, that a fraction of the fluorescence signal results from biological matters attached to the clay minerals. In any case, both the SEM-EDX and micro-Raman analyses indicated that mineral dust particles act as efficient ice nuclei under conditions relevant for mixed phase cloud formation.*

This finding is in good agreement with the findings of previous work. For example, several laboratory studies showed that mineral dust particles are capable of nucleating ice crystals at relatively high temperatures, and may be important ice nuclei, especially at temperatures below approximately -15 ˚C (Murray et al., 2012). Additionally, several in-situ field studies performed within a mixed phase cloud at Jungfraujoch, a high elevation site in the Swiss alpine region, reported that mineral dust was the most abundant component, comprising 40 - 70 % of the ice residue particles by number (Worringen et al., 2015; Ebert et al., 2011; Kamphus et al., 2010).

Nonetheless, questions remain concerning the factors controlling the IN properties of mineral dust. These particles exist as internal mixtures of several minerals. Strictly speaking, therefore, the mineralogical composition of mineral dust is unique to each particle. Recently, several studies have pointed out that the feldspar group, especially K-feldspar, is an important mineral component for ice nucleation within mixed phase clouds at higher temperatures (Atkinson et al., 2013; Harrison et al., 2016; Boose et al., 2016). Also, quartz has been proposed to contribute to the relatively strong ice nucleation activity of natural desert dusts (Boose et al., 2016), whose stronger ice nucleation activity in immersion mode than that of clay minerals is thought to be related to defects present on the surface of quartz particles (Zolles et al., 2015).

In this study, standard K-feldspar (-20.3 ˚C) and quartz (-25.7 ˚C) samples were indeed more efficient ice nuclei than ADS (-26.6 ˚C). However, most of the collected atmospheric particles formed ice crystals at temperatures below -25 ˚C. These ice nucleation onset temperatures are similar to those reported for several natural dust samples from different regions around the world (Boose et al., 2016; Kaufmann et al., 2016).

The mineral dust particles can be further separated into K-feldspar and Na/Ca-feldspar groups using ~~an Al-K-(Ca+Na)~~ *a Na-Ca-K* ternary plot (Fig. 7). Mineral particles composed mainly of other clay minerals and mica should appear near the center of the Al-K-(Ca+Na) ternary plot *(Fig. S-5)*. However, K-feldspar dominated particles were rarely observed in the atmospheric mineral dust particles analyzed in this study, although Na/Ca-feldspar (plagioclase feldspar), mica, and clay minerals were present. Also, peaks of feldspar (2 %) or quartz (19 %) were rarely identified in the Raman spectra of the analyzed mineral dust particles, further suggesting the absence of K-feldspar enriched particles. Even where feldspar and quartz peaks were observed, they also contained other mixtures such as fluorescent material, organic matter, or sulfates, which were not particularly IN active. Therefore, highly IN active dust particles composed of single component minerals, such as feldspar or quartz, were very rare or non-existent in the ambient aerosols collected in this study. Although we may have miscounted some IN active particles due to the aforementioned coalescence with adjacent particles during ice crystal growth, even the most rapidly growing crystals initiated ice nucleation below - 25 ˚C. Thus, it would have been noticed if particles as active as *the standard* K-feldspar were nucleating at *higher* temperatures ~~as high as -20.3 ˚C~~.

~~Previous studies have~~ *A previous study has* reported that clay and mica account for 51 % of the Asian dust particles over Japan, while quartz (10 %) and feldspar (5 %) are minor mineral components, based on similar identification criteria to that employed in this study (Iwasaka et al., 2009). Simulated Asian mineral dust has also been investigated, and the detection frequency of K-feldspar was significantly lower (2 %) than that of Na/Ca-feldspar (12 %) (Yabuki et al., 2002). The results of onset temperature and related particle mineralogy (both in terms of SEM-EDX and micro-Raman spectroscopy), suggested that IN mineral dust particles as efficient as pure component K-feldspar or quartz are extremely rare in the atmosphere (at least in East Asia, which is affected by Asian dust). ~~Furthermore, it was demonstrated that most IN particles above -30 ˚C were mineral dust particles composed mainly of clay minerals, with or without minor mixing of other mineral components, that involve fluorescence, most likely as a result of defects and/or impurities (e.g. humic organics) in their crystal structure (Gaft et al., 2005; Jung et al., 2014; Sovanska et al., 2014).~~ *Furthermore, we even found that all the fresh ADS particles (believed to be dominated largely by clay minerals) showed the fluorescence. This fluorescence is likely derived from the defects and/or impurities (e.g. humic organics) in their crystal structure (Gaft et al., 2005; Jung et al., 2014; Sovanska et al., 2014). Therefore, the fluorescent particles associated with elements of crustal origin (by EDX analysis) were regarded as clay minerals. It was also demonstrated that the most IN particles active above -30 ˚C were dominated by such fluorescence mineral dust particles.*

More recently, Kaufmann et al. (2016) found no significant differences between the freezing temperatures of dust samples collected from ground soil of various arid dust source regions. Mineral components with extremely high ice nucleation activity, such as the alkali feldspar microcline, were found only as minor components. Their results further suggested that

dust mixing in the natural environment reduces high ice nucleation efficiency (Kaufmann et al., 2016). Additionally, minerals in the natural environment are decomposed by reactions with water (chemical weathering processes), thus forming Al-rich clay minerals. Our results are consistent with these findings, such that the distribution of freezing temperatures of the studied natural dusts is much more compact and falls within a narrower temperature range than that reported for a variety of reference minerals. It is worth noting that our results are based on actual atmospheric aerosol samples rather than sieved surface soil, and that the freezing experiment and characterization were made on a single particle basis by the coupling of IDFM, micro-Raman spectroscopy, and SEM-EDX. Therefore, our results should be representative of the ice nucleation activity expected within mixed phase clouds.

4.2 Sea salt particles

While mineral dust particles were found with the highest frequency among the particles that nucleate ice crystals, sea salt particles were the most dominant particle type in non-active particles (Fig. 6).

Although sea salt particles were assigned based on the largest atomic concentration of Na and Cl by EDX analysis, many particles had a combined Na and Cl concentration of less than 65 % with low Cl/Na ratios. *Note however, that this elemental fraction of sea salt components is based on SEM-EDX and does not reflect potential contribution from organics and therefore must be regarded as the upper limit*. This is an indication that many sea salt particles were aged and mixed with other components. In EDX analysis, in particular, most of these sea salt mixtures were characterized by a large S fraction, indicating that they were internally mixed with sulfates. Moreover, those particles showed peaks of organic matter, sulfates, or nitrates (in particular $MgNO_3$), in the Raman spectra. Therefore, these particles can be considered as aged sea salt particles that were internally mixed with nitrates, sulfates, or organics. The freezing experiments clearly demonstrated that these aged sea salt particles are not efficient ice nuclei in mixed phase cloud formation.

Ice nucleation by sea salt particles has been suggested by previous field studies but under conditions relevant for cirrus cloud formation instead (Cziczo et al., 2013). Meanwhile, ice nucleation by sea salt particles under mixed phase cloud conditions has not been fully confirmed by previous field studies, due to the geographical limitation of research facilities and technical difficulties related to the direct collection of ice residue particles (Worringen et al., 2015). Laboratory studies have reported ice nucleation by crystalline sea salt at much lower temperatures (Wise et al., 2012). Recently, Wilson et al. (2015) reported that sea spray organic aerosols derived from the sea surface microlayer nucleate ice under conditions relevant for mixed phase clouds and ice cloud formation at high-altitudes, but the sea water itself did not contribute markedly to ice nucleation. ~~Based on the results of this study, we suggest that large and aged sea salt particles internally mixed with sulfates, nitrates, or organics will not nucleate ice in any event, although the possibility remains for ice nucleation by pure sea salt and sea spray organic particles in the atmosphere.~~ *Based on the results of this study, we suggest that large and aged sea salt particles internally mixed with sulfates, nitrates, or organics are less likely to nucleate ice, although the possibility remains for ice nucleation by sea spray organic particles in the atmosphere. The lower freezing temperature of NaCl solution relative to*

pure water droplets (Fig. S-4) and the degree of dilution (Table S-1) involved in the experiment suggest that the weak IN activity of sea salt particles could be explained by the molar depression of freezing point by the soluble salt.

A ternary diagram of Na-(Al+Mg+Fe)-(Ca+S) showing the compositions of all analyzed particles is shown in Fig. 8. Interestingly, the diagram clearly indicates that particles with Na greater than 35 % were dominant amongst non-active particles. This indicates that internal mixing with sea salt may act as an important inhibiting factor for ice nucleation within mixed phase clouds. For example, particles containing mineral dust components (often found among IN active particles), showing clear mixing with sea salt, were rarely found among IN active particles, but were rather common in the non-active particle group.

4.3 Ca-rich and sulfate particles

As shown in Fig. 6, both relatively pure Ca-rich particles and sulfate particles (without inclusions) were detected with similar frequencies among the IN active and non-active particles. The particles enriched in Ca can be related to mineral dusts such as calcite ($CaCO_3$), dolomite ($CaMg(CO_3)_2$), and gypsum ($CaSO_4$). Calcite or dolomite dominated particles can be inferred by the elemental ratio of Mg/Ca (calcite: Mg/Ca < 0.5, dolomite: Mg/Ca > 0.5). The presence of pure gypsum can be inferred from the S/Ca ratio of 1 in the Ca-rich particle group (Trochkine et al., 2003), but a S/Ca ratio of < 1 is expected because gypsum is typically regarded as occurring in a mixture with calcite (Iwasaka et al., 2009). The dolomite dominated particles with high Mg contents were rare among the Ca-rich particles. Most of the Ca-rich particles were classified as calcite or gypsum with Mg as a minor component.

There seems to be no marked difference between the IN active and non-active Ca-rich particles in terms of their mixing states with other mineral components (e.g. Al, Mg, Fe) from the SEM-EDX analysis (Fig. 9). Interestingly, however, Ca-rich particles with small S content (S/Ca < 0.2), which can be regarded as predominantly calcite, were more common in non-active particles (i.e. bottom right corner in Fig. 9). Of the non-active Ca-rich particles, 50 % were detected with a carbonate peak in the Raman spectra, confirming the presence of calcite. In contrast, carbonate peaks were hardly detected in Ca-rich particles in the IN active group. In terms of compounds identified by micro-Raman analysis, the detection frequencies of fluorescence, sulfates, or organic matter among Ca-rich particles were difficult to compare as no obvious differences were found between the IN active and non-active particles. Meanwhile, nitrate peaks, in particular the $Ca(NO_3)_2$ peak, were more frequently detected in non-active particles than in IN active Ca-rich particles. In other words, we suggest that Ca-rich particles mixed with nitrates *are less likely to* form ice ~~much less easily~~ than Ca-rich particles mixed with organics and sulfates.

Frequent detection of $Ca(NO_3)_2$ has several important implications related to the physical state of the Ca-rich particles in the atmosphere. It is reported that originally solid Ca-rich ($CaCO_3$) particles readily deliquesce and are converted into aqueous droplets following the atmospheric reaction with gaseous HNO_3 to form $Ca(NO_3)_2$ (Laskin et al., 2005; Matsuki et al., 2005). Indeed, we found that the aspect ratios of non-active Ca-rich particles measured by AFM tended to show smaller values closer to 1. Furthermore, AFM topographic images of such particles typically showed thin coatings around the core (core-

shell structure) as shown in Fig. 10b, very much resembling the morphological features of the Ca-rich aqueous droplets described in the literature. Note also that the core of the particle showed a peak for Al in the EDX spectra, suggesting the presence of alumino-silicate (e.g. clay) particle in the center. Such Ca-rich spherical particles were exclusively found among non-active particles rather than the IN active Ca-rich particles (Fig. 10a), suggesting that nitrate containing Ca-rich spherical particles are less likely to act as ice nuclei in the mixed phase clouds. It is worth pointing out that, $Ca(NO_3)_2$ is an extremely soluble salt with a solubility of 121.2 g/100g H_2O at 20 ˚C. Therefore, the liquefied $Ca(NO_3)_2$ coating is expected to show strong molar depression of freezing point, which could explain their weak IN ability *(Table S-1)*. ~~Therefore, t~~*T*hese Ca-rich spherical particles mixed with nitrates were found to be less IN active than Ca-rich particles mixed with organics or sulfates, regardless of the composition of their core particles (e.g. with or without clay mineral particles). Tobo et al. (2010) reported similar liquefied particles can be formed through reaction with gaseous HCl to form $CaCl_2$. Such chloride particles are also expected to behave similarly to the Ca-rich particles having $Ca(NO_3)_2$.

There is still a slight discrepancy among previous studies concerning the ice nucleation activity of carbonates. For example, several laboratory studies regarded calcite as an inefficient ice ~~nuclei~~ *nucleus* (Murray et al., 2012; Atkinson et al., 2013), while one laboratory experiment and field study reported that Ca-rich particles act as ice nuclei (Zimmermann et al., 2008; Worringen et al., 2015). Although the number of analyzed particles is rather small, our result suggests that pure calcite (i.e. fresh) particles or their mixture with nitrate are less likely to nucleate ice under mixed phase cloud conditions.

Particles with S/Ca > 0.8 were grouped into sulfate particles. In terms of elemental composition determined by SEM-EDX analysis, there were no differences between the sulfate dominated particles that were IN active and non-active. However, from the micro-Raman analysis, 43 % of non-active sulfate particles showed a peak of $(NH_4)_2SO_4$, while none of the IN active sulfate particles showed this peak. Particles identified as $CaSO_4$, or those with fluorescent peaks, showed a relatively higher abundance among IN active particles.

Sulfate particles are generally believed to nucleate ice crystals only under cirrus forming conditions (Abbatt et al., 2006). However, field studies have reported the presence of sulfate particles in ice residues, although potential bias from sampling artifacts cannot be entirely excluded (Prenni et al., 2009; Worringen et al., 2015; Ebert et al. 2011).

With regard to the Ca-rich and sulfate particles studied here, in summary, our results suggest that $(NH_4)_2SO_4$, intact calcite, or Ca-rich spherical particles mixed with nitrates in the atmosphere are less likely to nucleate ice. Meanwhile, Ca-rich particles with internally mixed sulfate (e.g. $CaSO_4$), or sulfate dominated particles internally mixed with clay minerals, may have a higher chance of nucleating ice under mixed phase cloud formation conditions.

4.4 Organic matter

Various organic matter are believed to be involved in ice nucleation. For example, some primary biological particles such as bacteria and pollen can act as efficient ice nuclei (Möhler et al., 2008a; Pummer et al., 2012; Hara et al., 2016). Soot particles and humic-like substances also act as ice nuclei in immersion mode, although with variable freezing temperatures (Diehl and Mitra, 1998; DeMott et al., 1999; Brooks et al., 2014; O'Sullivan et al., 2014). Based on Raman spectroscopy,

70 % of particles showed the broad peak indicating the presence of organic matter in both the IN active and non-active particles analyzed in this study. The frequent detection of organic matter in this study is in agreement with other field measurements on atmospheric particles (Baustian et al., 2012).

Particles detected with and without organic matter showed no significant difference in terms of the particle groups and their fractions identified by SEM-EDX for both IN active and non-active particles. This implies that the organics detected in this study had a secondary effect on ice nucleation above -30 ˚C, or simply that the current definition of organic matter (based on the C-H stretching band alone) is not capable of resolving IN active and non-active compounds.

In the Raman analysis, 98 % of particles detected with a broad peak arising from the intermolecular hydroxyl groups (3,200-3,650 cm^{-1}) were associated with particles containing the organic matter peak (C-H). It is worth noting that a similar association of hydroxyl groups with organic matter was reported for IN particles under cirrus cloud conditions (Baustian et al., 2012). The detected OH broad peaks associated with organic matter are not as strong as the Raman intensities from water typically observed with particle deliquescence and, therefore, clearly distinguishable. As shown in Fig. 5, non-active particles (53 %) showed a higher detection frequency of organic particles with OH broad peaks than IN active particles (39 %).

Past laboratory studies reported that biomass burning particles, organic acid, and secondary organic particles have the potential to nucleate ice in the conditions relevant for cirrus cloud formation (Petters et al., 2009; Prenni et al., 2009b; Hoose and Möhler, 2012). Möhler et al. (2008b) suggested that thick coatings of organic matter can inhibit the depositional freezing of mineral dust. Moreover, the ice nucleation activity of mineral dust particles is enhanced due to mixing with heat sensitive organic substances supposedly of biological origin (Conen et al., 2011; Tobo et al., 2014). The ice nucleation activity of oxidized organic matter has also been reported from several laboratory experiments and field studies, but for conditions of cirrus cloud formation (Knopf et al., 2010; Baustian et al., 2012). In this respect, the effects of mixing with either oxidized or non-oxidized organic matter on ice nucleation in mixed phase clouds have not been fully confirmed, either by laboratory or field experiments.

Nonetheless, the impact of major particle components other than the organic matter (e.g. mineral dust and sea salt) were more apparent in terms of the different ice nucleation activity observed under simulated mixed phase cloud conditions. Therefore, we suggest that observed ice nucleation activity above -30 ˚C cannot be linked directly to the oxidative state of the organic matter on the surface of the particles. Instead, ice nucleation activity may be controlled more strongly by the major components governing their particle types. Furthermore, the IN active and non-active fractions showed different frequencies in terms of particles containing oxidized and less oxidized organic matter. Also, IN active particles were more often associated with BBC peaks, which are suggestive of the presence of complex organic matter. The possibility remains, therefore, that less oxidized organic matter and BBC may partly be responsible for, or even enhance, the ice nucleation activity of the host particles.

4.4 Sampling conditions: influence of aged Asian dust particles

~~The study area, Kanazawa City, is located along the west coast of mainland Japan, and further upstream of the westerly continental outflow are the vast arid regions of inland China and Mongolia. Every spring, frequent dust outbreaks are observed, transporting a massive amount of mineral dust aerosols (Asian dust) across the region and beyond (Iwasaka et al., 2009).~~ *The study area, Kanazawa City, is located along the west coast of mainland Japan. Further upstream of the westerly continental outflow are the vast arid regions of inland China and Mongolia. Every spring, frequent dust outbreaks are observed, transporting a massive amount of mineral dust aerosols (Asian dust) across the region and beyond (Iwasaka et al., 2009a).*

Backward trajectories suggested that the air mass at 3,000 m altitude over the sampling location during the two sampling dates in February and April 2016, had traveled over Chinese and Mongolian regions (Fig. 11; redrawn from http://ready.arl.noaa.gov/HYSPLIT.php; Stein et al., 2015; Rolph, 2017). The range of coarse particle (D > 1.0 μm) and number concentrations monitored by an optical particle counter (OPC KC-01E, RION, Japan) at the NOTO Ground-based Research Observatory ~~(NOTOGRO; 37.45°N, 137.36°E)~~ *(NOTOGRO; 37.45°N, 137.36°E; 116km north east of the sampling location)* (Iwamoto et al., 2016) during the sampling periods was significantly higher than the background concentrations (0.31 ± 0.12 particles/cm^3) during the 2016 spring season. ~~Although the observed concentrations in February were not as high as that expected during major Asian dust events (3.27 ± 1.80 particles/cm^3), the sporadic nature of the increasing particle concentration and air-mass transport patterns suggested that the samples were collected under the influence of a modest Asian dust event.~~ *The average concentration observed during Asian dust events in February 2016 was 3.27 ± 1.80 particles/cm^3, so the concentrations observed during February sampling period were not as high as that expected during major Asian dust events*. The April sampling date is reported as an Asian dust event day by the Japanese Meteorological Agency (http://www.data.jma.go.jp/gmd/env/kosahp/kosa_table_2016.html). Indeed, the coarse particle concentration in April (2.45 ± 0.09 particles/cm^3) was three times as high as that in the February (0.85 ± 0.08 particles/cm^3) sampling period at the sampling location, and five times higher (2.38 ± 0.07 particles/cm^3) than that in February (0.49 ± 0.04 particles/cm^3) at NOTOGRO.

As discussed above, the mineral dust particles were the dominant group of IN active particles. The higher ice nucleation active fraction observed for the April sample (5.6E -03) compared to the February sample (3.6E -03) can be related to the stronger influence of Asian dust particles.

Based on the result of individual particles analysis, the dust particles collected at the sampling location were internally mixed with sulfates, nitrates, sea salt, and organics. On the other hand, the ADS did not show signs of mixing with sulfates or nitrates, although they did contain either organic matter or BBC. This finding is in agreement with previous reports on Asian dusts collected at the desert surface, which are reported to contain organics originating from biomass burning and unsaturated fatty acid derived from plants (Kawamura and Gagosian, 1987; Kawamura et al., 2004). Therefore, our ice nucleation experiment is representative of the Asian dust plume, originally emitted from Chinese and Mongolian deserts,

experiencing aging during long-range transport across the urban areas of China and/or the Sea of Japan, where particles became internally mixed with sulfates, nitrates, or sea salt (Zhang et al., 2003).

The results of this study revealed that the influences of dust aging and associated mixing during transport on ice nucleation activity is very complex because, in certain cases, the aging process may act to both promote or inhibit ice nucleation in mixed phase clouds. For example, while the mixing of sulfates and nitrates with clay minerals may not significantly affect the original ice nucleation activity, mixing with sea salt was shown to inhibit the IN activity of the mineral dust particles. Moreover, relatively pure calcite and sulfate particles such as $(NH_4)_2SO_4$ may nucleate ice following mixing with other components (except for the mixing of calcite with nitrate). These results suggest that, in addition to the original composition and related ice nucleation activities, the aging process in the atmosphere must also be considered when precisely predicting the ice nucleation activity of ambient aerosols.

5 Conclusions

Ice nucleation experiments on both standard mineral samples and ambient aerosol particles were performed on an individual particle basis by the individual droplet freezing method, simulating conditions relevant for mixed phase cloud formation. In addition, the morphology and chemical composition of both IN active and non-active particles were directly measured by three individual particle analysis methods.

Standard feldspar and quartz particles were shown to be more ice nucleation active than atmospheric particles. Among the ambient aerosol particles, alumino-silicate mineral dust and internally mixed Ca-rich and sulfate particles were identified as IN active particle types. Other IN active particles were identified as internal mixtures including sulfates, nitrates, and organics, but commonly contained mineral dust as a major component. ~~These mineral dust inclusions were suggested to be mixtures of several mineral components (including defects and impurities in crystal structure such as mineral clay) rather than single mineral species.~~ *These mineral dust particles were suggested to be mixtures of several clay mineral components rather than single mineral species, having defects in their crystal structure and contain impurities*.

Dust particles consisting of pure mineral components, associated with high ice nucleation activity (e.g. K-feldspar) in previous laboratory experiments, were extremely rare or non-existent in the atmosphere, even under the influence of Asian dust transport. Therefore, the majority of immersion and condensation modes IN particles in the atmosphere were identified as clay mineral particles on an individual particle basis. Our result suggests that the freezing temperatures of individual ice nuclei in the atmosphere do not show large variation, and fall in a relatively narrow range that can be represented by the ice nucleation activity of clay minerals. This claim is consistent with those inferred from bulk analysis (Kaufmann et al., 2016).

Moreover, aged sea salt, pure calcite, mixtures of Ca-rich spherical particles with nitrates, and pure sulfate particles were found to be less active as ice nuclei. In particular, internal mixing with sea salt particles during transport over the ocean was shown to be an important factor inhibiting the ice nucleation activity of mixed counterparts. Cloud processing has been proposed as an efficient mechanism for mixing mineral dust and sea salt particles (Niimura et al., 1998), and such depression

in the ice nucleation activity has important implications for subsequent condensation and immersion freezing pathways. ~~Although pure calcite and sulfate particles were identified as an inert particle group, interestingly, their internal mixture (i.e. sulfate + Ca-rich) showed relatively higher ice nucleation activity. This also suggests that atmospheric aging (including cloud processing) could potentially enhance the originally inert ice nucleation activity of calcite and sulfate particles.~~ *Although relatively pure calcite and sulfate particles such as* $(NH_4)_2SO_4$ *were identified as an inert particle group, interestingly, these particles may nucleate ice following mixing by themselves (i.e. sulfate + Ca-rich), or with other components (except for the mixing of calcite with nitrate). This also suggests that atmospheric aging (including cloud processing*) could potentially enhance the originally inert ice nucleation activity of calcite and sulfate particles. These results suggest that, the influences of dust aging and associated mixing during transport on ice nucleation activity is very complex, because in certain cases, the aging process may act to both promote or inhibit ice nucleation in mixed phase clouds. Therefore, *in addition to the original composition and related ice nucleation activities, the aging process in the atmosphere must also be considered when precisely predicting the ice nucleation activity of ambient aerosols*.

The mineral dust particles were found to contain organic matter already at the emission source. Mixing with organics was found to show only a secondary effect on the ice nucleation activity of the host particles. The possibility remains, however, that the oxidation state of the organics and the presence of BBC on the particle surface may be partly involved in ice nucleation. Therefore, there is a further need to characterize the surface and coating state of atmospheric particles to better understand the specific factors responsible for ice nucleation in mixed phase clouds. This is because ice nucleation is probably most sensitive to the particle surface or the first few layers below the surface, as ice germs are believed to grow from cracks, crevices, or pores.

In conclusion, this study successfully related immersion and condensation mode ice nucleation activity of actual atmospheric particles to their morphology, chemical composition, and mixing states on an individual particle basis. This was made possible by the direct and comprehensive particle analysis of individual IN particles. We believe that this method can be used to verify previously proposed aerosol ice nucleation theories that are mostly based on experiments using single components and/or bulk samples.

Acknowledgement

We thank Shoji Arai, Tomoyuki Mizukami (Kanazawa University), and Norikatsu Akizawa (Kyoto University) for providing experimental equipment. We gratefully acknowledge the Fourth Laboratory, Forecast Research Department, Meteorological Research Institute for providing the ATD and valuable comments. The authors also acknowledge the NOAA Air Resources Laboratory (ARL) for provision of the HYSPLIT transport and dispersion model and/or the READY website (http://www.ready.noaa.gov) used in our work. This study was supported by the Japan Society for Promotion of Science (JSPS) Funding Program for Next Generation World-Leading Researchers (# GR045).

References

Abbatt, J.P.D., Benz, S., Cziczo, D.J., Kanji, Z., Lohmann, U., and Möhler, O.: Solid ammonium sulfate aerosols as ice nuclei: a pathway for cirrus cloud formation, Science, 313, 1770–1773, doi: 10.1126/science.1129726, 2006.

Adachi, K., Chung, S.H., Friedrich, H., and Buseck, P.R.: Fractal parameters of individual soot particles determined using electron tomography: Implications for optical properties, J. Geophys. Res. Atmos., 112, D14202, doi:10.1029/2006JD008296, 2007.

Akizawa, N., Tamaru, A., Fukushi, K., Yamamoto, J., Mizukami, T., Python, M., and Arai, S.: High-temperature hydrothermal activities around suboceanic Moho: An example from diopsidite and anorthosite in Wadi Fizh, Oman ophiolite, Lithos, 263, 66-87, 2016.

Ardon-Dryer, K., and Levin, Z.: Ground-based measurements of immersion freezing in the eastern Mediterranean, Atmos. Chem. Phys., 14, 5217–5231, doi:10.5194/acp-14-5217-2014, 2014.

Atkinson, J.D., Murray, B.J., Woodhouse, M.T., Whale, T.F., Baustian, K.J., Carslaw, K.S., Dobbie, S., O'Sullivan, D., and Malkin, T.L.: The importance of feldspar for ice nucleation by mineral dust in mixed-phase clouds, Nature, 498, 355-358, doi: 10.1038/nature12278, 2013.

Augustin-Bauditz, S., Wex, H., Denjean, C., Hartmann, S., Schneider, J., Schmidt, S., Ebert, M., and Stratmann, F.: Laboratory generated mixtures of mineral dust particles with biological substances: characterization of the particle mixing state and immersion freezing behavior, Atmos. Chem. Phys., 16, 5531–5543, doi:10.5194/acp-16-5531-2016, 2016.

Ault, A.P., Zhao, D., Ebben, C.J., Tauber, M.J., Geiger, F.M., Prather, K.A., and Grassian, V.H.: Raman microspectroscopy and vibrational sum frequency generation spectroscopy as probes of the bulk and surface compositions of size-resolved sea spray aerosol particles, Phys. Chem. Chem. Phys., 15, 6206-6212, doi: 10.1039/C3CP43899F, 2013.

Batonneau, Y., Sobanska, S., Laureyns, J., and Bremard, C.: Confocal microprobe Raman imaging of urban tropospheric aerosol particles, Environ. Sci. Technol, 40, 1300-1306, doi: 10.1021/es051294x, 2006.

Baustian, K.J., Cziczo, D.J., Wise, M.E., Pratt, K.A., Kulkarni, C., Hallar, A.G., and Tolbert, M.A.: Importance of aerosol composition, mixing state, and morphology for heterogeneous ice nucleation: A combined field and laboratory approach, J. Geophys. Res., 117, D06217, doi: 10.1029/2011JD016784, 2012.

Baustian, K.J., Wise, M.E., and Tolbert, M.A.: Depositional ice nucleation on solid ammonium sulfate and glutaric acid particles, Atmos. Chem. Phys., 10, 2307–2317, 2010.

Boose, Y., Welti, A., Atkinson, J., Ramelli, F., Danielczok, A., Bingemer, H.G., Plötze, M., Sierau, B., Kanji, Z.A., and Lohmann, U.: Heterogeneous ice nucleation on dust particles sourced from nine deserts worldwide – Part 1: Immersion freezing, Atmos. Chem. Phys., 16, 15075-15095, doi:10.5194/acp-16-15075-2016, 2016.

Brooks, S.D., Suter, K., and Olivarez, L.: Effects of chemical aging on the ice nucleation activity of soot and polycyclic aromatic hydrocarbon aerosols, J. Phys. Chem. A, 118, 10036–10047, doi:10.1021/jp508809y, pMID: 25280086, 2014.

Cantrell, W., and Heymsfield, A.: Production of ice in tropospheric clouds: A review, Bull. Am. Meteorol. Soc., 86, 795–807, doi:10.1175/ BAMS-86-6-795, 2005.

Conen, F., Morris, C.E., Leifeld, J., Yakutin, M.V., and Alewell, C.: Biological residues define the ice nucleation properties of soil dust, Atmos. Chem. Phys., 11, 9643–9648, doi:10.5194/acp-11- 9643-2011, 2011.

Connolly, P.J., Möhler, O., Field, P.R., Saathoff, H., Burgess, R., Choularton, T., and Gallagher, M.: Studies of heterogeneous freezing by three different desert dust samples, Atmos. Chem. Phys., 9, 2805–2824, doi:10.5194/acp-9-2805-2009, 2009.

Cziczo, D.J., DeMott, P.J., Brock, C., Hudson, P.K., Jesse, B., Kreidenweis, S.M., Prenni, A.J., Schreiner, J., Thomson, D.S., and Murphy, D.M.: A method for single particle mass spectrometry of ice nuclei, Aerosol Sci. Technol., 37, 460–470, doi:10.1080/02786820300976, 2003.

Cziczo, D.J., Froyd, K.D., Hoose, C., Jensen, E.J., Diao, M., Zondlo, M.A., Smith, J.B., Twohy, C.H., and Murphy, D.M.: Clarifying the dominant sources and mechanisms of cirrus cloud formation, Science, 340, 1320–1324, doi: 10.1126/science.1234145, 2013.

Cziczo, D.J., Stetzer, O., Worringen, A., Ebert, M., Weinbruch, S., Kamphus, M., Gallavardin, S.J., Curtius, J., Borrmann, S., Froyd, K.D., Mertes, S., Möhler, O., and Lohmann, U.: Inadvertent climate modification due to anthropogenic lead, Nat. Geosci., 2, 333–336, doi:10.1038/ngeo499, 2009.

DeMott, P.J., Chen, Y., Kreidenweis, S.M., Rogers, D.C., and Sherman, D.E.: Ice formation by black carbon particles, Geophys. Res. Lett., 26, 2429−2432, doi: 10.1029/1999GL900580, 1999.

DeMott, P.J.: An exploratory study of ice nucleation by soot aerosols, J. Appl. Meteorol., 29, 1072–1079, doi: 10.1175/1520-0450(1990)029<1072:AESOIN>2.0.CO;2, 1990.

Diehl, K., and Mitra, S.K.: A laboratory study of the effects of a kerosene-burner exhaust on ice nucleation and the evaporation rate of ice crystals, Atmos. Environ., 32, 3145−3151, doi: 10.1016/S1352-2310(97)00467-6, 1998.

Ebert, M., Worringen, A., Benker, N., Mertes, S., Weingartner, E., and Weinbruch, S.: Chemical composition and mixing-state of ice residuals sampled within mixed phase clouds, Atmos. Chem. Phys., 11, 2805–2816, doi:10.5194/acp-11-2805-2011, 2011.

Escribano, R., Sloan, J.J., Siddique, N., Sze, N., and Dudev, T.: Raman spectroscopy of carbon-containing particles, Vib. Spectrosc., 26, 179–186, doi: 10.1016/S0924-2031(01)00106-0, 2001.

Flato, G., Marotzke, J., Abiodun, B., Braconnot, P., Chou, S.C., Collins, W., Cox, P., Driouech, F., Emori, S., Eyring, V., Forest, C., Gleckler, P., Guilyardi, E., Jakob, C., Kattsov, V., Reason, C. and Rummukainen, M.: Evaluation of Climate Models. In: Climate Change 2013: The Physical Science Basis. Contribution of Working Group I to the Fifth Assessment Report of the Intergovernmental Panel on Climate Change (eds. T.F. Stocker, D. Qin, G.-K. Plattner, M. Tignor, S.K. Allen, J. Boschung, A. Nauels, Y. Xia, V. Bex and P.M. Midgley), Cambridge University Press, Cambridge, UK and New York, NY, USA, pp. 741–866, 2013.

Fornea, A.P., Brooks, S.D., Dooley, J.B., and Saha, A.: Heterogeneous freezing of ice on atmospheric aerosols containing ash, soot, and soil, J. Geophys. Res., 114, D13201, doi:10.1029/2009JD011958, 2009.

Gaft, M., Reisfeld, R., and Panczer, G.: Modern Luminescence Spectroscopy of Minerals and Materials; Springer-Verlag: Berlin, Heidelberg, doi: 10.1007/b137490, 2005.

Hara, K., Maki, T., Kakikawa, M., Kobayashi, F., and Matsuki, A.: Effects of different temperature treatments on biological ice nuclei in snow samples, Atmos. Environ., 140, 415-419, doi: 10.1016/j.atmosenv.2016.06.011, 2016.

Harrison, A.D., Whale, T.F., Carpenter, M.A., Holden, M.A., Neve, L., O'Sullivan, D., Temprado, J.V., and Murray, B.J.: Not all feldspars are equal: a survey of ice nucleating properties across the feldspar group of minerals, Atmos. Chem. Phys., 16, 10927–10940, doi: 10.5194/acp-16-10927-2016, 2016.

Hiranuma, N., Brooks, S.D., Gramann, J., and Auvermann, B.W.: High concentrations of coarse particles emitted from a cattle feeding operation, Atmos. Chem. Phys., 11, 8809–8823, doi: 10.5194/acp-11-8809-2011, 2011.

Hoose, C., and Möhler, O.: Heterogeneous ice nucleation on atmospheric aerosols: a review of results from laboratory experiments, Atmos. Chem. Phys., 12, 9817–9854, doi: 10.5194/acp-12-9817-2012, 2012.

Huffman, J. A., Sinha, B., Garland, R. M., Snee-Pollmann, A., Gunthe, S. S., Artaxo, P., Martin, S. T., Andreae, M. O., and Pöschl, U.: Size distributions and temporal variations of biological aerosol particles in the Amazon rainforest characterized by microscopy and real-time UV-APS fluorescence techniques during AMAZE-08, Atmos. Chem. Phys., 12, 11997–12019, doi:10.5194/acp-12-11997-2012, 2012.

Ivleva, N.P., Messerer, A., Yang, X., Niessner, R., and Pöschl, U.: Raman microspectroscopic analysis of changes in the chemical structure and reactivity of soot in a diesel exhaust aftertreatment model system, Environ. Sci. Technol., 41, 3702-3707, doi: 10.1021/es0612448, 2007.

Iwamoto,Y., Kinouchi, K., Watanabe, K., Yamazaki, N., and Matsuki, A.: Simultaneous measurement of CCN activity and chemical composition of fine mode aerosols at Noto Peninsula, Japan, in autumn 2012, Aerosol Air Qual. Res., 16, 2107–2118, doi: 10.4209/aaqr.2015.09.0545, 2016.

~~Iwasaka, Y., Nishikawa, M., Yamada, M., and Hong, C.S.: KOSA, Kokin Shoin Press, Tokyo, 342 p., 2009 (in Japanese).~~

Iwasaka, Y., Nishikawa, M., Yamada, M., and Hong, C.S.: KOSA, Kokin Shoin Press, Tokyo, 342 p., 2009a (in Japanese).

Iwasaka, Y., Shi, G. Y., Yamada, M., Kobayashi, F., Kakikawa, M., Maki, T., Chen, B., Tobo, Y., and Hong, C.: Mixture of Kosa (Asian dust) and bioaerosols detected in the atmosphere over the Kosa particles source regions with balloon-borne measurements: possibility of long-range transport, Air. Qual. Atmos. Health., 2, 29–38, 2009b.

Jung, H.J., Eom, H.J., Kang, H.W., Moreau, M., Sobanska, S., and Ro, C.U.: Combined use of quantitative ED-EPMA, Raman microspecrometry, and ATR-FTIR imaging techniques for the analysis of individual particles, Analyst, 139, 3949–3960, doi: 10.1039/c4an00380b, 2014.

Kamphus, M., Ettner-Mahl, M., Klimach, T., Drewnick, F., Keller, L., Cziczo, D.J., Mertes, S., Borrmann, S., and Curtius, J.: Chemical composition of ambient aerosol, ice residues and cloud droplet residues in mixed-phase clouds: single

particle analysis during the Cloud and Aerosol Characterization Experiment (CLACE 6), Atmos. Chem. Phys., 10, 8077–8095, doi:10.5194/acp-10-8077-2010, 2010.

Kaufmann, L., Marcolli, C., Hofer, J., Pinti, V., Hoyle, C.R., and Peter, T.: Ice nucleation efficiency of natural dust samples in the immersion mode, Atmos. Chem. Phys., 16, 11177–11206, doi: 10.5194/acp-16-11177-2016, 2016.

Kawamura, K., Kobayashi, M., Tsubonuma, N., Mochida, M., Watanabe, T., and Lee, M.: Organic and inorganic compositions of marine aerosols from East Asia: Seasonal variations of water-soluble dicarboxylic acids, major ions, total carbon and nitrogen, and stable C and N isotopic composition, Geochemical Investigation in Earth and Space Science: A Tribute to Isaac R. Kaplan (eds. R.J. Hill, J. Leventhal, Z. Aizenshtat, M.J. Baedecker, G. Claypool, R. Eganhouse, M. Goldhaber, and K. Peters), The Geochemical Society Special Publications Elsevier, 9, 243-265, 2004.

Kawamura, K., and Gagosian, R.B.: Implications of ω-oxocarboxylic acids in the remote marine atmosphere for photo-oxidation of unsaturated fatty acids, Nature, 325, 330–332, doi:10.1038/325330a0, 1987.

Kireeva, E.D., Popovicheva, O.B., Persiantseva, N.M., Khokhlova, T.D., and Shonija, N.K.: Effect of black carbon particles on the efficiency of water droplet freezing, Colloid J., 71, 353–359, doi: 10.1134/S1061933X09030090, 2009.

Klein, H., Haunold, W., Bundke, U., Nillius, B., Wetter, T., Schallenberg, S., and Bingemer, H.: A new method for sampling of atmospheric ice nuclei with subsequent analysis in a static diffusion chamber, Atmos. Res., 96, 218–224, doi:10.1016/j.atmosres.2009.08.002, 2010.

Knopf, D. A., Alpert, P. A., Wang, B., O'Brien, R. E., Kelly, S. T., Laskin, A., Gilles, M. K., and Moffet, R. C.: Microspectroscopic imaging and characterization of individually identified ice nucleating particles from a case field study, J. Geophys. Res. Atmos., 119, JD021866, doi:10.1002/2014JD021866 , 2014.

Knopf, D.A., Wang, B., Laskin, A., Moffet, R.C., and Gilles, M.K.: Heterogeneous nucleation of ice on anthropogenic organic particles collected in Mexico City, Geophys. Res. Lett., 37, L11803, doi:10.1029/ 2010GL043362, 2010.

Koop, T., Luo, B. P., Tsias, A., and Peter, T.: Water activity as the determinant for homogeneous ice nucleation in aqueous solutions, Nature, 406, 611–614, 2000.

Korolev, A.: Limitations of the Wegener-Bergeron-Findeisen Mechanism in the Evolution of Mixed-Phase Clouds, J. Atmos. Sci., 64, 3372–3375, doi:10.1175/JAS4035.1, 2007.

Kulkarni, G., Sanders, C., Zhang, K., Liu, X., and Zhao, C.: Ice nucleation of bare and sulfuric acid-coated mineral dust particles and implication for cloud properties, J. Geophys. Res. Atmos., 119, 9993–10011, doi:10.1002/2014JD021567, 2014.

Kupiszewski, P., Weingartner, E., Vochezer, P., Schnaiter, M., Bigi, A., Gysel, M., Rosati, B., Toprak, E., and Baltensperger, U.: The ice selective inlet: a novel technique for exclusive extraction of pristine ice crystals in mixed-phase clouds, Atmos. Meas. Tech., 8, 3087–3106, doi: 10.5194/amt-8-3087-2015, 2015.

Laskin, A., Iedema, M.J., Ichkovich, A., Graber, E.R., Taraniuk, I., and Rudich, Y.: Direct observation of completely processed calcium carbonate dust particles, Faraday Discuss., 130, 453– 468, doi:10.1039/b417366j, 2005.

Laskina, O., Young, M.A., Kleiber, P.D., and Grassian, V.H.: Infrared extinction spectroscopy and micro-Raman spectroscopy of select components of mineral dust mixed with organic compounds, J. Geophys. Res. Atmos, 118, 6593–6606, doi:10.1002/jgrd.50494, 2013.

Lohmann, U. and Feichter, J.: Global indirect aerosol effects: a review, Atmos. Chem. Phys., 5, 715–737, doi: 1680-7324/acp/2005-5-715, 2005.

Maki, T., Susuki, S., Kobayashi, F., Kakikawa, M., Tobo, Y., Yamada, M., Higashi, T., Matsuki, A., Hong, C., Hasegawa, H., and Iwasaka, Y.: Phylogenetic analysis of atmospheric halotolerant bacterial communities at high altitude in an Asian dust (KOSA) arrival region, Suzu City, Sci. Total Environ., 408, 4556–4562, doi:10.1016/j.scitotenv.2010.04.002, 2010.

Maring, H., Savoie, D. L., Izaguirre, M. A., Custals, L., and Reid, J. S.: Mineral dust aerosol size distribution change during atmospheric transport, J. Geophys. Res., 108(D19), 8592, doi:10.1029/2002JD002536, 2003.

Mason, R.H., Chou, C., McCluskey, C.S., Levin, E.J.T., Schiller, C.L., Hill, T.C.J., Huffman, J.A., DeMott, P.J., and Bertram, A.K.: The micro-orifice uniform deposit impactor–droplet freezing technique (MOUDI-DFT) for measuring concentrations of ice nucleating particles as a function of size: improvements and initial validation, Atmos. Meas. Tech., 8, 2449–2462, doi: 10.5194/amt-8-2449-2015, 2015.

Matsuki, A., Iwasaka, Y., Osada, K., Matsunaga, K., Kido, M., Inomata, Y., Trochkine, D., Nishita, C., Nezuka, T., Sakai, T., Zhang, D., and Kwon, S.-A.: Seasonal dependence of the long-range transport and vertical distribution of free tropospheric aerosols over east Asia: On the basis of aircraft and lidar measurements and isentropic trajectory analysis. J. Geophys. Res., 108, 8663, doi: 10.1029/2002JD003266, 2003.

Matsuki, A., Iwasaka, Y., Shi, G.Y., Zhang, D.Z., Trochkine, D., Yamada, M., Kim, Y.S., Chen, B., Nagatani, T., Miyazawa, T., Nagatani, M., and Nakata, H.: Morphological and chemical modification of mineral dust: Observational insight into the heterogeneous uptake of acidic gases, Geophys. Res. Lett., 32, L22806, doi:10.1029/2005GL024176, 2005

Mertes, S., Verheggen, B., Walter, S., Connolly, P., Ebert, M., Schneider, J., Bower, K.N., Cozic, J., Weinbruch, S., Baltensperger, U., and Weingartner, E.: Counterflow virtual impactor based collection of small ice particles in mixed-phase clouds for the physico-chemical characterization of tropospheric ice nuclei: Sampler description and first case study, Aerosol Sci. Technol., 41, 848–864, doi:10.1080/02786820701501881, 2007.

Morris, C.E., Georgakopoulos, D.G., Sands, D.C.: Ice nucleation active bacteria and their potential role in precipitation. J. Phys. *IV*. Fr., 121, 87-103, doi: 10.1051/jp4:2004121004, 2004.

Murray, B. J., Broadley, S. L., Wilson, T. W., Atkinson, J. D., and Wills, R. H.: Heterogeneous freezing of water droplets containing kaolinite particles, Atmos. Chem. Phys., 11, 4191–4207, doi:10.5194/acp-11-4191-2011, 2011.

Murray, B.J., Broadley, S.L., Wilson, T.W., Bull, S.J., Wills, R.H., Christenson, H.K., and Murrary, E.J.: Kinetics of the homogeneous freezing of water, Phys. Chem. Chem. Phys., 12, 10380–10387, doi: 10.1039/C003297B, 2010.

Murray, B.J., O'Sullivan, D., Atkinson, J.D., and Webb, M.E.: Ice nucleation by particles immersed in supercooled cloud droplets, Chem. Soc. Rev., 41, 6519–6554, doi: 10.1039/C2CS35200A, 2012.

Möhler, O., Benz, S., Saathoff, H., Schnaiter, M., Wagner, R., Schneider, J., Walter, S., Ebert, V., and Wagner, S.: The effect of organic coating on the heterogeneous ice nucleation efficiency of mineral dust aerosols, Environ. Res. Lett., 3, 025007, doi:10.1088/1748-9326/3/2/025007, 2008a.

Möhler, O., Georgakopoulos, D.G., Morris, C.E., Benz, S., Ebert, V., Hunsmann, S., Saathoff, H., Schnaiter, M., and Wagner, R.: Heterogeneous ice nucleation activity of bacteria: new laboratory experiments at simulated cloud conditions, Biogeosciences, 5, 1425–1435, doi: 10.5194/bg-5-1425-2008, 2008b.

Niemand, M., Möhler, O., Vogel, B., Vogel, H., Hoose, C., Connolly, P., Klein, H., Bingemer, H., DeMott, P., Skrotzki, J., and Leisner, T.: A particle-surface-area-based parameterization of immersion freezing on desert dust particles, J. Atmos. Sci., 69, 3077–3092, doi:10.1175/Jas-D-11-0249.1, 2012.

Niimura, N., Okada, K., Fan, X.B., Kai, K., Arao, K., Shi, G.Y., and Takahashi, S.: Formation of Asian dust-storm particles mixed internally with sea-salt in the atmosphere, J. Meteorol. Soc. Jpn., 76, 275–288, 1998.

O'Sullivan, D., Murray, B.J., Malkin, T.L., Whale, T.F., Umo, N.S., Atkinson, J.D., Price, H.C., Baustian, K.J., Browse, J., and Webb, M.E.: Ice nucleation by fertile soil dusts: Relative importance of mineral and biogenic components, Atmos. Chem. Phys., 14, 1853–1867, doi:10.5194/acp-14-1853-2014, 2014.

Petters, M.D., Parsons, M.T., Prenni, A.J., DeMott, P.J., Kreidenweis, S.M., Carrico, C.M., Sullivan, A.P., McMeeking, G.R., Levin, E., Wold, C.E., Collett Jr., J.L., and Moosmüller, H.: Ice nuclei emissions from biomass burning, J. Geophys. Res., 114, D07209, doi: 10.1029/2008JD011532, 2009.

Prenni, A. J., DeMott, P. J., Sullivan, A. P., Sullivan, R. C., Kreidenweis, S. M., and Rogers, D. C.: Biomass burning as a potential source for atmospheric ice nuclei: Western wildfires and prescribed burns, Geophys. Res. Lett., 39, L11805, doi:10.1029/2012GL051915, 2012.

Prenni, A.J., Demott, P.J., Rogers, D.C., Kreidenweis, S.M., McFarquhar, G.M., Zhang, G., and Poellot, M.R.: Ice nuclei characteristics from M-PACE and their relation to ice formation in clouds, Tellus B, 61, 436–448, doi:10.1111/j.1600-0889.2009.00415.x, 2009a.

Prenni, A.J., Petters, M.D., Faulhaber, A., Carrico, C.M., Ziemann, P.J., Kreidenweis, S.M., and DeMott, P.J.: Heterogeneous ice nucleation measurements of secondary organic aerosol generated from ozonolysis of alkenes, Geophys. Res. Lett., 36, L06 808, doi: 10.1029/2008GL036957, l06808, 2009b.

Pruppacher, H.R., and Klett, J.D.: Microphysics of Clouds and Precipitation, Kluwer Academic Publishers, Dordrecht, The Netherlands,1997.

Pummer, B.G., Bauer, H., Bernardi, J., Bleicher, S., and Grothe, H.: Suspendable macromolecules are responsible for ice nucleation activity of birch and conifer pollen, Atmos. Chem. Phys., 12, 2541–2550, doi:10.5194/acp-12-2541-2012, 2012.

Rogers, D.C., DeMott, P.J., Kreidenweis, S.M., and Chen, Y.: Measurements of ice nucleating aerosols during SUCCESS, Geophys. Res. Lett., 25, 1383–1386, doi: 10.1029/97GL03478, 1998.

Rolph, G.D.: Real-time Environmental Applications and Display sYstem (READY), Website (http://www.ready.noaa.gov), National Oceanic and Atmospheric Administration (NOAA), Air Resources Laboratory (ARL), College Park, MD, USA, 2017.

Rosenfeld, D., Lohmann, U., Raga, G.B., O'Dowd, C.D., Kulmala, M., Fuzzi, S., Reissel, A., and Andreae, M.O.: Flood or drought: How do aerosols affect precipitation?, Science, 321, 1309–1313, doi: 10.1126/science.1160606, 2008.

Rosenfeld, D., and Woodley, W.L.: Deep convective clouds with sustained supercooled liquid water down to -37.5 ˚C, Nature, 405, 440–442, doi: 10.1038/35013030, 2000.

Sadezky, A., Muckenhuber, H., Groyhe, H., Niessner, R., and Pöschl: Raman microspectroscopy of soot and related carbonaceous materials: Spectral analysis and structural information, Carbon, 43 1731–1742, doi: 10.1016/j.carbon.2005.02.018, 2005.

Schrod, J., Danielczok, A., Weber, D., Ebert, M., Thomson, E. S., and Bingemer, H. G.: Re-evaluating the Frankfurt isothermal static diffusion chamber for ice nucleation, Atmos. Meas. Tech., 9, 1313–1324, doi:10.5194/amt-9-1313-2016, 2016.

Schrod, J., Weber, D., Drücke, J., Keleshis, C., Pikridas, M., Ebert, M., Cvetkovic, B., Nickovic, S., Marinou, E., Baars, H., Ansmann, A., Vrekoussis, M., Mihalopoulos, N., Sciare, J., Curtius, J., and Bingemer, H. G.: Ice nucleating particles over the Eastern Mediterranean measured by unmanned aircraft systems, Atmos. Chem. Phys., 17, 4817–4835, https://doi.org/10.5194/acp- 17-4817-2017, 2017.

Sobanska, S., Falgayrac, G., Rimetz-Planchon, J., Perdrix, E., Brémard, C., and Barbillat, J.: Resolving the internal structure of individual atmospheric aerosol particle by the combination of Atomic Force Microscopy, ESEM–EDX, Raman and ToF–SIMS imaging, Microchem. J., 114: 89–98, doi: 10.1016/j.microc.2013.12.007, 2014.

Sobanska, S., Hwang, H., Choel, M., Jung, H.-J., Eom, H.-J., Kim, ¨ H., Barbillat, J., and Ro, C.-U.: Investigation of the chemical mixing state of individual Asian dust particles by the combined use of electron probe X-ray microanalysis and Raman microspectrometry, Anal. Chem., 84, 3145–3154, 2012.

Stein, A.F., Draxler, R.R, Rolph, G.D., Stunder, B.J.B., Cohen, M.D., and Ngan, F.: NOAA's HYSPLIT atmospheric transport and dispersion modeling system, Bull. Amer. Meteor. Soc., 96, 2059-2077, doi: 10.1175/BAMS-D-14-00110.1, 2015.

Sullivan, R. C., Guazzotti, S. A., Sodeman, D. A., and Prather, K. A.: Direct observations of the atmospheric processing of Asian mineral dust, Atmos. Chem. Phys., 7, 1213–1236, 10 doi:10.5194/acp-7-1213-2007, 2007.

Sullivan, R.C., Petters, M.D., DeMott, P.J., Kreidenweis, S.M., Wex, H., Niedermeier, D., Hartmann, S., Clauss, T., Stratmann, F., Reitz, P., Schneider, J., and Sierau, B.: Irreversible loss of ice nucleation active sites in mineral dust particles caused by sulphuric acid condensation, Atmos. Chem. Phys., 10, 11471–11487, doi:10.5194/acp-10-11471-2010, 2010.

Tang, I.N., and Fung, K.H.: Characterization of inorganic salt particles by Raman spectroscopy, J. Aerosol Sci., 20, 609-617, doi: 10.1016/0021-8502(89)90106-7, 1989.

Tobo, Y., DeMott, P.J., Hill, T.C.J., Prenni, A.J., Swoboda-Colberg, N.G., Franc, G.D., and Kreidenweis, S.M.: Organic matter matters for ice nuclei of agricultural soil origin, Atmos. Chem. Phys., 14, 8521–8531, doi:10.5194/acp-14-8521-2014, 2014.

Tobo, Y., Zhang, D., Matsuki, A., and Iwasaka, Y.: Asian dust particles converted into aqueous droplets under remote marine atmospheric conditions, Proc. Natl. Acad. Sci. USA, 107, 17905–17910, doi: 10.1073/pnas.1008235107, 2010.

Tong, H.-J., Reid, J. P., Bones, D. L., Luo, B. P., and Krieger, U. K.: Measurements of the timescales for the mass transfer of water in glassy aerosol at low relative humidity and ambient temperature, Atmos. Chem. Phys., 11, 4739–4754, doi:10.5194/acp-11-4739- 2011, 2011.

Trochkine, D., Iwasaka, Y., Matsuki, A., Yamada, M., Kim, Y.-S., Nagatani, T., Zhang, D., Shi, G.-Y., and Shen Z.: Mineral aerosol particles collected in Dunhuang, China, and their comparison with chemically modified particles collected over Japan, J. Geophys. Res., 108, 8642, doi:10.1029/2002JD003268, 2003.

Twohy, C. H., McMeeking, G. R., DeMott, P. J., McCluskey, C. S., Hill, T. C. J., Burrows, S. M., Kulkarni, G. R., Tanarhte, M., Kafle, D. N., and Toohey, D. W.: Abundance of fluorescent biological aerosol particles at temperatures conducive to the formation of mixed-phase and cirrus clouds, Atmos. Chem. Phys., 16, 8205–8225, https://doi.org/10.5194/acp-16-8205-2016, 2016.

Ueda, S., Osada, K., and Takami, A.: Morphological features of soot-containing particles internally mixed with water-soluble materials in continental outflow observed at Cape Hedo, Okinawa, Japan. J. Geophys. Res., Atmos., 116, D17207, doi: 10.1029/2010JD015565, 2011.

Whale, T.F., Murray, B.J., O'Sullivan, D., Wilson, T.W., Umo, N.S., Baustian, K.J., Atkinson, J.D., Workneh, D.A., and Morris, G.J.: A technique for quantifying heterogeneous ice nucleation in microlitre supercooled water droplets, Atmos. Meas. Tech., 8, 2437–2447, doi: 10.5194/amt-8-2437-2015, 2015.

Wilson, T.W., Ladino, L.A., Alpert, P.A., Breckels, M.N., Brooks, I.M., Browse, J., Burrows, S.M., Carslaw, K.S., Huffman, J.A., Judd, C., Kilthau, W.P., Mason, R.H., McFiggans, G., Miller, L.A., Nájera, J.J., Polishchuk, E., Rae, S., Schiller, C.L., Si, M., Temprado, J.V., Whale, T.F., Wong, J.P.S., Wurl, O., Yakobi-Hancock, J.D., Abbatt, J.P.D., Aller, J.Y., Bertram, A.K., Knopf, D.A., and Murray, B.J.: A marine biogenic source of atmospheric ice-nucleating particles. Nature 525, 234–238, doi: 10.1038/nature14986, 2015.

Wise, M.E., Baustian, K.J., Koop, T., Freedman, M.A., Jensen, E.J., and Tolbert, M.A.: Depositional ice nucleation onto crystalline hydrated NaCl particles: a new mechanism for ice formation in the troposphere, Atmos. Chem. Phys., 12, 1121-1134, doi: 10.5194/acp-12-1121-2012, 2012.

Worringen, A., Kandler, K., Benker, N., Dirsch, T., Mertes, S., Schenk, L., Kästner, U., Frank, F., Nillius, B., Bundke, U., Rose, D., Curtius, J., Kupiszewski, P., Weingartner, E., Vochezer, P., Schneider, J., Schmidt, S., Weinbruch, S., and Ebert, M.: Single-particle characterization of ice-nucleating particles and ice particle residuals sampled by three different techniques, Atmos. Chem. Phys., 15, 4161-4178, doi: 10.5194/acp-15-4161-2015, 2015.

Yabuki, S., Kanayama, S., Honda, M.: Mineral composition of certified reference material: China loess (CJ1) and simulated asian mineral dust (CJ2), Chikyu Kankyo, 7, 171–179, 2002 (in Japanese).

Zhang, D., Iwasaka, Y., Shi, G., Zang, J., Matsuki, A., and Trochkine, D.: Mixture state and size of Asian dust particles collected at southwestern Japan in spring 2000. J. Geophys. Res., 108, 4760, doi: 10.1029/2003JD003869, 2003.

Zimmermann, F., Weinbruch, S., Schütz, L., Hofmann, H., Ebert, M., Kandler, K., and Worringen, A.: Ice nucleation properties of the most abundant mineral dust phases, J. Geophys. Res., 113, D23204, doi: 10.1029/2008JD010655, 2008.

Zolles, T., Burkart, J., Häusler, T., Pummer, B., Hitzenberger, R., and Grothe, H.: Identification of ice nucleation active sites on feldspar dust particles, J. Phys. Chem. A, 119, 2692–2700, doi:10.1021/jp509839x, 2015.

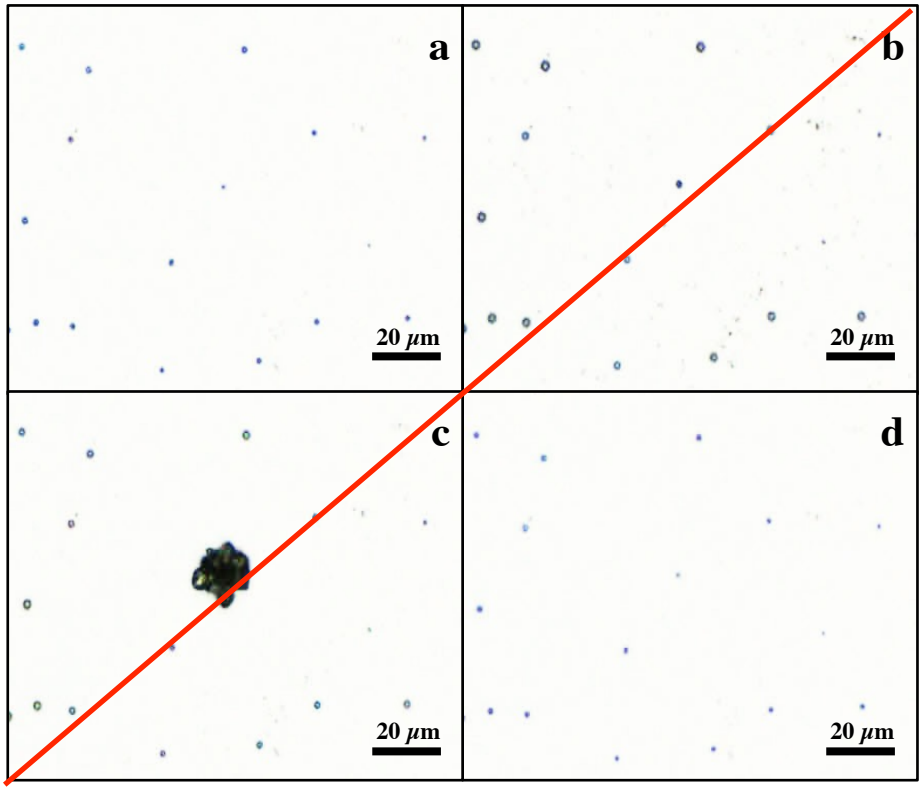

Figure 2: Optical images of sample particles deposited on Si wafer substrate before the freezing experiment (a), after exposure to water super saturation conditions at -9 °C (b), after cooling to -30 °C (c), and after evaporation by dry air (d).

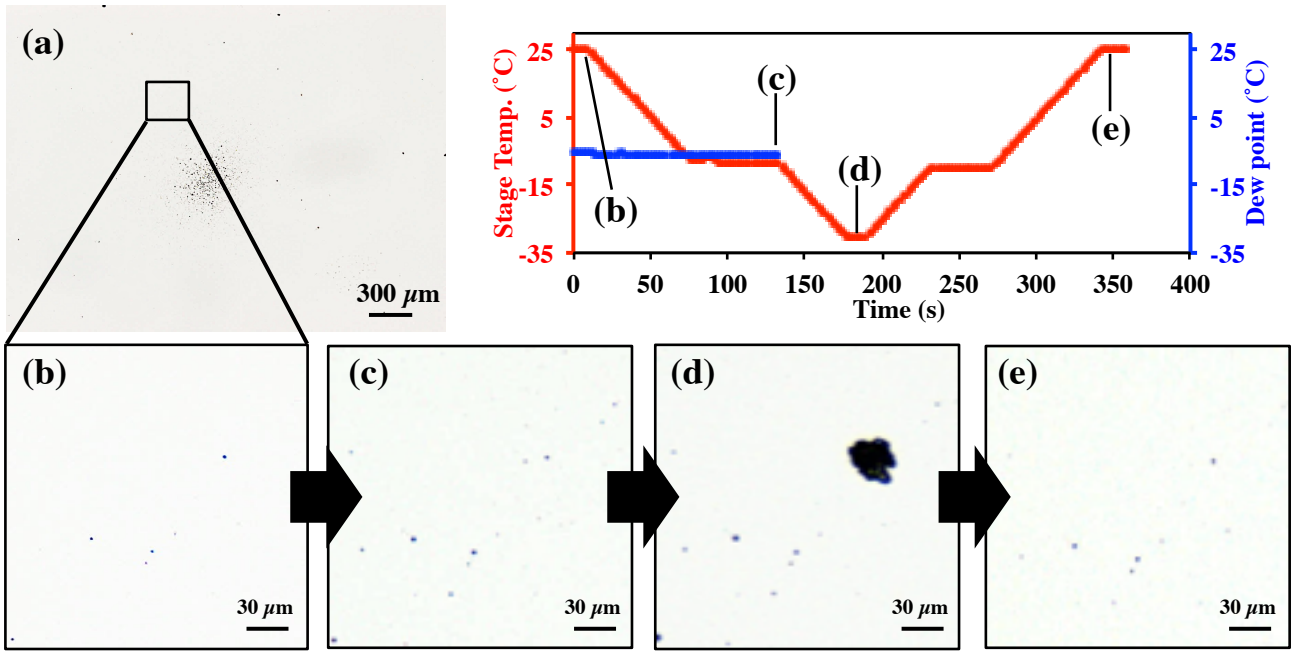

Figure 1: Optical images of sample particles deposited on Si wafer substrate before the freezing experiment (a, b), after exposure to water super saturation conditions at -9 ˚C (c), after cooling to -30 ˚C (d), and after sublimation and evaporation by dry air (e). The inset graph shows the stage temperature and the dew point of the wet air introduced into the cell before exposing the stage to water super saturation.

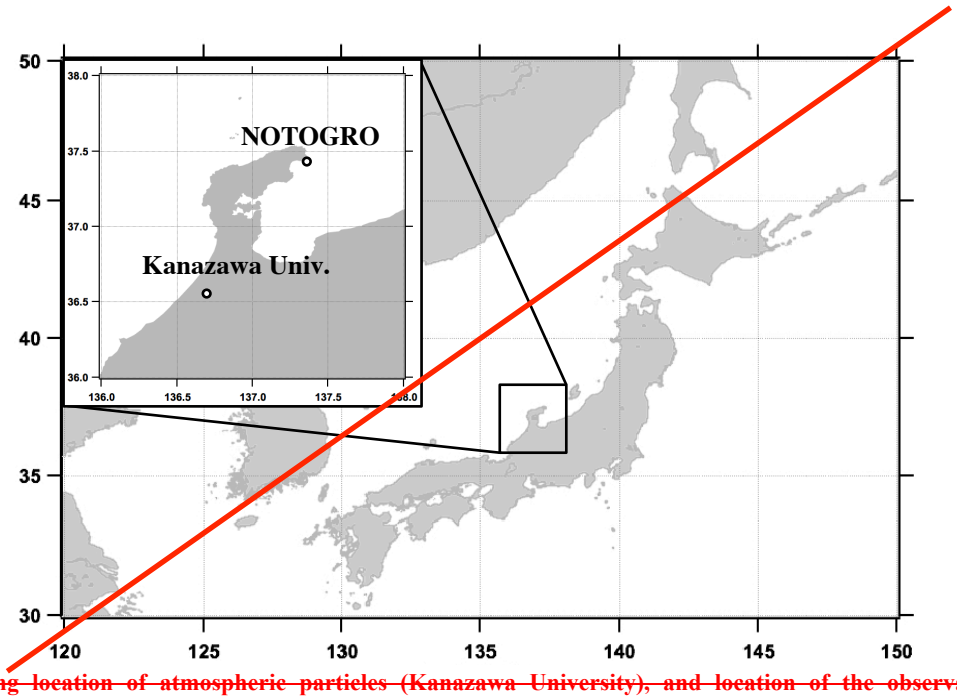

~~Figure 3: Sampling location of atmospheric particles (Kanazawa University), and location of the observatory for particle concentration monitoring (NOTO Ground-based Research Observatory: NOTOGRO).~~

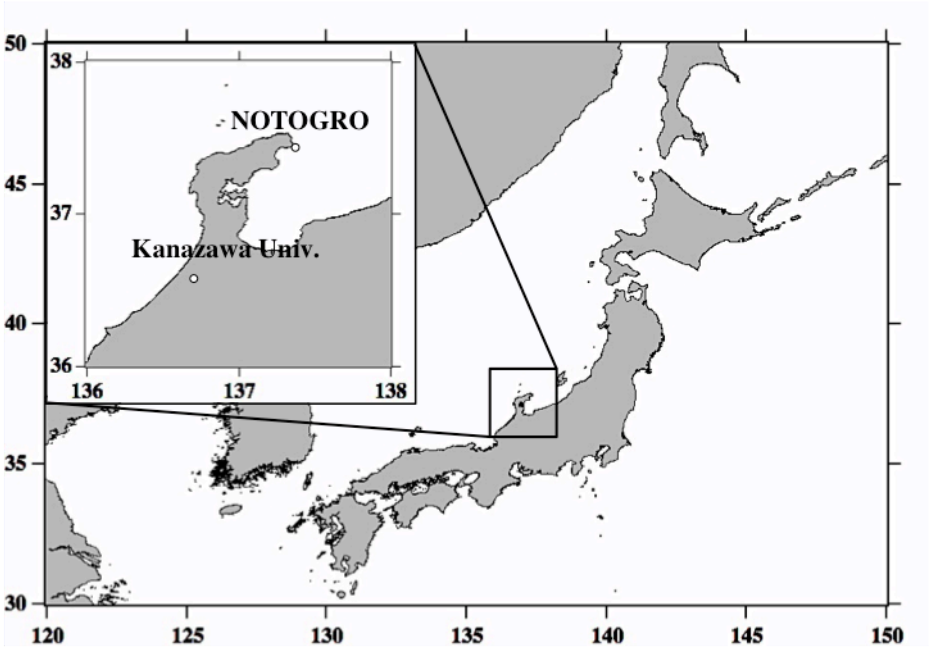

Figure 2: Sampling location of atmospheric particles (Kanazawa University), and location of the observatory for particle concentration monitoring (NOTO Ground-based Research Observatory: NOTOGRO).

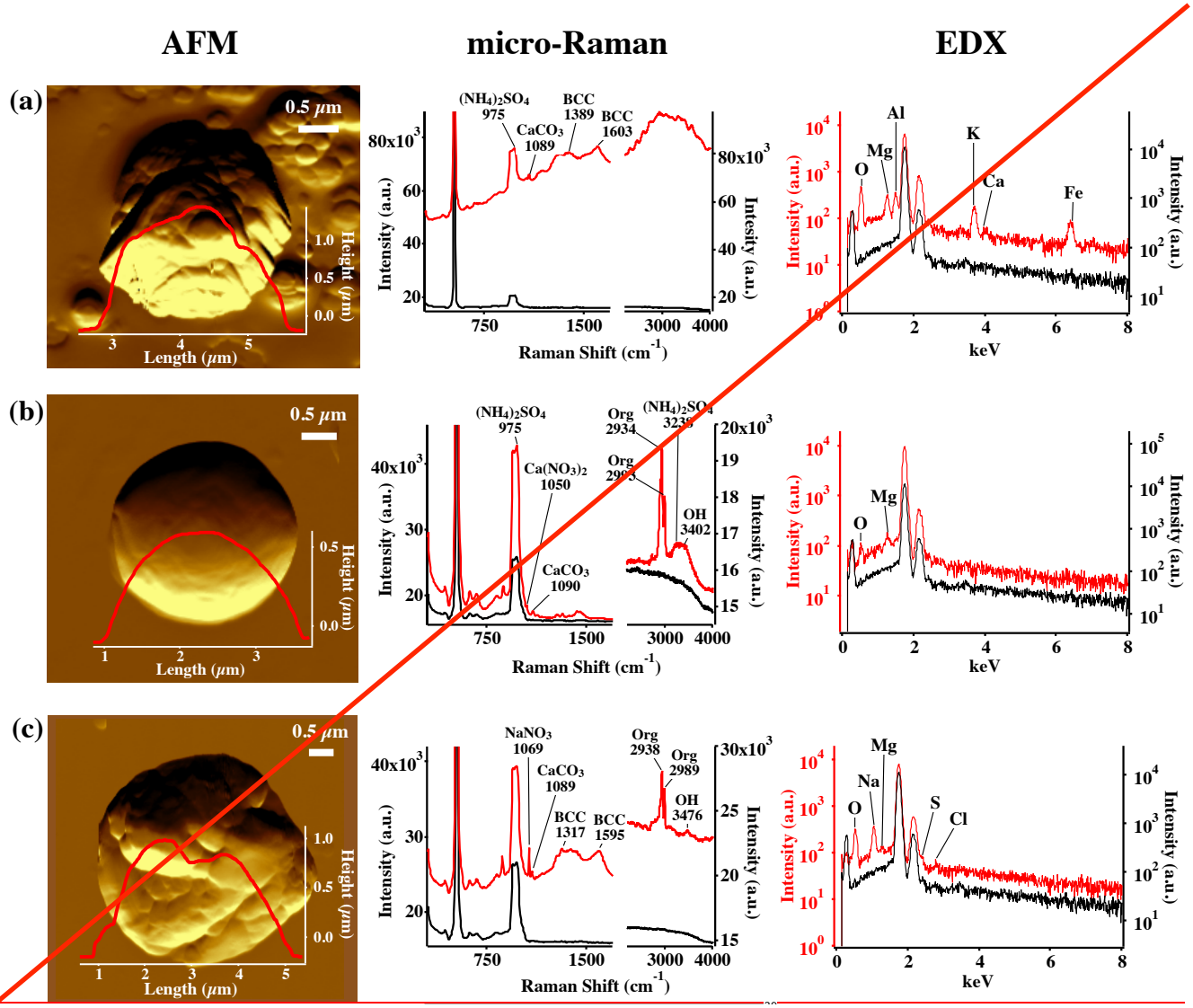

~~Figure 4: AFM topographic images of representative IN active particle (a) and non-active particle (b, c) groups, and their corresponding Raman and EDX spectra. The AFM images were obtained in probe amplitude mode. The inset in the AFM image shows the height of each particle. The red and black curves indicate the spectra of the particles and the substrate background, respectively~~.

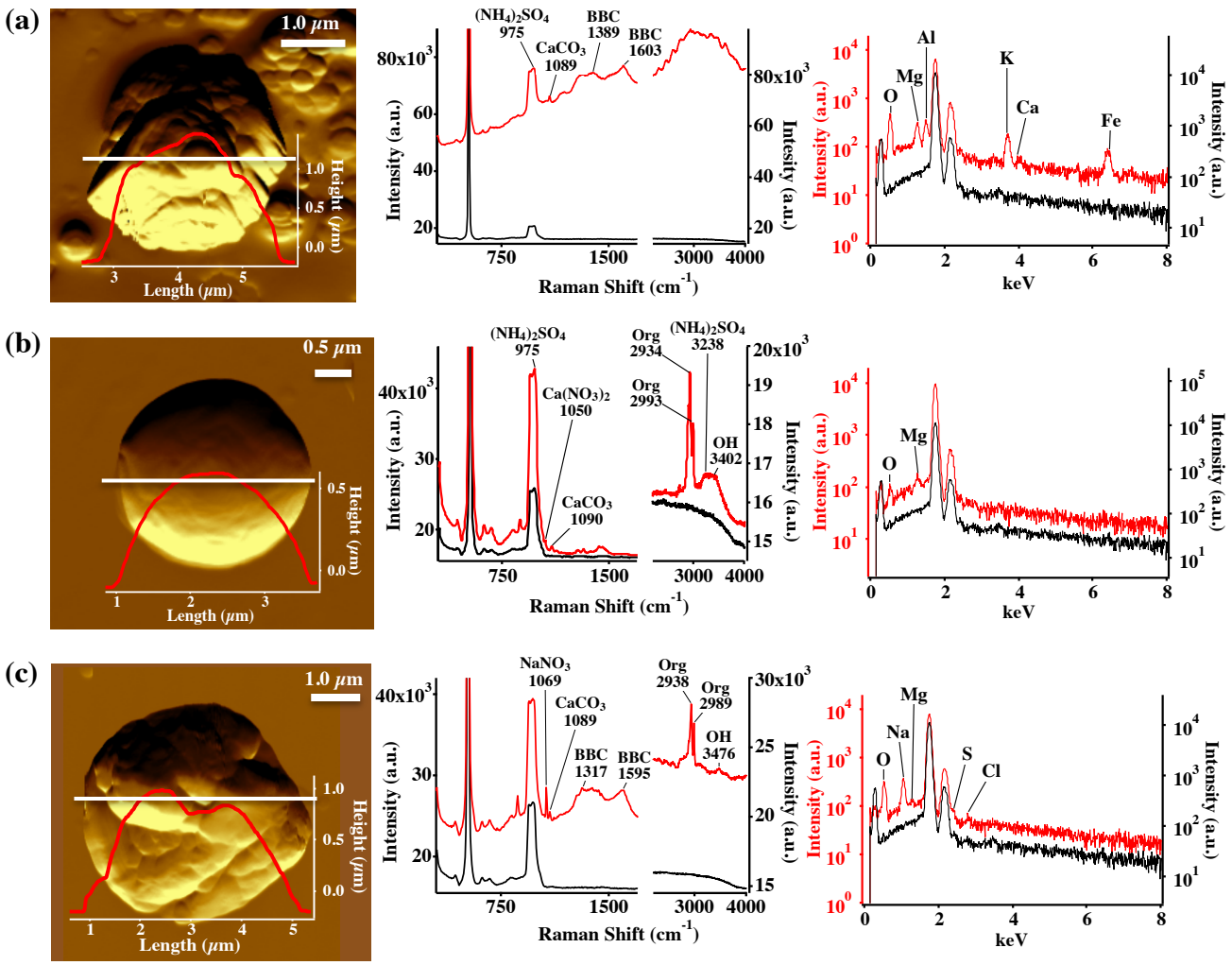

Figure 3: AFM topographic images of representative IN active particle (a) and non-active particle (b, c) groups, and their corresponding Raman and EDX spectra. The AFM images were obtained in probe amplitude mode. The inset in the AFM image shows the scanned height along the white transect of each particle. The red and black curves indicate the spectra of the particles and the substrate background, respectively.

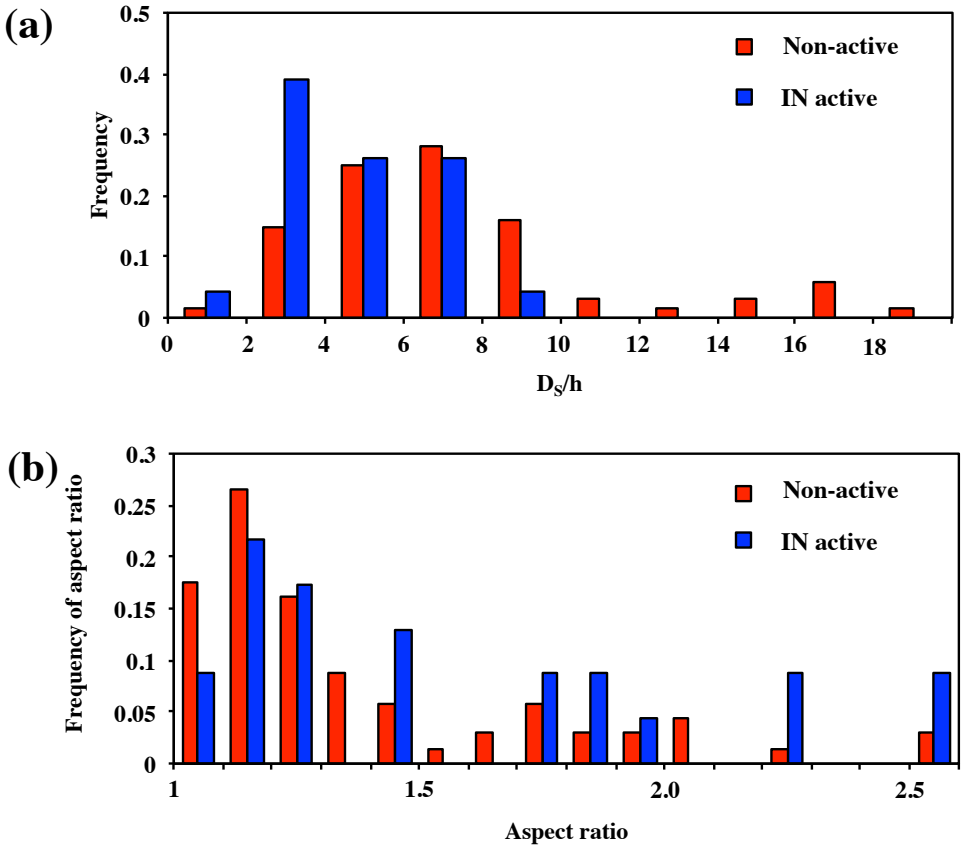

Figure 5: Frequency distributions of D_S/h (a) and aspect ratio (b), for non-active and IN active particles from AFM observation.

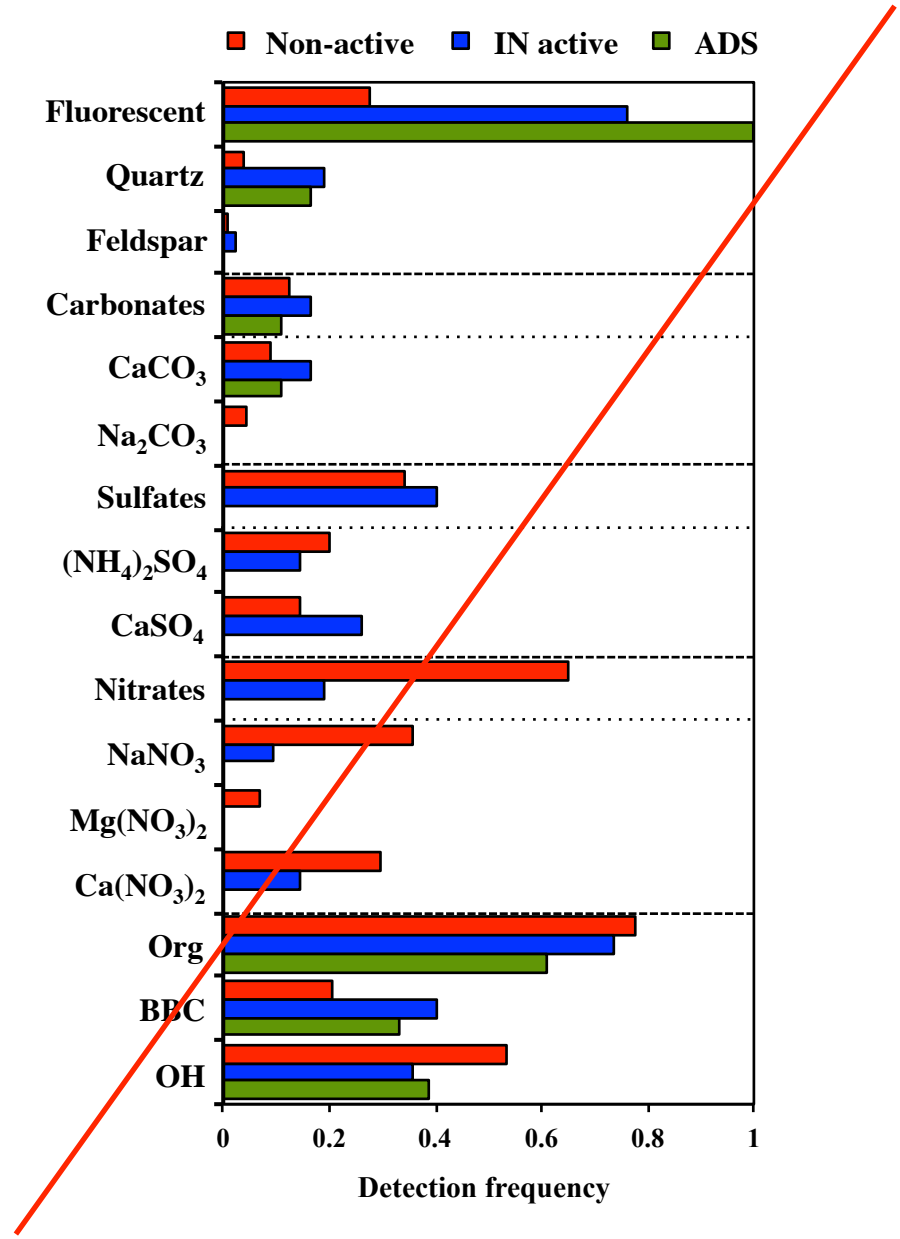

~~Figure 6: Summary of the detection frequencies of the assigned components in non-active and IN active particles by micro-Raman analysis. Data from Asian dust source (ADS) particles are shown for comparison. The detection frequencies of sulfates, carbonates and nitrates are further classified based on the counter cations (NH_4, Na, Mg, and Ca).~~

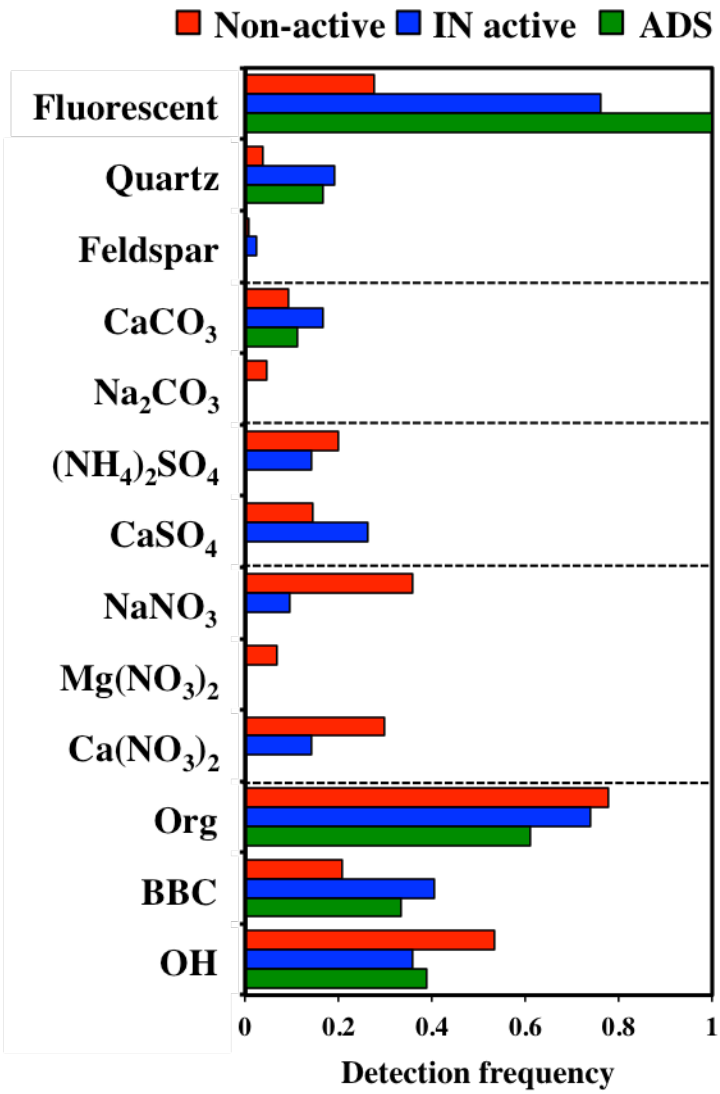

Figure 5: Summary of the detection frequencies of the assigned components in non-active and IN active particles by micro-Raman analysis. Data from Asian dust source (ADS) particles are shown for comparison.

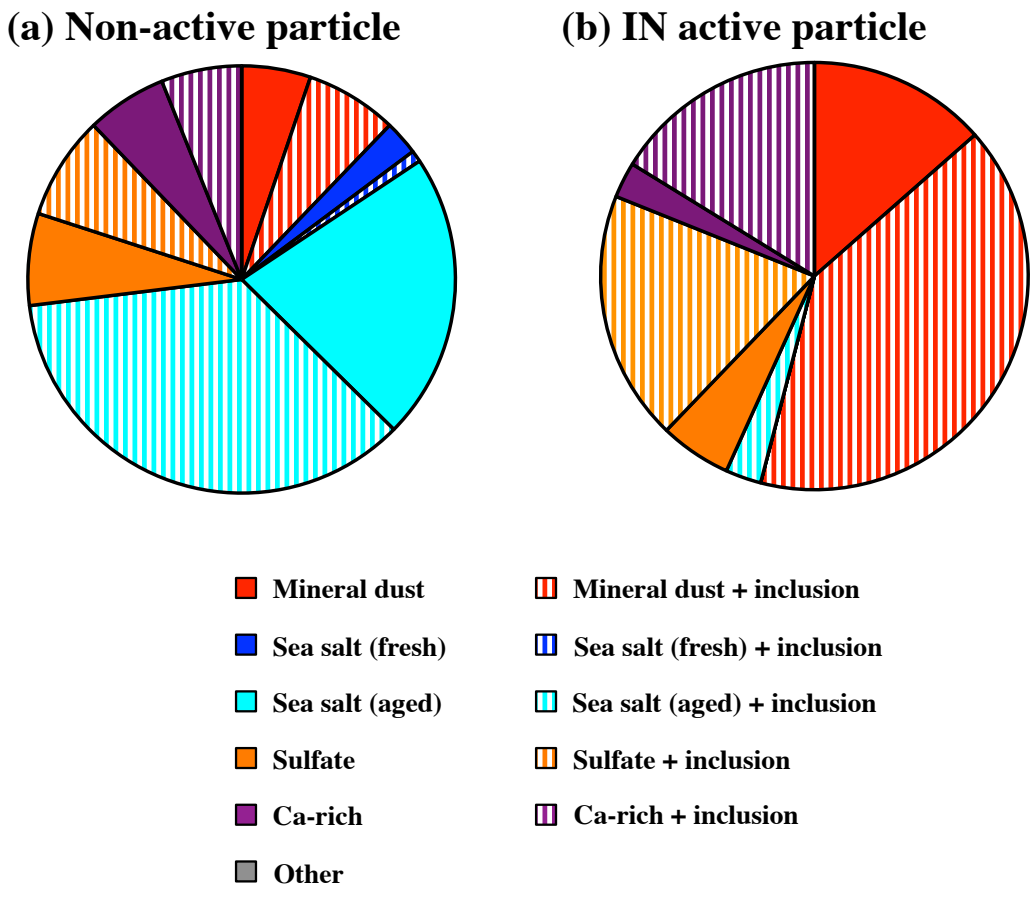

Figure 7: Relative abundance of the particle groups identified by SEM-EDX for non-active and IN active particles. April and February samples are combined.

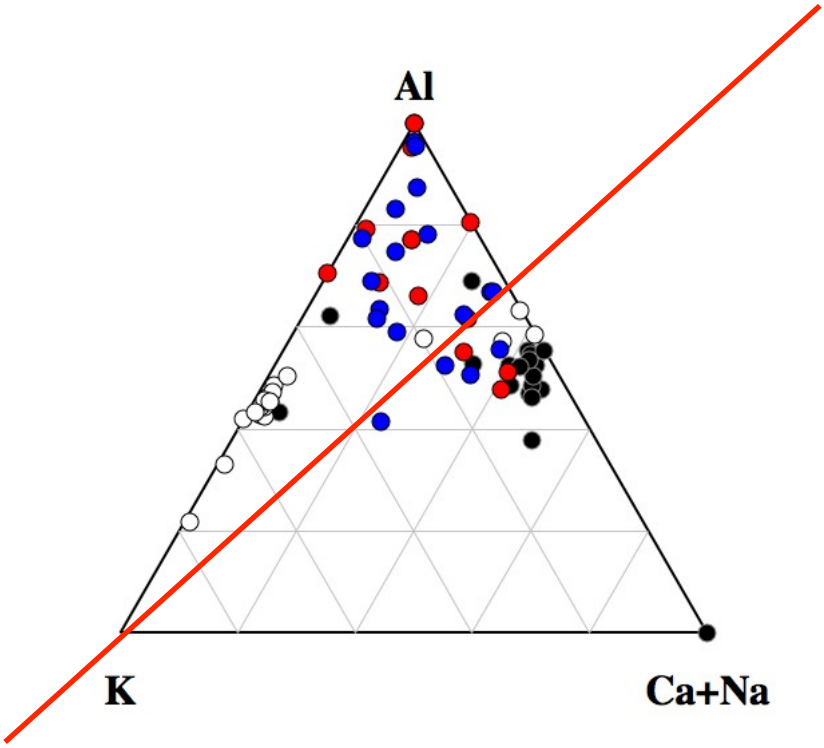

~~**Figure 8: Ternary diagram of Al-K-(Ca+Na) components, showing the compositions of mineral dust particles identified by SEM-EDX analysis. Data presented in relative atomic proportions. The circle symbols indicate non-active particles (red) and IN active particles (blue). Particles of Na-feldspar (black) and K-feldspar (white) are also shown for comparison.**~~

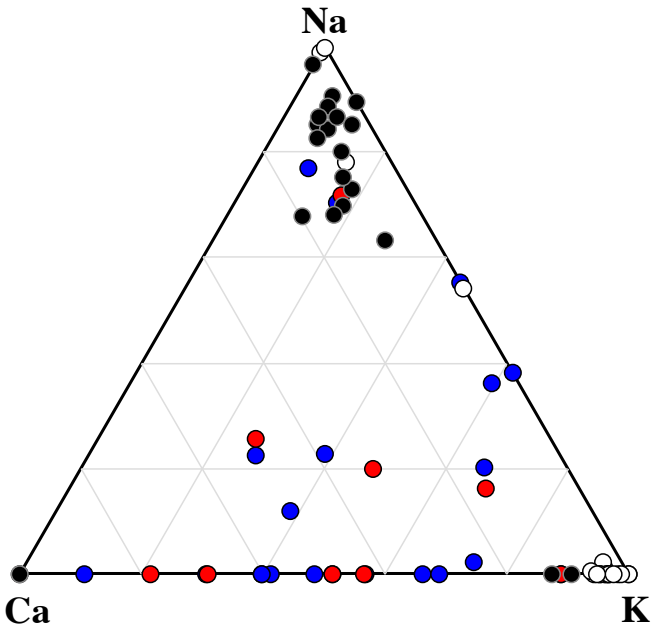

Figure 7: Ternary diagram of Na-Ca-K components, showing the compositions of mineral dust particles identified by SEM-EDX analysis. Data presented in relative atomic proportions. The circle symbols indicate non-active particles (red) and IN active particles (blue). Particles of Na-feldspar (black) and K-feldspar (white) are also shown for comparison.

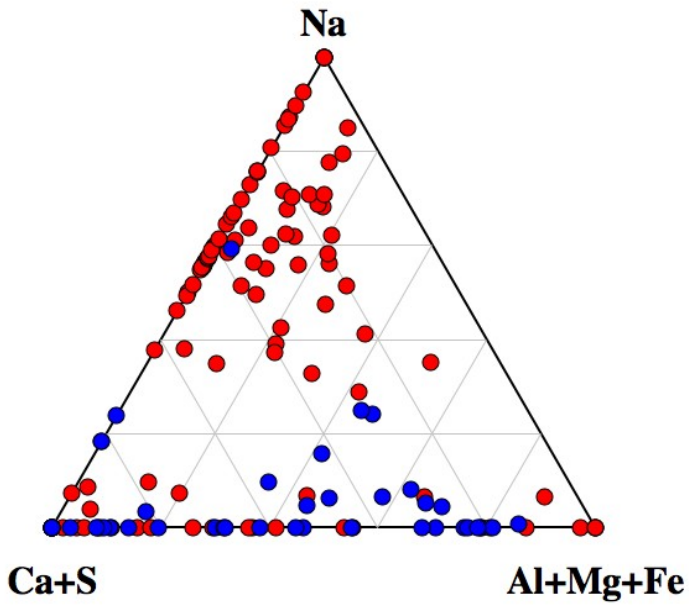

Figure 9: Ternary diagram of Na-(Ca+S)-(Al+Mg+Fe) components, showing the compositions of all particles analyzed by SEM-EDX analysis. Data presented in relative atomic proportions. The circle symbols indicate the non-active (red) and IN active particles (blue).

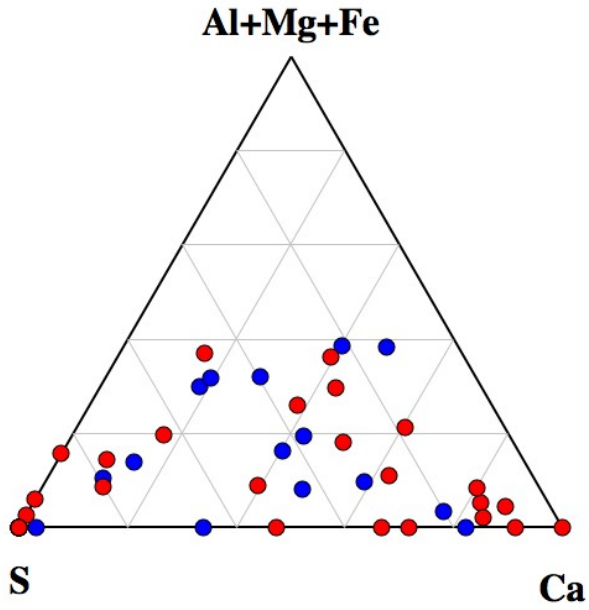

Figure 10: Ternary diagram of (Al+Mg+Fe)-S-Ca for Ca-rich and sulfate particles analyzed by SEM-EDX analysis. Data presented in relative atomic proportions. The circle symbols indicate the non-active (red) and IN active particles (blue).

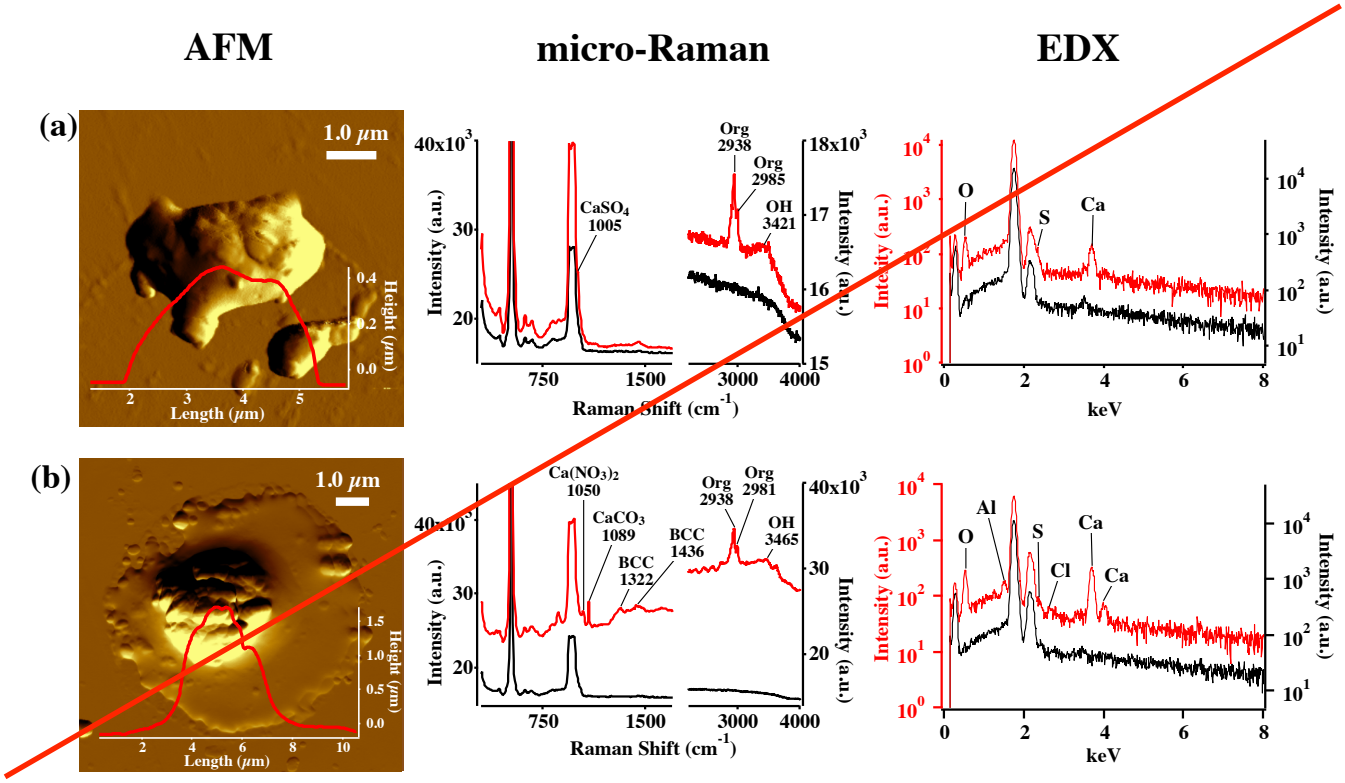

~~Figure 11: AFM topographic images of representative Ca-rich particles in IN active (a) and non-active (b) groups, and their corresponding Raman and EDX spectra. The AFM images were obtained in probe amplitude mode. The inset in the AFM image shows the height of each particle. The red and black curves indicate the spectra of the particle and the substrate background, respectively~~.

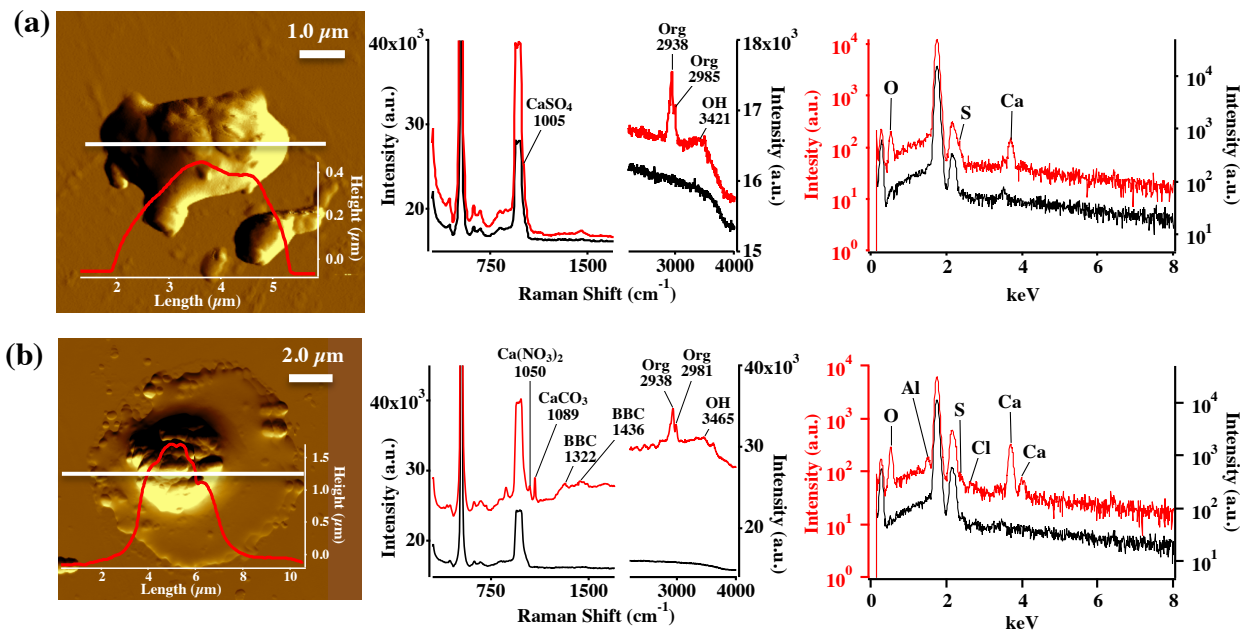

Figure 10: AFM topographic images of representative Ca-rich particles in IN active (a) and non-active (b) groups, and their corresponding Raman and EDX spectra. The AFM images were obtained in probe amplitude mode. The inset in the AFM image shows the scanned height along the white transect of each particle. The red and black curves indicate the spectra of the particle and the substrate background, respectively

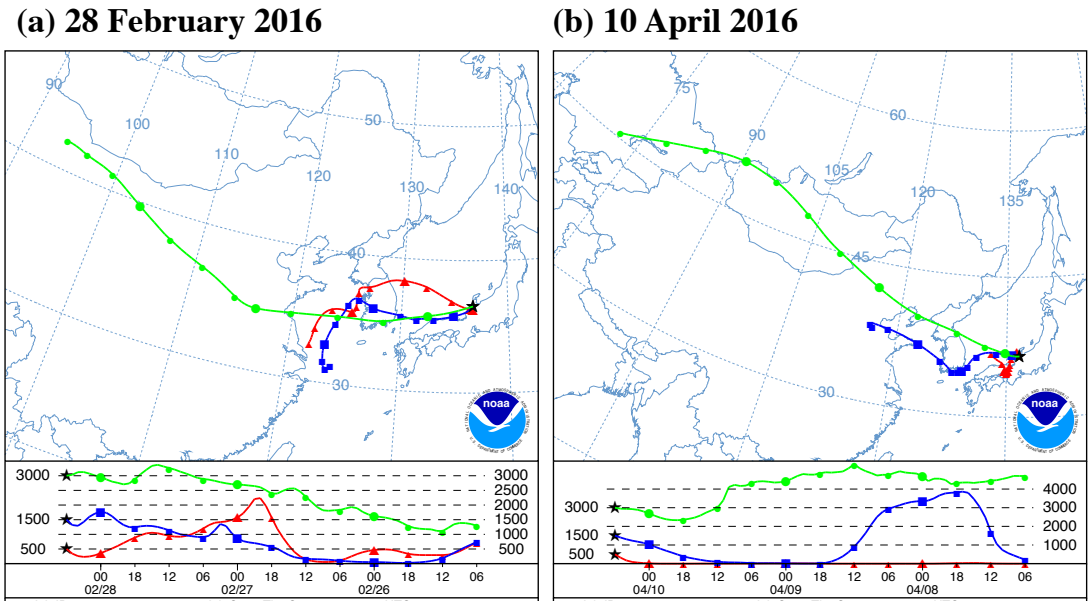

Figure 11: Backward trajectories of air masses that arrived at 3,000 m, 1,500 m, and 500 m over the sampling location during the sampling periods on the 28 February and 10 April, 2016.

Table 1: Peak assignments for Raman spectra obtained in this study.

Raman peak assignments		
	Raman Shift (cm^{-1})	Literature
Feldspar	485	Freeman et al., 2008
Quartz	465	Laskina et al., 2013
$CaCO_3$	1089	Laskina et al., 2013
Na_2CO_3	1080	Hiranuma et al., 2011
$(NH_4)_2SO_4$	975	Tang and Fung, 1989
$CaSO_4$	1005	Hiranuma et al., 2011
Na_2SO_4	990	Tang and Fung, 1989
$NaNO_3$	1069	Tang and Fung, 1989
$Mg(NO_3)_2 \cdot 6H_2O$	1059	Tang and Fung, 1989
$Ca(NO_3)_2 \cdot 4H_2O$	1050	Tang and Fung, 1989
C-H vibration (Organics)	2800 - 3100	Baustian et al., 2012
Black and brown carbon	1200 - 1700	Ivleva et al., 2007
Bonded OH stretch	3200 - 3650	Baustian et al., 2012
Fluorescent	- 4000	